VIETNAM NATIONAL UNIVERSITY

HANOI UNIVERSITY OF SCIENCE

VIENGTHONG XAYAVONG

APPLICATION OF GEOPHYSICAL EXPLORATION METHODS FOR GROUNDWATER INVESTIGATION IN LAOS

DOCTORAL THESIS IN PHYSICS

Hanoi – 2023

VIETNAM NATIONAL UNIVERSITY

HANOI UNIVERSITY OF SCIENCE

VIENGTHONG XAYAVONG

APPLICATION OF GEOPHYSICAL EXPLORATION METHODS FOR GROUNDWATER INVESTIGATION IN LAOS

Major: Physics of The Earth

Code: 9440130.06

DOCTORAL THESIS IN PHYSICS

Scientific Supervisor:

Assoc. Prof. Dr. Vu Duc Minh

Hanoi – 2023

Statutory declaration

I hereby declare that this thesis is my own research work under the direction of Assoc. Prof. Dr. Vu Duc Minh. The results stated in the thesis project are honest and have never been published in any other works.

Thesis author

Viengthong Xayavong

Acknowledgements

To complete this thesis, I would like to express my deepest gratitude to my supervisor, Assoc. Prof. Dr. Vu Duc Minh for giving me the opportunity to enter the world of research and working with groundwater problems in Laos; for his invaluable feedback in the writing process of articles and the thesis to complete my PhD study program. I would also like to express my sincere thanks to Dr. Nguyen Anh Duong and Dr. Vu Minh Tuan, who helped me with their suggestions, valuable discussions, encouragement when reading and editing some draft manuscripts. Thanks to Dr. Do Anh Chung, Dr. Pham Thanh Luan, Dr. David Gomez-Ortiz, Dr. Ahmed M. Eldosouky for their important contributions to my articles. A special thanks to Professor Roland Roberts and Professor Thomas Kalscheuer, Department of Earth Sciences, Uppsala University, Sweden for reviewing the article. My sincere appreciation goes to the anonymous reviewers for taking their time to contribute with constructive criticism and improve my articles. Special thanks go to my field work team, Dr. Sonexay Xayheuangsy and Mr. Thiengsamome Sounsuandao and BSc students in geophysics in Physics Department, Faculty of Natural Science, National University of Laos for the hard fieldwork assistance.

I gratefully acknowledge the funding of the International Programme in the Physical Sciences (IPPS), Uppsala University, Sweden with grateful thanks to Prof. Dr. Carla Puglia and Dr. Barbara Brena, Director and Deputy Director of the IPPS respectively. Many thanks also go to Assoc. Prof. Dr. Ernst Van Groningen and Prof. Dr. Lennart Hasselgren, past Director of the IPPS for giving me the chance to obtain this research fund. The author would like to thank the VNU University of Sciences, Faculty of Physics, Department of Physics of the Earth for supporting course fee and the SuperSting R8/IP (USA) to geophysical data acquisition. Special thanks go to the International Center of Physics, Institute of Physics, Vietnam, Grant number ICP.2019.09 for research grant in this research work.

Finally, I send my loving thanks to my family, relatives and friends and especially to my wife, Bouakham Douangpanya and my daughter, Valatthaya Xayavong for encouraging and supporting me throughout my work.

Thesis author

Viengthong Xayavong

TABLE OF CONTENTS

LIST OF SYMBOLS AND ABBREVIATIONS

Abbreviations	Full name
VES	Vertical Electrical Sounding
IES	Improved Electrical Sounding
MEE	Multi-Electrode Electrical Exploration
IMES	Improved Multi-Electrode Electrical sounding
AMES	Advanced Multi-Electrode Electrical Sounding
IMEE	Improved Multi-Electrode Electrical Exploration
MRS	Magnetic Resonance Sounding
ERT	Electrical Resistivity Tomography
2D ERT	2D Electrical Resistivity Tomography
2D ERI	2D Electrical Resistivity Imaging
SRT	Seismic Refraction Tomography
TDS	Total Dissolved Solids
EC	Electrical Conductivity of water
pH	Potential of Hydrogen
SP	Self-Potential method
IP	Induced Polarization method
EM	Electromagnetic method
Ra	Radiometric method
GPR	Ground Penetrating Radar method
M	Magnetic method
S	Seismic method
G	Gravity method
E	Electrical resistivity method
WHO	World Health Organization
USEPA	United State Environmental Protection Agency
JICA	Japan International Cooperation Agency

LIST OF TABLES

LIST OF FIGURES

INTRODUCTION

Groundwater is an essential source of freshwater in many regions in the world. A growing number of countries in Southeast Asia have encountered serious groundwater quantity and quality issues such as declining groundwater tables, subsidence, groundwater quality, and overexploitation leading to unsustainable management of groundwater resources. These are major problems that currently challenge hydrogeologists and relevant organizations. Groundwater is also a renewable resource with volumes that vary with the seasons and the local geological characteristics. Although, Laos is abundant of surface water, but available volumes of surface water may vary very strongly over time, and surface water can be susceptible to various forms of pollution. Particularly in the central parts of Laos, has grown for groundwater utilization. At the same time there is limitation of groundwater potential information, monitoring and evaluation activities regarding groundwater quantity and quality have not yet been carried out to any significant degree in this region.

Groundwater is an important source for irrigation, industries, and for both eating, drinking water and domestic use [32]. Groundwater information and groundwater quantity and quality monitoring and assessment programs remain limited in Laos. For example, a drilling project in the 1990s in Vientiane Province was implemented by the Japan International Cooperation Agency (JICA) for domestic supply in rural areas. Unfortunately, 60% of the 118 deep drilled wells were unusable due to poor water quality, such as high salinity [39]. Groundwater is one of the major sources of drinking water in Laos for both urban and rural areas. In 1998, only 60% of the urban and 51% of the rural residents had direct access to water supply. Not only is groundwater mainly used in the plateaus located far from surface water in the south and west of Champasack Province or other large areas without perennial rivers in the country, but also in places with a plentiful source of surface water in the Vientiane Plain. The use of groundwater help increases food security in regions such as Savannakhet province by increasing the number of crops annually.

Meanwhile, dug wells are unsafe sources of drinking water due to biological contamination and usually dry out during the dry season. Moreover, the use of surface water sources for eating and drinkingcan result in outbreaks of water-borne diseases because they may easily be contaminated with domestic waste from farm animals [60,77]. In addition, more than 100 boreholes were drilled in Outhomphone district, with a success rate of 50-60%, and approximately 50 boreholes were selected for production wells [45].

Water shortage remains the main problem in many areas of the research sites because the growth of economy and population leads to an increasing demand for water. Besides there are no mechanisms for data collection, compilation and storage, no protocols or entities responsible for implementing new groundwater resources. As well, no unit is responsible for strategic planning and there is virtually no coherent regulatory framework for groundwater usage and monitoring.

The three geophysical methods were selected for groundwater investigation in different study areas of the central part of Laos. The combination of resistivity and induced polarization techniques can delineation fresh and saline water and high groundwater potential zones, while seismic methods have been applied for identifying water table, thickness of aquifers and groundwater potential in the selected study areas. However, due to the main limitation of the magnetic resonance sounding (MRS) method is electromagnetic interference (EM), the noise can be caused by magnetic storms, thunderstorms, etc., and we don’t have MRS equipment that is very expensive, due to the main limitation of the vertical electrical sounding (VES) technique cannot be taken into account the horizontal variation in the subsurface earth resistivity, thus these methods were not selected in this thesis work.

The geophysical results of this study will probably verify the advantages of the application of geophysical methods for groundwater investigation in the selected research areas of Laos. On the other hand, this study allows to determine groundwater potential zone including water table, thickness of aquifers, fresh and saline groundwater in the three research areas. Therefore, geophysical exploration is

necessary to delineate locations of the freshwater and saline water zones in order to plan well drilling in the future in the study areas. Thus, we chose the thesis title "Application of Geophysical Exploration Methods for Groundwater Investigation in Laos". Three selected study areas in Central Laos are Vientiane, Khammouane and Savannakhet Provinces.

The objectives of the thesis

- To apply geophysical methods to find groundwater in three research areas: defining water table, depth and thickness of aquifers; delineating freshwater aquifers and saline aquifers.

- To determine groundwater quality directly from geophysical parameters and water samples from different wells in the first selected area.

- To provide the groundwater information in three research areas to assist water resource managers in the development of groundwater exploration and use plans.

Mission of the thesis

- To research and conduct integrated analysis of achievements of domestic and foreign scientists that related to the application of geophysical methods for groundwater investigation in Laos.

- To learn and study the application of the multi-electrode electrical exploration, the improved multi-electrode electrical exploration (both resistivity and induced polarization) and refractive seismic methods for groundwater investigation in Laos.

- To apply the above methods for groundwater investigation in three areas of Laos.

- To drill and check the results obtained by the application of geophysical methods in the survey areas and determine groundwater quality in the first selected area.

- To report the groundwater information in the three research areas to the Department of Water Resources, Ministry of Natural Resources and Environment, Lao PDR for managers in planning exploitation and the use of groundwater resources.

New results of the thesis

- Using the multi-electrode electrical exploration and refractive seismic methods simultaneously, especially the first use of the improved multi-electrode electrical exploration (both resistivity and induced polarization) for groundwater investigation in Laos has increased the accuracy of the research results.

- Providing new geophysical results at three research areas such as depth of groundwater tables or aquifers, the thickness of aquifers, and groundwater quality in the first selected area.

- Providing the groundwater information in three research areas to assist water resource managers in the development of groundwater exploration and use plans.

Scientific and practical significance

- The simultaneous use of the multi-electrode electrical exploration and the seismic refraction methods, especially for the first time using the improved multi-electrode electrical exploration method (both resistivity and induced polarization) to survey groundwater in Laos have complemented each other and increased the accuracy of research results while the field time is faster, the implementation cost is less.

- The results of the thesis will be a useful reference for future researchers who are interested in the field of groundwater exploration and evaluation in the three studied areas. At the same time, the results of this study will contribute directly to the managers in the planning, exploitation and use of water resources in the three studied areas; used as a public awareness strategy to promote safe and sustainable groundwater use in these areas.

Thesis Layout

- Chapter 1: An overview of groundwater research using geophysical methods

- Chapter 2: Geophysical exploration methods applied to survey groundwater in the research areas

- Chapter 3: Groundwater survey results in Central Laos

CHAPTER 1
AN OVERVIEW OF GROUNDWATER RESEARCH USING GEOPHYSICAL METHODS

1.1. GEOPHYSICAL METHODS FOR GROUNDWATER INVESTIGATION

Geophysical exploration methods are conducted on the earth's surface to define geological structures or target bodies by measuring certain physical property such as density, elastic moduli, electrical conductivity, electrical capacitance, magnetic susceptibility and magnetic moment of the hydrogen nucleus in the subsurface earth influenced by the Earth's subsurface distribution of physical properties or water saturation in the porous rocks. Geophysical exploration methods comprise of measurement of signals from natural or induced phenomena of physical properties of subsurface earth. The application of geophysical exploration methods depends on specific purposes related to the distribution of the physical property of the earth layers. Thus, for example, the gravity method is very suitable for the delineation of salt dome by dint of their density contrast of earth layers whereas seismic or electrical techniques are appropriate for the identification of water table or aquifers because saturated subsurface may be distinguished from dry earth layers by their different seismic velocity and electrical resistivity. The geophysical methods, measured parameters and operative physical property are listed in Table 1.1.

Table. 1.1. Geophysical methods and relevant measured geophysical parameter (modified from [41])

Method	**Measured geophysical parameter**	**Operative physical property**
Seismic	Travel times of reflected or refracted seismic waves	Density and elastic moduli
Gravity	The strength of the gravitational field of the Earth	Density
Magnetic	The strength of the Earth magnetic field	Magnetic susceptibility and remanence
Resistivity	Earth resistance	Electrical conductivity

Induced polarization	Polarization voltages	Electrical capacitance
Electromagnetic	Electromagnetic signals	Electrical conductivity and inductance
Magnetic resonance sounding	Proton magnetic relaxation signal in water	Spin and magnetic moment of the hydrogen nucleus

Geophysical methods apply the principles of physics to the investigation of the earth's subsurface structures. Geophysical data processing and interpretation can identify subsurface characterization for groundwater sources, environmental problems, and understand the influence of subsurface geological conditions as shown in many geophysical investigation reports [10, 20, 30-31, 41, 49-50, 59, 69].

Geophysical exploration methods have been widely applied to many investigation purposes such as conductive ore or mineral deposits, hydrocarbon deposits, engineering or construction sites, archaeology, including groundwater investigation. The most appropriate geophysical methods have been selected for available investigations (Table 1.2).

Table. 1.2. Geophysical exploration applications (modified from [41])

Applications	Appropriate survey methods*
Hydrocarbon (oil, gas, coal) investigation	S, G, M, (EM)
Conductive ore deposits investigation	M, EM, E, SP, IP, R
Geological structures investigation	S, (E), (G)
Groundwater sources investigation	E, S, (G), (Rd)
Engineering/construction site investigation	E, S, Rd. (G), (M)
Archaeological investigation	Rd, E, EM, M, (S)

* G: gravity; M: magnetic; S: seismic; E: electrical resistivity; SP: self-potential; IP: induced polarization; EM: electromagnetic; R: radiometric; Rd: ground-penetrating radar. Subsidiary methods in brackets.

The aims of the geophysical exploration methods are to delineate subsurface earth or target bodies that possible to determine their dimensions and relevant physical properties. Since physical properties are determined to a considerable degree by lithology, discontinuities in physical properties often correspond to geological boundaries. A geophysical survey consists of a set of measurement, usually collected to a systematic pattern over the earth's surface by land, sea or air. Measurements may be of spatial variations of static fields of gravitational or magnetic "potential" or of characteristics of wave fields, more particularly of travel-times or electromagnetic waves. The surface geophysical methods are non-destructive geophysical methods, which can provide a more continuous image of subsurface geophysical properties than test drilling. On the other hand, the application of subsurface methods including test drilling and borehole geophysical logging methods for groundwater investigation are more expensive than the surface geophysical exploration methods. However, the disadvantage of each geophysical method depends on the accuracy of geophysical instruments and the variations of physical properties in the subsurface earth, these geophysical methods cannot be conducted without a contrast of physical properties in different subsurface conditions [41].

Seismic refraction method (SRT) is commonly applied to delineate the subsurface earth, the depth to water table, basement structures in engineering and construction sites. This method has been extensively used for a variety of purposes in various geological information in many countries around the world to map structural geology, including groundwater studies [19, 33-34,47, 54, 72, 75]. Nevertheless, this method is frequently used for subsurface detection and depth to water table with high accuracy [5, 9, 15, 27-29, 57, 73].

The main purpose of electrical methods is to detect the resistivity distribution in the Earth by performing measurements on the earth's surface. By these measurements, the true resistivity of the subsurface can be estimated. The earth resistivity is related to various geological parameters such as mineral and fluid

content, porosity and water saturation level in the rock. Electrical methods have been used for many decades in hydrogeological, mining and geotechnical investigations, including hydrogeology investigations [50].

The multi-electrode electrical exploration was developed over the last two decades. In this measurement, automatic acquisition systems and new inversion algorithms for Electrical Resistivity Tomography (ERT) have been applied to resolve the complex subsurface geology. The ERT method is a recent advantage in eletrical resistivity imaging, providing non-invasive measurment of subsurface characterization at different scales with better resolution than its conventional method. The 2D Electrical Resistivity Tomography (2D ERT) models obtained with a multi-electrode technique are used to study the shallow structures of the underground located a few tens of meters down to a hundred meters depth. These models provide complementary information to that obtained by the more traditional Vertical Electrical Sounding technique, which mainly aims to determine the depths of horizontal 1D structures from the surface to several hundred meters of depth. The use of multi-electrode systems for data acquisition in electrical resistivity exploration has significantly improved field productivity as well as the quality and reliability of the information obtained on the earth resistivity. Initially, multi-electrode systems with manual switching were used before the emergence of computer-controlled multi-electrode systems with automatic measurements and data quality control that has a considerable impact on data quality and data collection speed. Multi-channel transmitter and receiver systems are used to simultaneously conduct series of measurements. Electrical resistivity imaging is increasingly applied in groundwater investigation of saline water intrusion into freshwater aquifers, fault detection in the hard rock terrains, study of environmental problems in waste disposal areas, archaeological investigation of an ancient sites and investigation of metallic ore deposits [7, 43, 48-50].

The improved electrical sounding methods were developed in order to increase the efficiency of the methods using the 1D conventional electrode arrays

[2,80]. They developed three main advantages of the Improved Electrical Sounding (IES) methods such as the Petrovski parameters and electrode arrays, by using only an improved electrode array at each survey point and improved data processing and the IES analysis algorithm should only use simple and reliable algebraic formulas to convert the curves, without using unstable derivatives. Moreover, the combination of the IES methods and the Multi-Electrode Electrical Exploration (MEE) method provides advantages of both methods to create the Improved Multi-electrode Electrical Sounding (IMES) method [3] by using the (1D) improved multi-electrode arrays. These methods have been applied in Vietnam and have yielded better results than previous methods. However, these methods are still restricted to 1D survey due to each measurement by an improved electrode array, they only get one depth measurement point. In order to overcome the limitations, he has made a data reading program to have data files for each measuring point along the profile for data analysis. Then he continued to study and propose the Advanced Multi-Electrode Electrical Sounding (AMES) methods [81-82]. Now, he named exactly the Improved Multi-Electrode Electrical Exploration (IMEE) methods (using both resistivity and induced polarization) by using the (2D) improved multi-electrode arrays (abbreviated as MC array). These new development methods have high scientific reliability, really usefulness, scientific and practical significance. The detailed instruction of the IMEE methods as well as some results of model calculation, experimentation and practical application in Vietnam gave better results than previous methods, have been reported in many previous publications [24, 81-83].

At present, different geophysical methods and software have been developed to delineate subsurface structures at high precision and accuracy, including groundwater exploration [11, 16, 18, 22-23, 44, 58]. Whereas, the integration of electrical resistivity tomography and Seismic Refraction Tomography methods are the most common methods used to determine reliable subsurface structures for a variety of research purposes in many countries around the world, including finding groundwater sources [67,70-71]. These geophysical methods have been applied in

central parts of Laos where there are the sedimentary deposits, namely the Vientiane and Savannakhet basins. Many reports have shown that salt deposits in the subsurface at a depth of about 50 m, inevitably affect groundwater in these areas.

The combination of various geophysical exploration methods is applied to groundwater assessment capacity in the Vientiane Plain, Lao PDR [13]. The aim of this research work is to apply a variety of geophysical methods to evaluate groundwater potential, provide new skills in research activities through attending various stakeholder groups from relevant organizations, the university, and the community. The results of their article indicate that near-surface geophysical methods could evaluate groundwater potential and aquifer conditions. The integration of near-surface geophysical methods and water quality surveys could provide further opportunities to explore the capacity of deeper aquifers and groundwater quality in the Vientiane Plain. This project has supported local undergraduate and postgraduate training opportunities using several different near-surface geophysical and hydrogeologic methods, which have not been applied in Lao PDR.

Application of both Magnetic Resonance Sounding and Vertical Electrical Sounding was conducted in Vientiane Basin, Laos [60]. The objectives of their study are to determine and identify groundwater potential zones in the study areas and verify that both geophysical methods can be used to delineate saline and fresh water zones in the study areas. The results have shown that clay layer is usually situated between 25 and 50 m depth and regions with very low resistivity of 0.5 ohm-m are interpreted as thick clay layers which is likely related to layers of halite deposits, it seems that this clay layer is caused by salt deposits in this layer. The clay layer may serve as an indicator of the halite and it probably works as a salinity barrier for the overlying aquifers. Whereas both geophysical and water chemistry data were used to determine water quality parameters of aquifers in the Vientiane basin, Laos [61]. The aim of this study is to test the possibility of using geophysical methods with groundwater chemistry data from shallow and deep wells to distinguish freshwater aquifers from salt-affected groundwater and determine water quality parameters

directly from geophysical data. The results showed that the integration of geophysical and chemical data techniques was successful in distinguishing highly conductive clay from mudstone from water bearing layers, furthermore, freshwater aquifers from salt-affected water. Application of Magnetic Resonance Sounding and Vertical Electrical Sounding was performed in Vientiane province, Laos [56]. The results revealed that the combination of these techniques can define locations of good quality groundwater in the study area. However, he recommended that other geophysical methods such as seismic refraction, electrical resistivity, and electromagnetic methods should be applied to provide more reliable results. They have successfully applied the combination of resistivity and induced polarization analysis in Malaysia [53].

The purpose of the study is to delineate the subsurface geological formation through combination of resistivity and induced polarization analysis. The results showed that the electrical resistivity value from 700 to 2000 Ohm.m is overlapped with the low chargeability value ranging from 1 to 2 ms. This indicates groundwater occurrence. Induced polarization analysis can reduce the ambiguities in the resistivity data and distinguish clay from groundwater. The combination of resistivity and induced polarization data can identify the possible fractured areas.

They have successfully applied 2D electrical resistivity imaging and seismic refraction methods to delineate water table in Indonesia [68]. The results indicated that the resistivity values of less than 1 to 2 Ohm.m is brackish water intrusion while the bottom layer with the resistivity value of more than 20 Ohm-m is considered as marine alluvium. Meanwhile, the results of seismic refraction found velocity models with 1571 m/s are considered as the water table at depth of 5 to 8 m and the leachate (1229 to 1571 m/s) at the same location as indicated by 2-D inverse model resistivity. They succeeded in applying 2D electrical resistivity imaging and seismic refraction to underwater survey in Sweden [67]. The results demonstrated that the joint inversion approach combining ERT and seismic has very promising results for three reasons such as the reduced extent of the transition zone, the more reliable interpretation of two independent parameters and their combination by a clustering

approach. The reduced investigation depth of ERT is due to the fact that the current preferably flows through low-resistive bodies caused by water or sediments. This is the major disadvantage of this method. Therefore, the combination of geoelectrical and seismic refraction is recommended as the standard tool for site investigations under geologic conditions similar to these areas. Application of seismic refraction method to study the groundwater potential was carried out at the basement complex of Northern Nigeria [57]. The results of seismic models revealed that earth subsurface with seismic velocity regions of 1000 to 2500 m/s m/s at depth of 10 to 20 m was interpreted as sandy clay, clay and saturated soil of fine to medium and coarse grain size. Application of seismic refraction method was conducted in Ethiopia for groundwater assessment [37]. The results of research work showed that third layer's average velocity of 1858 m/s was interpreted as weathered basalts (water saturated) with 23m vertical extension, according to velocity and lithology of third layer that could form good reservoir for groundwater potential have been identified in this work. Application of seismic refraction method for delineation of structures favorable to groundwater occurrence was performed in Krishna district, Andhra Pradesh [76]. The results were examined by correlating the geophysical signals with the available geology of the area and were found to be an available zone for further exploration and exploitation of groundwater. Refraction seismic studies proved to be highly useful in accurately determining the thickness of various layers. The low seismic velocity value regions which are favorable for groundwater accumulation were also identified.

Groundwater is an essential source of freshwater in many regions in the world. A growing number of countries in Southeast Asia have encountered serious groundwater quantity and quality issues such as declining groundwater tables, subsidence, groundwater quality, and overexploitation leading to unsustainable management of groundwater resources. These are major problems that currently challenge hydrogeologists and relevant organizations. Properly managed, groundwater is a renewable resource with volumes that vary with the seasons and the

local geological characteristics. Available volumes of surface water may vary very strongly over time, and surface water can be susceptible to various forms of pollution. Even groundwater may contain, for example, an unhealthy content of heavy metals, but this content tends to be stable over time, and is thus, at least in principle, relatively easy to identify and monitor. Groundwater is an important source for irrigation, industries, and for both eating, drinking water and domestic use [32]. Groundwater information and groundwater quantity and quality monitoring and assessment programs remain limited in Laos. For example, a drilling project in the 1990s in Vientiane Province was implemented by JICA for domestic supply in rural areas [39]. Unfortunately, 60% of 118 deep drilled wells were unusable due to poor water quality, such as high salinity.

Groundwater is one of the major sources of drinking water in Laos for both urban and rural areas. In 1998, only 60% of the urban and 51% of the rural residents had direct access to water supply. Not only is groundwater mainly used in the plateaus located far from surface water in the south and west of Champasack Province or other large areas without perennial rivers in the country, but also in places with a plentiful source of surface water in the Vientiane Plain. In Laos in general and in the central parts of Laos in particular, groundwater usage has been increasing in regions such as Savannakhet province by increasing the number of crops annually. Meanwhile, dug wells are unsafe sources of drinking water due to biological contamination and usually dry out during the dry season. Moreover, the use of surface water sources for drinking water can result in outbreaks of water-borne diseases because they may easily be contaminated with domestic waste and feces from farm animals [52, 77]. In addition, more than 100 boreholes were drilled in Outhomphone district, with a success rate of 50-60%, and approximately 50 boreholes were selected for production wells [45]. Water shortage remains the main problem in many areas of the research sites because the growth of economy and population leads to an increasing demand for water. Besides there are no mechanisms for data collection, compilation and storage, no protocols or entities responsible for implementing new groundwater

resources. As well, no unit is responsible for strategic planning and there is virtually no coherent regulatory framework for groundwater usage and monitoring.

Vientiane basin is considered as a northwest extension of Sakon Nakhon basin of the Khorat Plateau, Thailand. This plateau is bounded by latitudes 14° N to 19° N and longitudes 101° E to 106° E, covering an area of about 170,000 square kilometers in northeastern of Thailand and central Laos. The bedrock of this plateau consists of a continental sequence of red-beds of Mesozoic age. The potash deposits in the MahaSarakham Formation of the Khorat basin is in Cretaceous age. The maximum thickness of the formation could exceed 1,000 meters. The PhuPhan range separates Khorat Plateau into two basins, the Khorat basin in south covers an area of about 36,000 square kilometers and SakonNakhon basin in north covers an area of about 21,000 square kilometers [59-62].

The MahaSarakham Formation is composed of claystone, shale, siltstone, sandstone, anhydrite, gypsum, potash, and rock salt. This formation is underlain by sandstone and siltstone of Khok Kraut Formation. A complete sequence from the bottom to top of this formation consists of a basal anhydrite, lower salt, potash zone, color-banded salt, lower anhydrite, lower clastic rocks, middle salt, middle anhydrite, middle clastic rocks, upper salt and upper anhydrite [25, 35, 42, 89].

The immense rock salt, rich potash and gypsum are deposited near Vientiane of Laos [26]. The salt deposits at shallow depth are in the northern extension of salt deposits of the northern Khorat Plateau. Drilling wells in the Khorat Plateau, Thailand near the Laos border indicated that 145-feet thick bed of carnallite of Cretaceous salt-bearing beds may develop into one of the world's largest potash deposits. In addition, Phosphate, halite, and potash deposits occur in central Laos and red-bed copper deposits are found in southeastern Laos (Figure 1. 1).

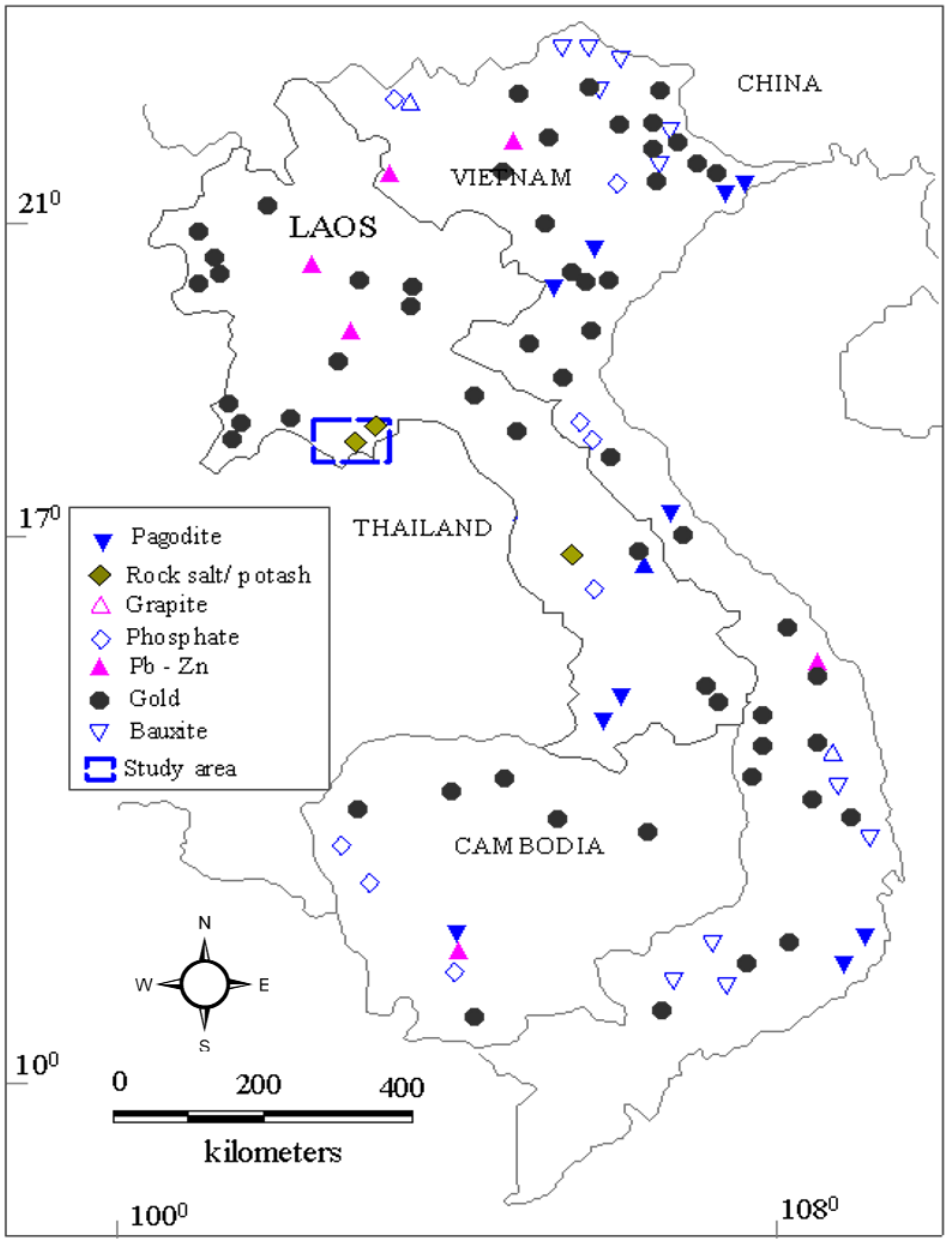

Figure 1.1. Mineral deposits of Indochina [26]

Laotian geological history is complex, and includes significant periods of marine deposition, uplift and erosion, as well as igneous activity and terrestrial deposition of e.g., coal, including in the Vientiane area which we focus on in this study. Although there has been some interest in prospecting for oil and gas, no commercially viable reserves have yet been identified in Laos. Coal resources are incompletely mapped, but there are reserves, mostly lignite. The largest known

deposit is in Songha, in the North of the Vientiane area [46]. Despite incompletely prospected, Laos is assessed to be relatively rich in various minerals, and about half of Laos exports are reported to be minerals or mineral products, largely gold, silver and copper from the Sepon and Phu Kham mines [55]. The potash reserves in the Thangon area of the Vientiane basin are considerable, with an estimated 50.3 billion tons of ore grading 15% potassium chloride [51]. Gypsum is mined e.g., at the Ban Iaomakkha mine in the Savannkhet area to the south, where reserves are estimated to be at least 50 million tons. While minerals are significant, the Lao economy is dominated by agriculture, which represents most of the employment in the country and about half of the GDP. With the climatic conditions, this means that effective management of water resources is vital to sustained and effective economic growth. As the economy has grown, loads on water resources have increased, requiring more advanced approaches to long-term management. Here, we study the application of some geophysical methods, primarily electrical resistivity tomography and induced polarization to shallow groundwater studies, to investigate how these methods may contribute. The specific targets were to measure the position of the water table, the thickness of the aquifers, and water quality in there. The obtained results of the field studies are compared to ground-truth from boreholes results, including the soil profile and analysis of water samples. The research work will also be used as a community awareness strategy to promote safe and sustainable use of groundwater in the selected areas. This research work will directly help water resource managers and drillers to get a deeper understanding of the resource and to further develop, where to locate domestic wells and irrigation wells to obtain the greatest yield and quality, while ensuring the security of the resource with optimal well-depth and extraction rate. Currently, there is little or no information on the groundwater resource which has led to limited knowledge and awareness of groundwater use that can often provide a safer and higher quality water resource, especially during the dry season or when the country is experiencing drought.

1.2. REASON FOR CHOOSING THE THESIS TITLE

Groundwater is an important source of water, which is also a renewable water source for households and drinking water for many people in rural communities. However, water scarcity remains a major problem in some research areas. This is due to the increasing economy and population associated with increasing demand for water, there is no mechanism for collecting, compilation and storage with the implementation of new groundwater resources for strategic planning resources, and there is almost no consistent regulatory framework for the use and monitoring of groundwater. Geophysical exploration techniques are commonly carried out on the earth surface to search for the many different purposes, including groundwater resources cause by some physical parameters like density, velocity, conductivity, resistivity, magnetic phenomena. Geophysical exploration techniques measure the physical properties contrast, or anomalies of physical properties within the earth's crust. The commonly geophysical methods have been useful for hydrogeology is the electrical, seismic, gravity, and magnetic methods. In this thesis work, the three geophysical exploration methods such as electrical exploration, polarization and seismic refraction methods were applied to study groundwater situations at three selected research areas in the central parts of Laos. The integration of resistivity and induced polarization methods can identify fresh and saline water and high groundwater potential zones, while seismic methods have been applied for identifying water table, thickness of aquifers and groundwater potential in research areas. The geophysical exploration methods are widely used in groundwater investigations to identify the extent and thickness of aquifers [12-13], including groundwater quality and groundwater flow [14, 16]. Some geophysical surveys have been carried out in the Vientiane Basin to identify of salt-affected groundwater in deeper aquifers and groundwater quality [61]. They applied vertical electrical sounding and magnetic resonance sounding methods to identify for groundwater potential zone or aquifers as well as groundwater quality in the Vientiane Basin. The main limitation of the VES technique cannot be taken into account in the horizontal

variation in the subsurface resistance. While the main limitation of the MRS method is electromagnetic interference (EM), the noise can be caused by magnetic storms, thunderstorms, etc., including man-made caused by wires, cars, electric fences, etc.

On the other hand, these geophysical results of their studies were not compared to ground-truth from new boreholes, the geophysical results were compared to previous boreholes where are relative far from sites of geophysical surveys. In addition, the application of geophysical methods is limited in central Laos, especially in the selected research areas. In this thesis work, three main geophysical techniques were chosen to assess groundwater investigation in central Laos, covering 3 provinces such as Vientiane, Khammouane and Savannakhet. The obtained results of this study may demonstrate the benefits of using geophysical methods for groundwater exploration in research areas and open up opportunities for future groundwater assessments and these geophysical methods can be used for other areas with similar geology formation. Therefore, it is necessary to conduct a geophysical survey to determine the location of freshwater and saltwater zones in order to plan future well drilling in the study area. Thus, we chose the thesis entitle "Application of Geophysical Exploration Methods for Groundwater Investigation in Laos**".**

CONCLUSION OF CHAPTER 1

✓ Groundwater is an invisible natural resource. It is also a renewable and alternative water source. The groundwater level depends on the season and the nature of the subsurface hydrogeology and different rock formations. The search for groundwater potential has increased due to lack of water resources and changes in groundwater table.

✓ Several geophysical methods were used to target groundwater potential zones. Geophysical surveys are conducted on the surface of the earth to explore groundwater resources based on certain physical parameters such as density, velocity, conductivity, electrical resistance. The purpose of geophysical exploration is to identify aquifers or locate potential groundwater for water exploitation. The results

were compared with the soil structure and water samples analyzed from these boreholes.

✓ One thing to keep in mind is how to ground the electrode when using the electrical exploration method, if the electrode is not grounded well, the results may not be obtained or the results may not be accurate. Choosing the grounding method of the electrodes while applying the Improved Multi-Electrode Electrical Exploration method has been noted in the research work [4].

✓ The obtained results of geophysical methods from previously published studies on groundwater finding in Vientiane province, Laos indicate ambiguity in the interpretation of the earth resistivity values, i.e., low resistivity values can consider as higher clay content or higher water content in earth subsurface. This includes the main limitation of the Vertical Electrical Sounding method in which the horizontal variation in subsurface resistivity cannot be taken into account, whereas the main limitation of the Magnetic Resonance Sounding method is electromagnetic interference, noise can be caused by magnetic storms. Meanwhile, the application of geophysical methods to search for groundwater remains limited to two study areas in Khammouane and Savannakhet provinces, central Laos.

✓ To overcome the above limitations, three main geophysical methods as: 2D Electrical Resistivity Tomography, Seismic Refraction Tomography, and the Improved Multi-electrode Electrical Exploration methods were chosen to use on groundwater finding in central Laos in this thesis work. Induced polarization and seismic refraction data analysis can reduce the ambiguities in the resistivity data and distinguish clay content from groundwater saturated sands in the earth subsurface in the three research areas.

CHAPTER 2
GEOPHYSICAL EXPLORATION METHODS APPLIED TO SURVEY GROUNDWATER IN THE RESEARCH AREAS

2.1. BASIC RESISTIVITY THEORY

The aim of electrical exploration is to determine the earth resistivity distribution by conducting measurements on the ground surface, the true resistivity of the subsurface can be estimated. The earth resistivity is related to various geological parameters such as the mineral and liquid content, porosity and degree of water saturation in the rock. The fundamental physical law used in resistivity surveys is Ohm's Law that governs the flow of current in the ground. The equation for Ohm's Law in vector form for current flow in a continuous medium is expressed in equation (2.1).

$$\vec{J} = \sigma\vec{E} \tag{2.1}$$

Where: σ is the conductivity of the medium, J is the current density and E is the electric field intensity. In resistivity surveys the medium resistivityρ, which is equals to the reciprocal of the conductivity ($\rho = 1/\sigma$), the relationship between the electric potential and the field intensity is given in equation (2.2)

$$\vec{E} = -\nabla V \tag{2.2}$$

Combining equations (2.1) and (2.2), we get

$$\vec{J} = -\sigma\nabla V \tag{2.3}$$

In resistivity surveys, the current sources are in the form of point sources. In this case, over an elemental volume ΔV surrounding a current source I, located at (x_s, y_s, z_s) the relationship between the current density and the current is given in equation (2.4)

$$\nabla.\vec{J} = \left(\frac{I}{\Delta V}\right)\partial(x - x_s)\partial(y - y_s)\partial(z - z_s) \tag{2.4}$$

Where: ∂ is the Dirac delta function.

Equation (2.3) can be rewritten as equation (2.5)

$$-\nabla \bullet [\sigma(x,y,z)\nabla V(x,y,z)] = \left(\frac{I}{\Delta V}\right)\partial(x-x_s)\partial(y-y_s)\partial(z-z_s) \qquad (2.5)$$

This is the basic equation that gives the potential distribution in the ground due to a point current source. This is the "forward" modeling problem, i.e., to determine the potential that would be observed over a given subsurface structure. Fully analytical methods have been used for simple cases, such as a sphere in a homogenous medium or a vertical fault between two areas each with a constant resistivity. Electrical resistivity measurements were carried out by injecting into the earth layers through two current electrodes and the resulting potential difference is measured at other two potential electrodes at the ground surface. For example, a half space solution, consider a single current electrode for a point source of current on the surface of a homogeneous-isotropic half space, injecting a current (I) into the subsurface. The flow of electric current will be radially symmetric in the half space (Figure 2. 1). The current flowing into the subsurface at the electrode with the total current flow out of a hemispherical surface. Now consider a single current electrode on the surface of a medium of uniform resistivity, ρ. The circuit is completed by a current sink at a large distance from the electrode. Current flows radially away from the electrode so that the current distribution is uniform over hemispherical shells centered on the source [50]. At a distance r from the electrode the shell has a surface area of $2\pi r^2$, so the current density J is given by

$$J = \frac{I}{2\pi r^2}$$

From equation (2.3), the potential gradient associated with this current density is

$$\frac{\partial V}{\partial r} = -\rho J = \frac{-\rho I}{2\pi r^2}$$

The potential V_r at distance r can be calculated by integration

$$V_r = \int \partial V = -\int \frac{\rho I}{2\pi r^2}\partial r = \frac{\rho I}{2\pi r}$$

We get the potential V_r at distance r is given in equation (2.6)

$$V_r = \frac{\rho I}{2\pi r} \qquad (2.6)$$

Where: r is the distance of a point current source in the medium, including the earth surface from the single electrode.

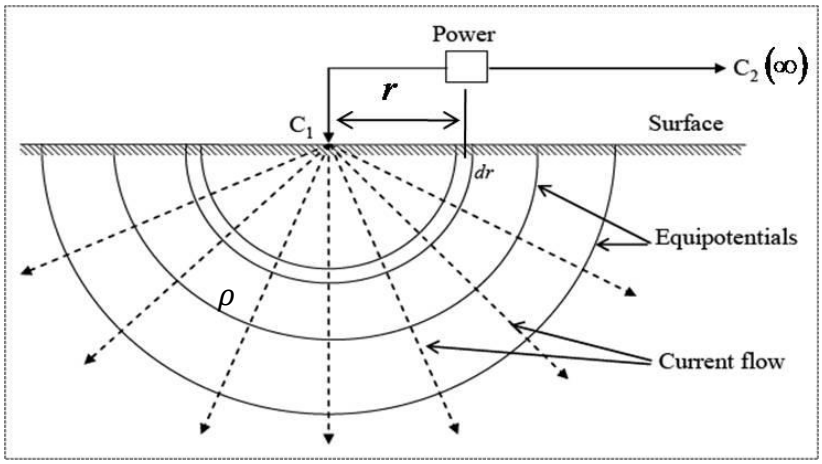

Figure 2.1. The current flow lines from a point source and the resulting equipotential distributions [50]

Equation (2.6) will be used for the calculation of the potential at any point on or below the surface of a homogeneous half -space. The hemispherical shells (Figure 2.1), mark surfaces of constant voltage and are termed equipotential surfaces.

In practice, all resistivity measurements use at least two current electrodes, a positive current and a negative current source. Now consider the case where the current sink is a finite distance from the source (Figure 2. 2). The potential at position M (V_M) at an internal electrode A is the sum of the potential contributions V_A and V_B from the current source at A and the sink at B.

$$V_M = V_A + V_B$$

From equation (2.6), now we consider the case where the current sink is a finite distance from the source (Figure 2.2). The potential at position M from the current source at A and the sink at B is calculated as below:

$$V_M = \frac{\rho I}{2\pi r}\left(\frac{1}{r_1} - \frac{1}{r_2}\right)$$

Similarly, the potential at position N, from the current source at A and the sink at B

$$V_N = \frac{\rho I}{2\pi r}\left(\frac{1}{r_3} - \frac{1}{r_4}\right)$$

Then, we can calculate the potential difference (ΔV) between positions M and N as shown below:

$$\Delta V = V_M\text{-}V_N$$

Thus, the potential difference (ΔV) between positions M and N can be calculated in equation (2.7)

$$\Delta V = \frac{\rho I}{2\pi}\left(\frac{1}{r_1} - \frac{1}{r_2} - \frac{1}{r_3} + \frac{1}{r_4}\right) \quad (2.7)$$

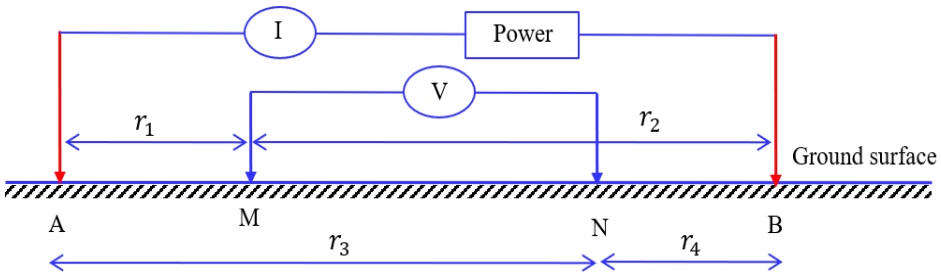

Figure 2.2. The generalized form of the electrode array used in resistivity measurements [41]

The equation (2.7) gives the potential difference that would be measured over a homogenous half space with the four electrodes. Actual field surveys are invariably conducted over an inhomogeneous medium where the subsurface resistivity has a 3-D distribution. The resistivity measurements are still made by injecting current into the ground through the two current electrodes C_1 at A and C_2 at B (Figure 2. 2), and measuring the resulting voltage difference at two potential electrodes (P_1 at M and P_2 at N). From the current (I) and potential (ΔV) values, an apparent resistivity (ρ_a) value is calculated by equation (2.8)

$$\rho_a = k\frac{\Delta V}{I} \quad (2.8)$$

Where: $$k = \frac{2\pi}{\left(\frac{1}{r_1} - \frac{1}{r_2} - \frac{1}{r_3} + \frac{1}{r_4}\right)}$$

k is a geometric factor that depends on the arrangement of the four electrodes. Resistivity measuring instruments normally give a resistance value, $R = \frac{\Delta V}{I}$, so in practice the apparent resistivity value is calculated by equation (2.9)

$$\rho_a = kR \tag{2.9}$$

The calculated resistivity value from equation (2.9) is not the true resistivity of the subsurface, but an "apparent" value that is the resistivity of a homogeneous ground that will give the same resistance value for the same electrode arrangement. The relationship between the "apparent" resistivity and the "true" resistivity is a complex relationship in order to determine the true subsurface resistivity from the apparent resistivity values is the "inversion" problem. Many common electrode arrays were used in resistivity surveys together with their geometric factors namely Wenner, Schlumberger, Dipole-Dipole and Pole-Dipole arrays. There are two more electrical based methods that are closely related to the resistivity method namely the Induced Polarization (IP) and the Spectral Induced Polarization (SIP) methods, both methods need instruments that are more sensitive than the normal resistivity method, as well has significantly higher currents. IP surveys are comparatively more common, particularly in mineral exploration. It is able to detect conductive minerals of very low concentrations that might otherwise be missed by resistivity or EM surveys [41]

The resistivity of these rocks is greatly dependent on the degree of fracturing, and the percentage of the fractures filled with ground water. Thus, a given rock type can have a large range of resistivity, from about 1000 to 10×10^6Ohm.m, depending on whether it is wet or dry. This characteristic is useful in the detection of fracture zones and other weathering features, such as in engineering and groundwater surveys. Sedimentary rocks, which are usually more porous and have higher water content, normally have lower resistivity values compared to igneous and metamorphic rocks. The resistivity values range from 10 to about 10000 Ohm.m, with most values below 1000 Ohm.m. The resistivity values are largely dependent on the porosity of the rocks, and the salinity of the contained water [50].

The resistivity varies greatly due to different geological materials. The various electrical geophysical techniques distinguish materials when a contrast exists in their electrical properties. The earth resistivity is function of porosity, permeability, water saturation and the concentration of dissolved solids in pore liquids within the

subsurface materials (Table 2.1) [66]. Rock resistivity of a clean sand, saturated aquifer can be explained by Archie's law:

$$\rho_r = a\rho_w\varphi^{-m} \quad (2.10)$$

Where: ρ_r, ρ_w are resistivities of rock and water respectively

a is the saturation coefficient $(0.6 < a < 2.0)$

m is the cementation factor $(1.3 < m < 2.2)$

φ is fractional porosity filled with the liquid

Table 2.1. Resistivity of various earth materials [66]

Materials	**Resistivity (Ohm.m)**
Top soil	1-300
Clay and silt	1-2000
Clayey sand	30-215
Clay	1-100
Gravel	100-5000
Sand	60-1000
Sandstone	8- 4000
Shale	20-2000
Sand and gravel saturated with fresh water	15-600
Groundwater	10-800
Fresh groundwater	20-160
Sediments with salt water	<10
Salt water	0.2

The earth resistivity value is dependent on the porosity as well as the clay content. Clayey soil normally has a lower resistivity value than sandy soil. However, note the overlap in the resistivity values of the different classes of rocks and soils. This is because the resistivity of a particular rock or soil sample depends on a number of factors such as the porosity, the degree of water saturation and the concentration

of dissolved salts. The resistivity of groundwater varies from 10 to 100 Ohm.m. depending on the concentration of dissolved salts. The low resistivity is estimate 0.2 Ω·m of seawater caused by the relatively high salt content. This makes the resistivity method an ideal survey for mapping the saline and fresh water interface in coastal areas [50].

2.2. BASIC INDUCED POLARIZATION THEORY

Induced polarization was performed to further clarify the distinction between groundwater and clay. The induced polarization measurements in the time domain involves the observation of the voltage decay between the two potential electrodes and was observed after the current had been turned off. The chargeability is calculated by integrating the voltage signal decay with respect to the time window; The apparent chargeability, *m* and has units of time in milliseconds can be expressed as equation [41]:

$$m = \frac{1}{V_0}\int_{t_1}^{t_2} V(t)\,.\,dt \qquad (2.11)$$

Where: V_0 is the off–time measured MN voltage at time t, and V(t) the observed voltage with an applied current.

The Induced Polarization (IP) technique is to measure the slow decay of voltage in the subsurface following the cessation of an excitation current pulse, which method measures the electrical properties of the mineral content, geochemistry and grain size of the subsurface medium through which electrical current passes. In the measurement, after the electrical current is suddenly switched off, the potential difference observed between the measuring electrodes does not vanish instantaneously but gradually decay in term of the chargeability in millisecond (ms). ERT and IP methods are the multi-electrode electric exploration methods with the research points changing in two directions: depth and measurement profile (2D image), or 3 directions: depth, measurement profile and perpendicular to the measurement profile (3D image). The nature of these methods is to study the change of electrical properties in 2D and 3D environments. ERT and IP methods measure the resistivity and induced polarization of the environment by using two A and B current

electrodes to be connected to the ground and measuring the voltage between the two M and N potential electrodes. By arranging many such electrode pairs on the profile, we will determine the distribution of resistivity and polarization of the survey environment. Based on the difference of resistivity and polarization, by the algorithms in the interpretation software, we can identify objects with different properties. The IP method is a method of studying the secondary electric field due to the physicochemical processes occurring in rocks and ores after interrupting the current flowing. This secondary electric field is of electrochemical origin, closely related to the processes taking place at the boundary of solid objects and solutions in pore rock.

Electrodes usually use two types: the generating electrode and the collecting electrode. The emitting electrode is usually made of iron, while the collecting electrode is a non-polar electrode usually made of porous porcelain containing a saturated salt solution of the core metal (such as copper core embedded in CuSO4 solution), which is conductive or metal with very small electrode polarity potential. This method is applied in hydrogeology to eliminate low resistivity anomalies, containing clay causing high polarization anomalies that are unable to contain water. This method measures the electrical properties of the mineral content, geochemistry and grain size of the subsurface medium through which electrical current passes. During the application of the electrical current, electrochemical reactions within the subsurface material take place and electrical energy is stored. After the electrical current is turned off the stored electrical energy is discharged which results in a current flow within the subsurface material. In the measurement, after the electrical current is suddenly switched off, the potential difference observed between the measuring electrodes does not vanish instantaneously but gradually decays in accordance with the chargeability in milliseconds. The chargeability of various materials is different (Table 2.2) [66].

Table 2.2. The chargeability of various earth materials [66]

Materials	**Chargeability (ms)**
Aquifers	0
Alluvium	1-4
Sandstone	3-12
Limestone	<1
Gravel	3-9
Quartzite	5-12
Gneiss	6-30
Shale	50-100

2.3. TRADITIONAL ELECTRICAL EXPLORATION METHODS

The application of electrical resistivity measurements for subsurface earth exploration has conducted in 1912 due to the work of Conrad Schlumberger who conducted the first electrical resistivity experiment in the fields of Normandy; a similar idea was developed by Frank Wenner in the United State of American (USA) in 1915. In this method, the center point of the electrode array remains fixed, but the spacing between the electrodes is increased to obtain more information about the deeper sections of the subsurface. The measured apparent resistivity values are normally plotted on a log-log graph paper. To interpret the data from such a survey, it is normally assumed that the subsurface consists of horizontal layers. In this case, the subsurface resistivity changes only with depth, but does not change in the horizontal direction. Since, electrical resistivity surveying has greatly improved, and has become an important and useful tool in hydrogeological studies, mineral prospecting and mining, as well as in environmental and engineering applications [18].

The aims of electrical resistivity survey are to measure the resistivity distribution in the subsurface layers by conducting measurements along the ground surface. The 2D Electrical Resistivity Tomography method is an important

geophysical exploration method used to provide a high-resolution earth subsurface image of the electrical resistivity values. The earth resistivity values vary greatly due to different subsurface geological information. The various geophysical exploration techniques distinguish subsurface when a contrast exists in their electrical properties. The 2D electrical resistivity measurement is conducted by injected current into the earth subsurface through the two current electrodes and measures the potential difference at the other two potential electrodes on ground surface. The commonly electrodes arrays of 2D resistivity measurement are usually arranged in a linear array. The apparent resistivity is known as the bulk average resistivity of earth subsurface layers affecting the current. The apparent resistivity can be calculated by the ratio between the measured potential difference and the input current, and multiplying by a geometric factor (coefficient of array) for the specific array [50].

In this thesis work, the Wenner electrode array was used for 2D resistivity data acquisition by manually and automatically with the ABEM Terrameter SAS 1000 for 49 electrodes system. In this measurement, the Wenner array and electrode spacing "a" is set as shown in Figure 2. 3.

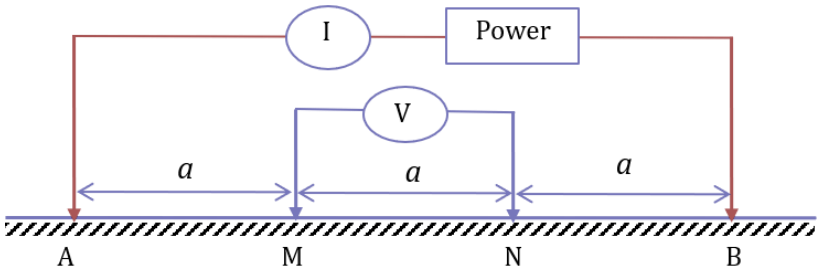

Figure 2.3. The Wenner electrode array [50]

The first procedure is to conduct all the measurements by using the Wenner array with electrode spacing of "1a". In the first measurement, electrodes number 1, 2, 3 and 4 are used. Notice that electrodes 1 and 4 are used as the first and second current electrodes (A) and (B) respectively, whereas electrodes 2 and 3 are used as the first and the second potential electrodes (M) and (N) respectively. For the second measurement, electrodes number 2, 3, 4 and 5 are used for (A), (M), (N) and (B)

respectively. This is repeated step by step of movement along the profile until electrodes 46, 47, 48 and 49 are used for the last measurement with “1a” spacing (Figure 2. 4). For a system with 49 electrodes note that there are 46 (49-3) possible measurements with “1a” spacing for the Wenner array**.**

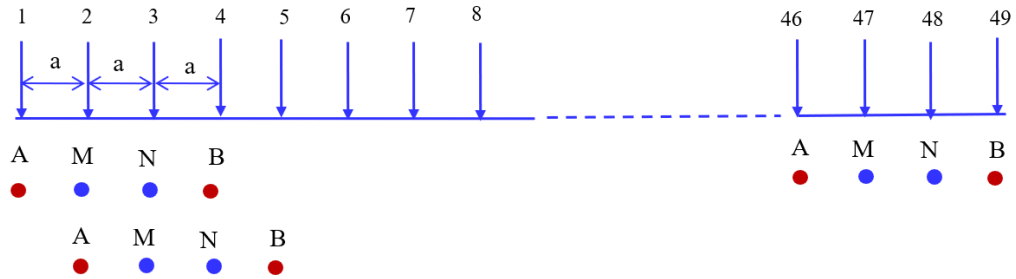

Figure 2.4. The arrangement of electrode system for a 2D- ERT survey for electrode spacing of “1a” [50]

After completing the sequence of measurements with “1a” spacing, the next sequence of measurements with “2a” electrode spacing is conducted. First electrodes 1, 3, 5 and 7 are used for the first measurement. The electrodes are chosen so that the spacing between adjacent electrodes is “2a”. For the second measurement, electrodes 2, 4, 6 and 8 are used. This process is repeated until reach electrodes 43, 45, 47 and 49 are used for the last measurement with spacing “2a”. For a system with 49 electrodes, note that there are 43 (49 - 2x3) possible measurements with “2a” spacing (Figure 2.5).

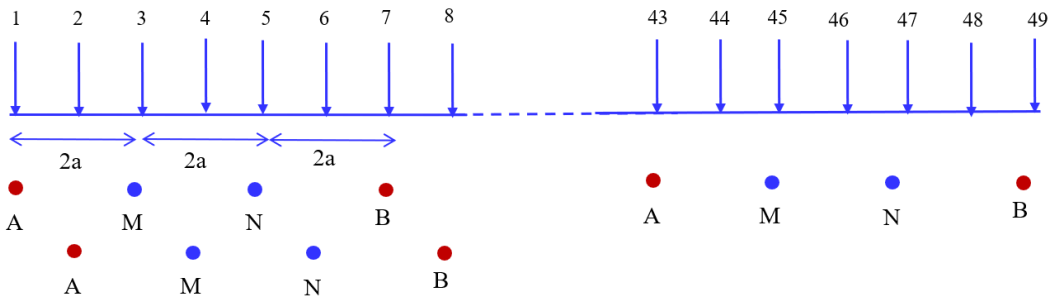

Figure 2.5. The arrangement of electrode system for a 2D- ERT survey for electrode spacing of “2a” [50]

The same procedure is repeated for measurements with “3a”, “4a”, “5a” up to “16a” spacings. To get the best results, the measurements in a field survey should be carried out in a systematic manner so that, as far as possible, all the possible measurements are conducted. In this work, we set a=10mindicated that the maximum electrode spacing of 160m and profile length of 480m.

The measured apparent resistivities are then presented in a contoured pseudo section, A pseudo section is a display technique, which involves plotting resistivity traverse data as a depth section, with each apparent resistivity being plotted as if it were the true resistivity of a point immediately below the center of the electrode array at a depth proportional to the electrode spacing. The contoured data provide an approximate image of the resistivity distribution in the plane of the section. The data integrated in the research area was processed by EarthImager software in order to determine an earth resistivity model that estimates the actual subsurface layers, the median depth of surveying is estimate 0.52 times the electrode spacing for the Wenner electrode array.

The electrical resistivity tomography is one of geophysical methods, that can be applied to image subsurface structures from tens of meters to several hundred meters in depth with still maintain higher resolution conventional methods, e.g. vertical electrical sounding. In this thesis work, the Wenner electrode array was selected for data acquisition, thus potential electrode spacing increases as current electrode spacing increases, which fewer sensitive voltmeters are required. Whereas, limitations of this method are basically to the depth of penetration of the technique is limited by the maximum electrical power that can be conducted into the ground and by the difficulties of laying out long lengths of electrical cable. Moreover, the topography and the influence of near-surface resistivity variations have an impact on the measurement results that need to be properly addressed.

2.4. IMPROVED MULTI-ELECTRODE ELECTRICAL EXPLORATION METHODS

The traditional horizontal layering method for interpreting electrical resistivity data are rapidly being replaced with two-dimensional (2D) and three-dimensional (3D) models of interpretations, especially in complex and heterogeneous subsurface media. In the field measurements have advanced from measurements made at separate and independent points to automated measuring systems with multi-electrode array along the measurement profiles. Data acquisition was more or less carried out manually till the 1980s, and this is labour intensive and slow, and the quality of the measured data might be poor. A range of fast automated multi-electrode and multi-channel data acquisition systems now exist that allows flexibility in the acquisition of electrical resistivity data [7]. A more accurate model of the subsurface is a two-dimensional (2-D) model where the resistivity changes in both the vertical and horizontal directions along the survey line. The present time, 2-D surveys are the most practical economic compromise between obtaining very accurate results and keeping the survey costs down. Typical 1D resistivity sounding surveys usually involve about 10 to 20 readings, whereas 2D imaging surveys involve about 100 to 1000 measurements. In comparison, 3D surveys usually involve several thousand measurements. In many geological situations, 2D electrical imaging surveys can give useful results that are complementary to the information obtained by other geophysical method. The development of the improved multi-electrode electrical exploration method was explained as follows: With the aim of increasing the efficiency of constant-current electrical sounding methods, the improved electrical sounding methods (IES) were successfully proposed [2, 80] using the (1D) conventional electrode arrays. The main advantages of the IES methods are: i) For the first time, the improved Petrovski parameters have been proposed and their scientifically theoretical base has been built; ii) For the improved electrode arrays, by using only an improved electrode array at each survey point, we still have all the information about the different types of curves after processing the obtained data; iii) The advantage of data processing and analysis algorithm of the IES methods is that

it only needs to use simple and reliable algebraic formulas to convert the curves, not using unstable derivatives as before.

Integrating the IES methods with the MEE method in order to promote the advantages of both methods to create the IMES method [3] by using the (1D) improved multi-electrode arrays. Correspondingly connecting the electrodes of the (1D) improved electrode array and the take-out of the SuperSting device together, they will have the (1D) improved multi-electrode arrays. These methods have been tested, applied in practice in Vietnam and gave better results than previous methods. However, the IES and IMES methods are only limited to 1D surveying because with each measurement by an improved electrode array, we only get one depth measurement point. Thus, he has built a data reading program to have data files for each measuring point along the profile for data analysis. The improved electrode array is irregular, so when processing 2D data, it is necessary to redefine the position of the electrodes to ensure that the recording points comply with the format requirements of the location of the data files and link the independent depth measuring points back into the profile.

To overcome the above limitations, especially to fully exploit the advantages of collecting and processing 2D data, he has investigated and proposed the AMES methods [81-82]. Now, he is called exactly the IMEE methods (using both resistivity and induced polarization) by using the (2D) improved multi-electrode arrays (abbreviated as MC array). This overcomes a very basic disadvantage that has existed up to now, which is to use the unstable derivative expression. These new proposals have high scientific reliability, really usefulness, scientific and practical significance. The detailed introduction of the IMEE methods as well as some results of model calculation, experimentation and practical application in Vietnam gave better results than previous methods, have been presented in previous publications [24, 80-83].

2.4.1. The improved multi-electrode arrays

The (1D) improved electrode array has uneven electrodes spacing (log coefficient increment), while the (2D) multi- electrode array has uniform electrodes

spacing (increase in natural numbers), so we have to convert the (1D) improved electrode array into the (1D) improved electrode array with uniform electrodes spacing, so that they can be put together into the (2D) improved multi- electrode array. For example, the principles of building an improved symmetric multi-electrode array (abbreviated as MC1 array) are shown as in Figure 2.6 , where A and B are the current-injecting electrodes, M and N are the potential-measuring electrodes, and MA refers to the separation between the M and A electrodes (Note that the principle of reciprocity in electrical sounding has been used, so the current-injecting electrodes should be arranged inside):

MA = AB = BN = n.a

MA = 4AB = BN = 4n.a (extended receiver)

MA = AB = BN = 3n.a (extended transmitter)

in which: a - the constant distance between adjacent electrodes;

n - the nth measurement for each configuration above.

Thus, the symmetrical MC multi-electrode array with the distance of first AB (in the position 27 and 28), we will have 2 measurement times with 2 MN distances (M1N1 in the position 26, 29 and M2N2 in the position 23, 32) that could be presented as in Figure 2.6.

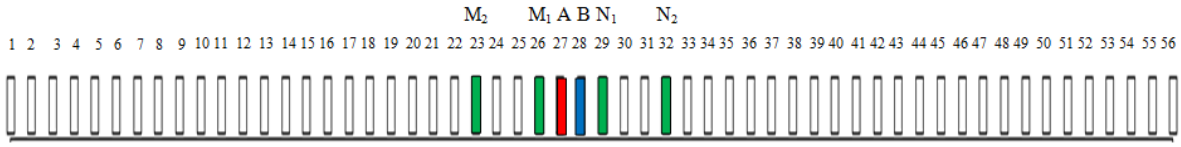

Figure 2.6. The arrangement of an improved symmetric multi-electrode array (with the distance of first AB in the position 27 and 28)

After that, we shall extend AB (in the position 26 and 29), we will get 2 measurement times with 2 MN distances (M1N1 in the position 23, 32 and M2N2 in the position 14, 41) that could be presented as in Figure 2.7.

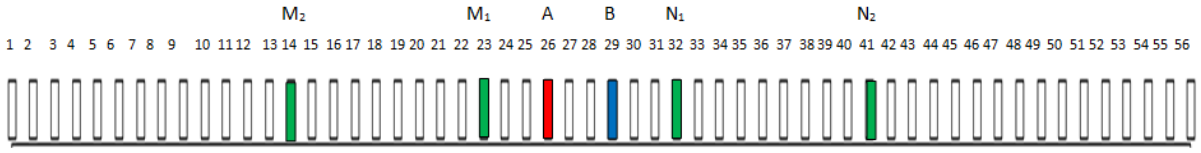

Figure 2.7. The arrangement of an improved symmetric multi-electrode array (with the distance of first AB in the position 26 and 29)

Corresponding to MC1 array, an improved dipole–dipole multielectrode array (abbreviated as MC2 array) is built according to the following principles:

3AB = 3BN = NM = 3.n.a (right hand side)

NM = 3MA = 3AB = 3.n.a (left hand side)

in which: a - the constant distance between adjacent electrodes;

n - the nth measurement for each configuration above.

For dipole MC array, at each measurement point with the distance of first AB (e.g. at position 14 and 15), we will have two measurements with the left and right hand sides of MN (M_TN_T at position 10, 13 and M_FN_F at position 16, 19), can be represented as in Figure 2.8.

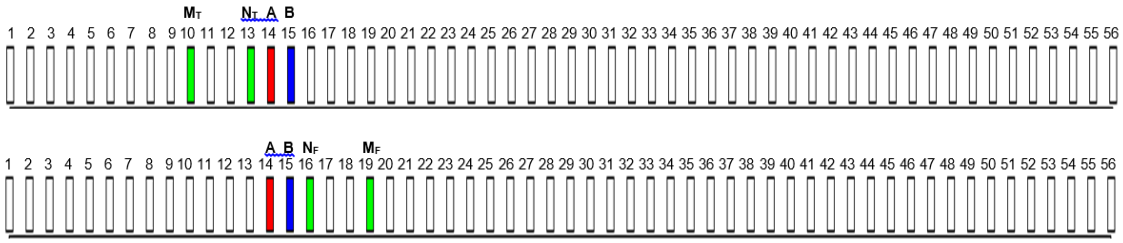

Figure 2.8. The arrangement of an improved dipole–dipole multielectrode array (with the distance of first AB in the position 14 and 15)

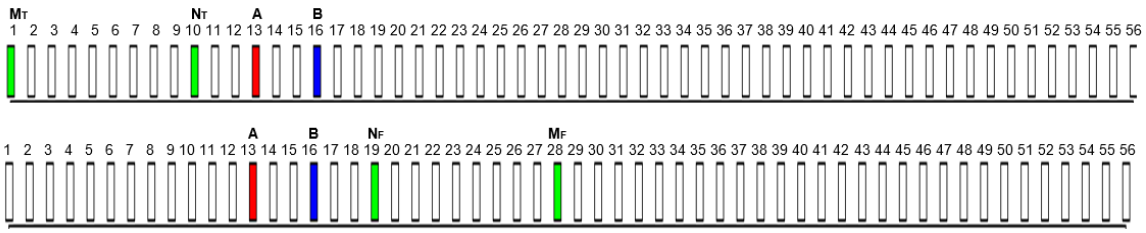

Figure 2.9. The arrangement of an improved dipole–dipole multielectrode array (with the distance of first AB in the position 13 and 16)

Then extending AB (at position 13 and 16), we will have 2 measurements with 2 MN sides (M_TN_T at positions 1, 10 and M_FN_F at position 19, 28), can be expressed in Figure 2.9.

On this basis, coupling and placement of electrodes shall be done in such a way that there is a 56-pole MC array on the principle of coupling of electrodes from the beginning to the end of the line.

So, the MC (MC1 and MC2) array shall get enough the features of the (1D) improved electrode array and the (1D) improved multi-electrode array and the conventional multi-electrode array.

2.4.2. The process of surveying, collecting and analyzing data

Based on the principles described above, a suitable array configuration, including switching between electrodes, is designed relative to the specific geological target, and this is the basis for setting up a control file that automatically collects the defined sequence of measurements from the entire array.

We used the SuperSting R8/IP equipment with 56 electrodes from Advanced Geosciences Inc. (US) with the MC array described above. The control file is manually set up and installed by us into the equipment before the fieldwork starts.

Note that, sometimes enhanced grounding methods may be necessary when contact resistance is high (for example, due to high surface resistance, etc. [1, 4]. For processing and analyzing the data to obtain the geo-electric sections from collected data files, two procedures are possible:

- Option 1: Use a self-built program to filter the data, calculate the value of ρ_s^{ct} and save it into a file with the same configuration as the input file of the required Res2DINV [65] or EarthImager 2D [6]. Then use any of this software to analyze and process ρ_s^{ct}.

- Option 2: Use a self-built program to filter the data and calculate the improved parameters according to the proposed algorithm on the basis of developing the data processing algorithm of the IMES and IES methods. At the same time, it is combined with EarthImager 2D and Surfer softwares to process and analyze the

obtained data and present the results (including the improved Petrovski parameter ρ_{pm}^{ct}).

Through the processing and analysis of the data collected in the field using the IMEE methods, we get not only the improved resistivity and polarization parameters, but also the improved Petrovski resistivity and polarization parameters.

In this thesis, option 1 with EarthImager 2D software was used to process and analyze data obtained through field trips.

2.4.3. Basis theories for 2D resistivity data processing

The final goal of geophysical measurements is to determine geological structures from geophysical data cause by the complex internal structure of the earth, which is a very difficult problem. Usually, we use a more or less simple model to approximate the real geology and try to determine the model parameters from the data [50]. We call this problem an inverse problem (Figure 2. 10)

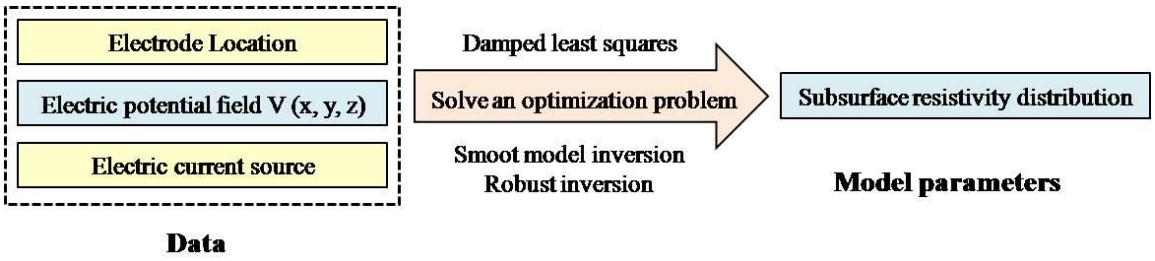

Figure 2.10. The traditional definition of the inverse problem [50]

In the automatic inversion routine, a homogeneous starting model of the earth resistivity distribution is used with logarithmic averages of the measured apparent resistivities. The earth layers are divided into a large number of rectangular cells, and the optimization method attempts to determine the resistivity distribution of the cells that minimizes the difference between the calculated and measured apparent values subject to certain constraints [48].

The inversion program is computer program that automatically generates 2D resistivity model of the subsurface for a data set from resistivity imaging surveys of conventional or non-conventional arrays with an almost unlimited number of possible

electrode arrays of uniform or non-uniform electrode spacing and for underwater and cross-borehole survey [50]. The inversion routine used by program is based on the smoothness-constrained least squares method that support both the quasi-Newton and Gauss-Newton least square optimization methods, Gauss-Newton method give slightly contrasts greater than 10:1 that can have an erratic resistivity zone, but slower than the quasi-Newton method. The Smoothness-constrained least squares method is based on equation (2.12)

$$(J^T J + uF)d = J^T g \qquad (2.12)$$

Where: $F = f_x f_x^T + f_z f_z^T$

f_x : horizontal flatness filter

f_z: vertical flatness filter

J : matrix of partial derivatives

u : damping factor

d : model perturbation vector

g : discrepancy vector

This mathematical inverse problem determines the subsurface distribution of resistivity from measurements of apparent resistivity data set to produce a subsurface inverted model that agrees mostly with the field apparent resistivity measurements based on predefined numbers of iterations for convergence. The subsurface is divided into a lot rectangular cells during the modeling. The resistivities of the cells are determined by the inversion algorithm, but might not always give the ideal resistivities because the cell-based inversion may employ a lot of assumptions to model complex geological structures [8]

A summary of the stages involved in inversion processes for data reductions and generating the final inversion model resistivity section (Figure 2. 11) is given as following [8]:

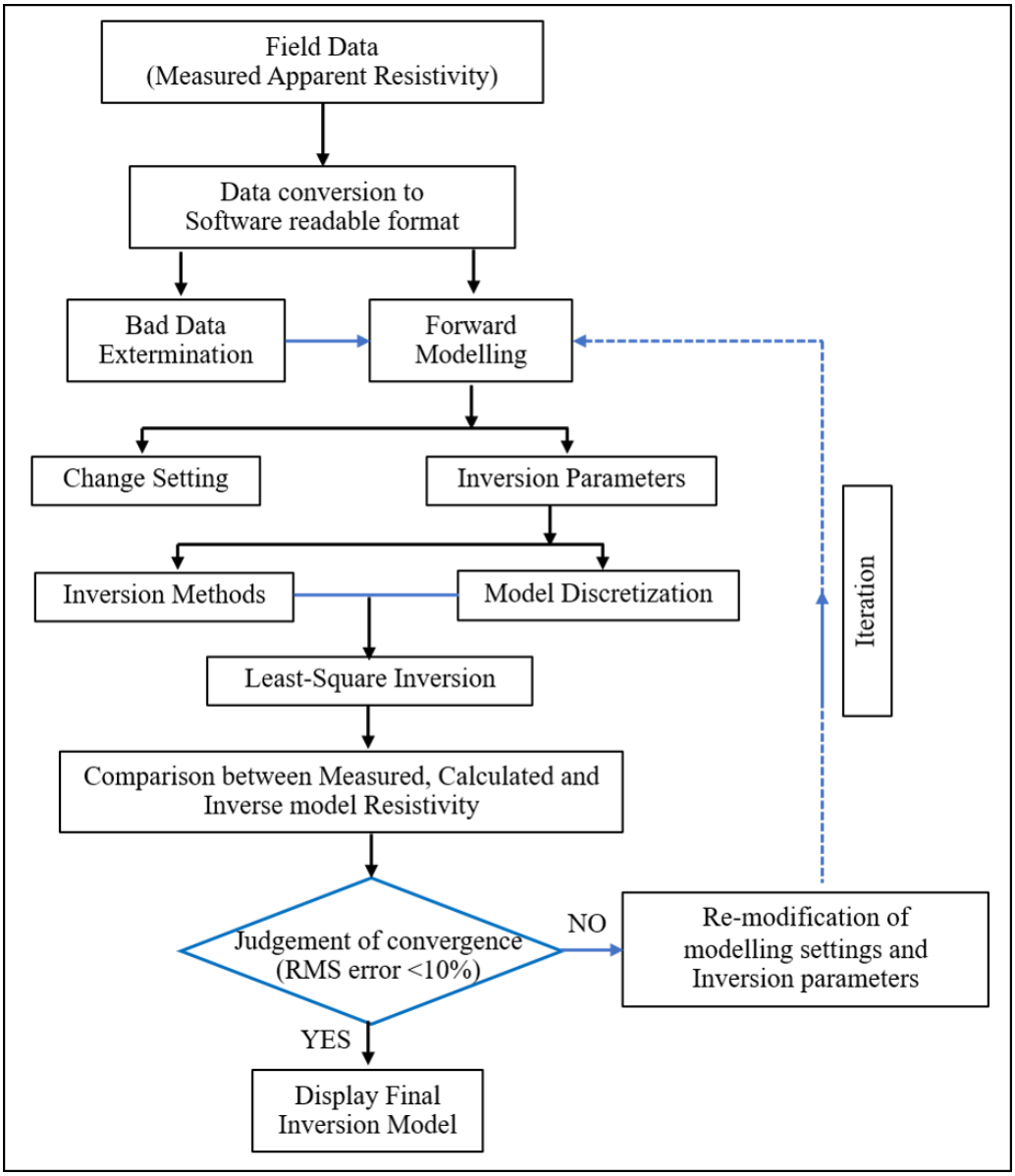

Figure 2.11. ERT data processing and inversion flow chart for RES2DINV software [8]

- Files in the Terrameter are saved in binary formats. This format is not compatible with the inversion software program so it has to be converted to a software readable file format.

- Data editing is performed to remove bad data points that have resistivity values which are clearly wrong due to the failure of relays at one of the electrodes, poor

electrode ground contact due to dry soil. The bad data points have apparent resistivity values that are obviously too large or too small compared to neighboring data points.

- Reciprocal measurement for data assessment and editing maybe to determine the percentage error resulting from interchanging of current and potential electrodes in contrast to the normal array of two current and two potential electrodes.

- Splicing is adopted for too large data sets in order to choose a section from the segmented data sets to be processed at a single time.

- Forward modeling subroutine-finite difference and finite–element methods. 2D or 3D model apparent resistivity and Jacobian matrix values are calculated through a mathematical link between the model parameter and the response model provided by finite-difference or finite-element methods. Finite-difference method is usually considered faster for data sets without topography while the finite-element method is used for data sets with topography.

- The ratio of vertical flatness filter (f_z) to horizontal flatness filter (f_x) is used for smoothing and reducing elongated vertical and horizontal anomalies in the pseudo-section. Higher vertical to horizontal flatness ratio values for elongated vertical anomalies and lower ratio values for elongated for horizontal anomalies are considered to produce a better pseudo-section.

- Models with very noisy and less noisy data sets, as well as unnatural oscillations in the lower section are taken care of during inversion by adjusting the damping factor (u) values. Relatively large damping factor is used for very noisy data sets and unnatural oscillations while a smaller damping factor is used for less noisy data sets to generate a better inversion model.

- The inversion refinement allows the user to choose a model with cell width with normal electrode spacing or cell width with half electrode spacing for optimum result. Cell width with half electrode spacing gives better resolution and smoothens the model than cell width of normal electrode spacing because the program attempts to reduce misfit of failure from the near surface variation that could lead to distortions in the lower section of the model.

- For achieving root mean square (rms) or absolute (Abs) error less than 10%, the iteration subroutine is usually set to 5 iterations for convergence, but can be continued to about 10 iterations in case model rms/Abs error is higher than the required convergence limit.

On the other hand, such 2D EarthImager software is a two-dimensional inversion modeling software for affordable resistivity and induced polarization (IP) imaging. It interprets data collected by the SuperSting™ Wi-Fi in just a few clicks, including parallel boreholes or on a surface line. The data set is processed into an easy-to-read and highly-visual 2D cross-section of the earth. The processed data can be output to various types of files and can be processed into reports ready for submission to your data set [6]. For data processing steps will be perform as folowing:

- Read data (*.stg, *.dat, *urf)
- Choose default settings (surface, borehole,….)
- Edit/Data Editing stistics (optional)
- Start Inversion
- View/Data Misfit Histogram to remove some data (optional)
- Start Inversion again after removeal of some noisy data
- Change settings
- View Inverted resistivity section
- Change Min/Max cour intervals
- Change vertical exaggeration factor
- Save image
- Save data in XYZ format
- Print image

In order to simply perform for data processing, it was done as shown in diagram (Figure 2. 12).

Many researchers have applied 2D resistivity and induced polarization data analysis to identify zones of potentially useful groundwater. This combination of methods is attractive because the resistivity of the soil is principally controlled by the

electrical conductivity of the pore liquid, whereas induced polarization is strongly affected by processes at the liquid-grain interface. It can be appropriate to infer that the chargeability of aquifers is 1 to 2 ms whereas lower values may be due to water interaction in clayey soil, allowing the method to distinguish aquifers from water in clayey soil [11- 12, 16, 56, 60-61, 67, 70-71].

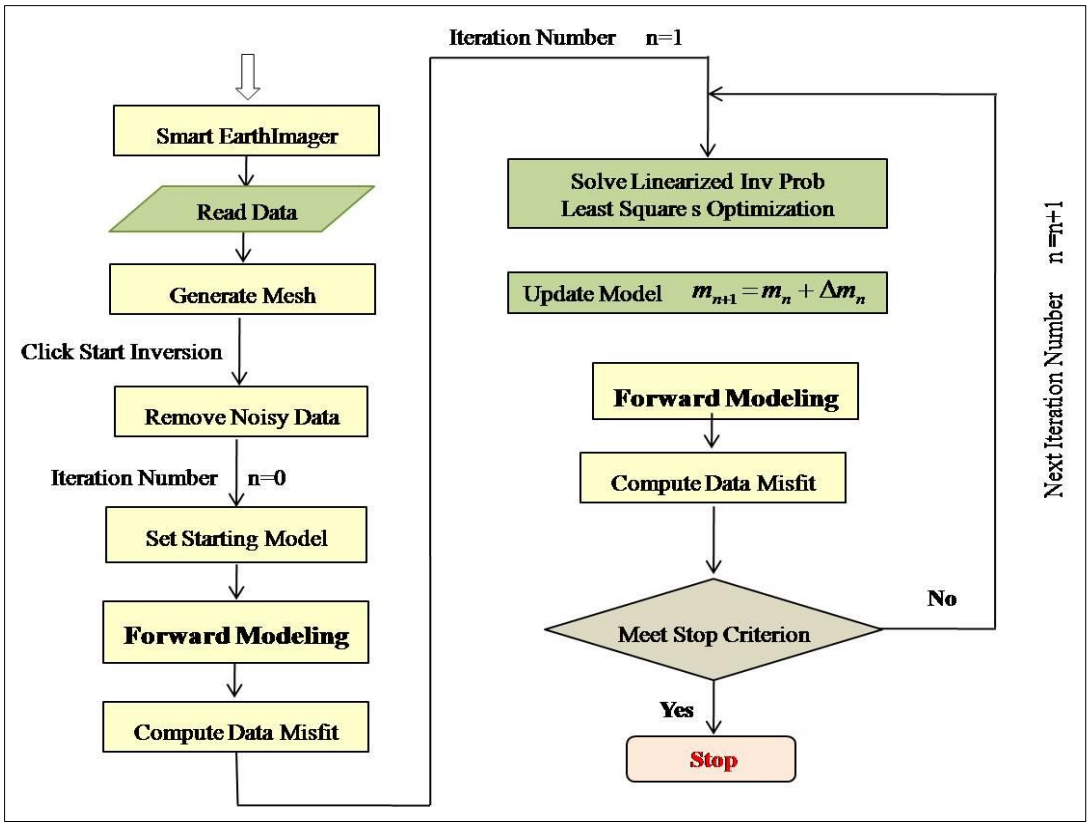

Figure 2.12. Diagram for inversion flow chart for EarthImager software [6]

The IMEE methods are more advantageous than the previous methods, the most prominent of which are: i) Build an (2D) improved multi-electrode arrays (abbreviated as MC array) to ensure easy 2D measurements; ii) The field data collection is fast and there is no data redundancy; iii) Data processing can use available software or a combination of its own program and available software depending on the research purpose; iv) Just using a certain array to collect data in the field, through processing and analysis by simple algebraic formulas, data of other

corresponding arrays can be obtained (including the improved Petrovski parameter with degree higher resolution). The limitations of this method are: This method has 02 options for data processing and analysis. With option 1 will have more accurate results with horizontal objects. As for option 2, there will be more accurate results with inclined or vertical surfaces. However, it has not been studied to be able to process and analyze the parameter ρ_{pm}^{ct} with EarthImager 2D software, so when the results are presented, they are not as expected.

2.5. BASIC THEORIES OF SEISMIC REFRACTION

2.5.1. Introduction

The seismic refraction method uses seismic energy that returns to the surface after travelling through the ground along refracted ray paths. The technique is normally used to determine refracting interfaces between layers of different seismic velocity, but the method is also applicable in cases where velocity varies smoothly as a function of depth or laterally. The vast majority of refraction surveying is conducted along profile which are arranged to be sufficiently long to ensure that refracted arrivals from target layers are recorded as first arrivals for at least half the length of the seismic profile. The seismic refraction profiles typically need to be between five and ten times as long as the required depth of investigation. The profile length required in any particular survey depends on the distribution of velocities with depth at that location. Refraction seismology is applied to a very wide range of scientific and technical problems, from engineering site investigation surveys to large-scale experiments designed to study the structure of the entire crust or lithosphere. The general assumptions relating to the ray path geometries considered below are that the subsurface is composed of a series of earth layers, separated by planar and possibly dipping interfaces. Also, within each layer seismic velocities are constant, and the velocities increase with layer depth. Finally, the ray paths are restricted to a vertical plane containing the profile [41].

The progressive positions of the wave front from a seismic source at A associated with energy travelling directly through an upper layer and energy critically

refracted in a lower layer. Direct and refracted ray paths to a detector at D, a distance *x* from the source (Figure 2.13)

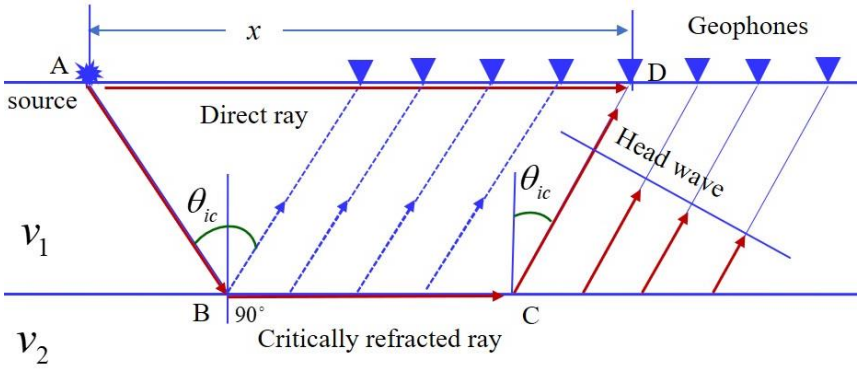

Figure 2.13. A Simplified diagram that shows seismic refraction ray parts for direct and refracted waves through a two-layer model [66]

The layer velocities are v_1 and $v_2\,(>v_1)$, and the refracting interface is at a depth *z*. The direct ray travels horizontally through the top of the upper layer from A to D at velocity v_1. The total travel time along the refracted ray path ABCD is given by the equation:

$$t = \frac{z}{v_1 \cos\theta} + \frac{(x - 2z\tan\theta)}{v_2} + \frac{z}{v_1 \cos\theta}$$

Regarding from Snell's law: $\sin\theta = v_1 / v_2$ and $\cos\theta = \left(1 - v_1^2 / v_2^2\right)^{1/2}$, the travel time equation is given in number of different forms, a useful general form being:

$$t = \frac{x}{v_2} + \frac{2z\cos\theta}{v_1} \tag{2.13}$$

We can rewrite equation (2.13) as following:

$$t = \frac{x}{v_2} + \frac{2z\left(v_2^2 - v_1^2\right)}{v_1 v_2} \tag{2.14}$$

Where, plotting *t* versus *x* (Figure 2.14), t_i is the intercept on the time axis of a travel-time plot or time–distance plot having a gradient of $1/v_2$. The intercept time t_i, is given by

$$t_i = \frac{2z\left(v_2^2 - v_1^2\right)}{v_1 v_2}$$

We can write travel time equation as new form.

$$t = \frac{x}{v_2} + t_i \tag{2.15}$$

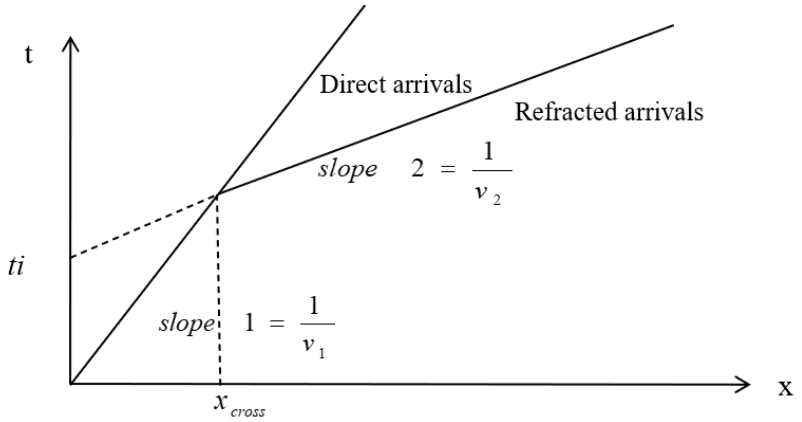

Figure 2.14. Travel-time curves for the direct wave and refracted wave from a single horizontal refractor.

In order to solve for refractor depth, it can be used by equation (2.16):

$$z = \frac{t_i v_1 v_2}{2z\left(v_2^2 - v_1^2\right)} \tag{2.16}$$

A useful way to consider the equations (2.13) to (2.15) is to note that the total travel time is the time that would have been taken to travel the total range x at the refractor velocity v_2 (that is x/v_2), plus an additional time to allow for the time it takes the wave to travel down to the refractor from the source, and back up to the receiver. The values of the best-fitting plane layered model parameters, v_1, v_2 and z, can be determined by analysis of the travel-time curves of direct and refracted arrivals:

• v_1 and v_2 can be derived from the reciprocal of the gradient of the relevant travel-time

• The refractor depth z, can be determined from the intercept time t_i.

At the crossover distance, x_{cros} the travel times of direct and refracted rays are equal:

$$\frac{x_{cross}}{v_1} = \frac{x_{cross}}{v_2} + \frac{2z\left(v_2^2 - v_1^2\right)}{v_1 v_2}$$

Thus, solving for the crossover distance, x_{cross}

$$x_{cross} = 2z\left[\frac{v_2 + v_1}{v_2 - v_1}\right]^{1/2} \tag{2.17}$$

From equation (2.17) it may be seen that the crossover distance is always greater than twice the depth to the refractor. The crossover distance equation (2.17) provides an alternative technique of calculating refractor depth *z*.

For multiple layered case we can apply the same process to determine layer thickness and velocity sequentially from the top later to bottom as following:

Head wave from top of layer 3, travel time equation is given in equation (2.18):

$$t = \frac{x}{v_3} + \frac{2z_1\sqrt{v_3^2 - v_1^2}}{v_3 v_1} + \frac{2z_2\sqrt{v_3^2 - v_2^2}}{v_3 v_2} \tag{2.18}$$

Thus, head wave from top of layer n, travel time equation is given as equation (2.19):

$$t = \sum_{j=1}^{n-1}\left(\frac{2z_j\sqrt{v_n^2 - v_j^2}}{v_n v_j}\right) + \frac{x}{v_n} \tag{2.19}$$

2.5.2. Seismic velocity

The seismic technique is based on a seismic wave's propagation in the subsurface which depends on the velocity variation in difference medium, but it is applicable in cases where velocity varies smoothly as a function of depth. The thickness and velocity of ground between an interface can be calculated by determining the arrival times for direct and refracted waves from seismic section. The velocities of longitudinal waves, P-wave, V_P and of transverse waves, S-wave, V_S in a homogeneous and isotropic medium are given by the equation (2.19). The factors affecting seismic velocity depend on their various compositions, textures (i.e., grain shape and degree of sorting), porosities and contained pore liquids, rocks differ in

their elastic moduli and densities (Table 2.3) shows seismic velocity value varies with mineral content, lithology, porosity, density and degree of compaction [41].

$$V_P = \sqrt{\frac{\lambda+2\mu}{\rho}} \quad \text{and} \quad V_S = \sqrt{\frac{2\mu}{\rho}} \tag{2.19}$$

Table 2.3. The P-wave velocity of various earth materials [41]

Materials	**P-wave velocity (m/s)**
Air	332
Water	1400-1600
Sandstone and shale	2000-4500
Limestone	2000-6000
Sand and gravel	500-1500
Shale	2000-4500
Alluvium	500-2000
Sand (dry)	200-1000
Sand (Saturated)	1500- 2000
Clay	1000- 2500

By virtue of their various compositions, textures, e.g., grain shape and degree of sorting, porosities and contained pore liquids, rocks differ in their elastic moduli and densities and, hence, in their seismic velocities. Information on the compressional and shear wave velocities, V_P and V_S, of rock layers encountered by seismic surveys is important for two main reasons: firstly, it is necessary for the conversion of seismic wave travel times into depths; secondly, it provides an indication of the lithology of a rock.

Factors affecting seismic velocity depend on their various compositions, textures (i.e., grain shape and degree of sorting), porosities and contained pore liquids, rocks differ in their elastic moduli and densities and their seismic velocities. A typical rock texture can be regarded as having mineral grains making up most of the rock, with the remaining volume being occupied by void space. The fractional volume of pore space is the porosity(f) of the rock. For simplicity it may be assumed

that all the matrix grains have the same physical properties. This is a surprisingly good approximation since the major rock-forming minerals, quartz, feldspar and calcite, have quite similar physical properties. The simplest case is for the density of a rock, where the bulk density ρ_b can be related to the matrix and pore liquid densities (ρ_m, ρ_f):

$$\rho_b = \rho_f \phi + (1-\phi)\rho_m \tag{2.20}$$

For P-wave velocity a similar relationship exists, but the velocity weighting is proportional to the percentage of travel-time spent in each component of the system, which is inversely proportional to velocity, giving the relationship:

$$\frac{1}{v_b} = \frac{\phi}{v_f} + \frac{(1-\phi)}{v_m} \tag{2.21}$$

From the above equations it is possible to produce cross-plot graphs (Figure 2.15) which allow the estimation of the matrix grain type and the porosity of a rock, purely from the seismic P-wave velocity and density. For S-wave velocity, the derivation of bulk velocity is more complex since S-waves will not travel through pore spaces at all. This is an interesting point, since it suggests that the S-wave velocity depends only on the matrix grain properties and their texture whereas while the P-wave velocity is also influenced by the pore liquids. In principle it is then possible, if both the P-wave and S-wave velocity of a formation are known, to detect variations in pore liquid [41].

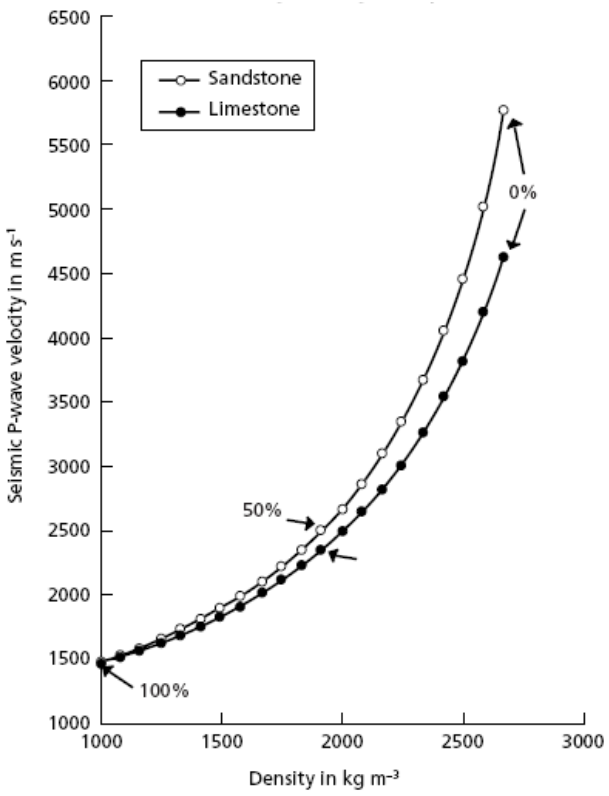

Figure 2.15. The relationship of seismic velocity and density to porosity, calculated for mono-mineralic granular solids: open circles – sandstone, calculated for a quartz matrix; solid circles – limestone, calculated for a calcite matrix [41]

The relationship between earth subsurface proprieties and body wave velocity has been studied for many years, as a means of indirectly characterizing porous aquifers. In existing literature, different approaches have been proposed some cases the water table is attributed to specific primary wave velocity (V_P) values. In the seismic refraction method, the magnitude of wave velocity values for the estimation of the depth of the aquifer has ambiguity for interpretation because a wide range of V_P values in connection to the water table level and these values are not uniquely correlated to the aquifer layer. Some authors attribute P-wave velocities around 1500 m/s to represent a saturated layer [34]. Meanwhile, another report proposes a P-wave velocity between 1200 and 1800m/s in porous aquifers [29].

2.5.3. Seismic data processing

The SeisImager software was performed for seismic refraction data interpretation in order to map subsurface geology in the thesis work. This software

has a system package for picking the first arrival time for P-wave known as the PICKWin program (Figure 2.16). This software uses nonlinear traveltime tomography consisting of ray tracing for forward modeling and simultaneous iterative reconstruction technique (SIRT) for inversion. The main features of the algorithm are: an initial model is constructed so that the velocity is layered and increased with depth, the first arrival traveltimes and ray paths are calculated by the ray tracing method based on the shortest path calculation and a traveltime between a source and a receiver is defined as the fastest traveltime of all ray paths. The velocity model is updated by SIRT and the seismic velocity of each cell is also updated during the process [8]. The flow chart of seismic refraction data processing (Figure 2.16) and the procedures in seismic refraction inversion processes are explained as flowing:

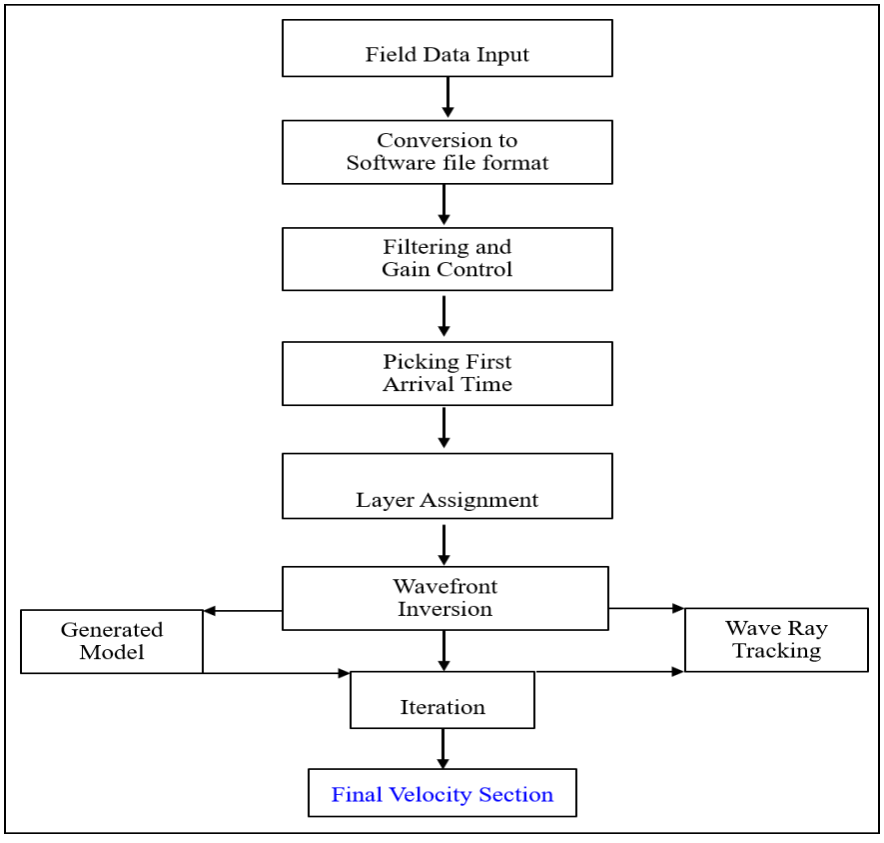

Figure 2.16. Flow chart of seismic refraction data processing [8]

- The field data file is based on readable file format of the software for the data analysis and processing.

- Gain control is conducted to the data to accentuate weak arrival times and other wavelets to improve the quality of the wavelet traces when to be picked.

- First arrival times are manually picked through visual inspection from collected time record on software like PickWin and saved for subsequent analysis (Figure 2.17).

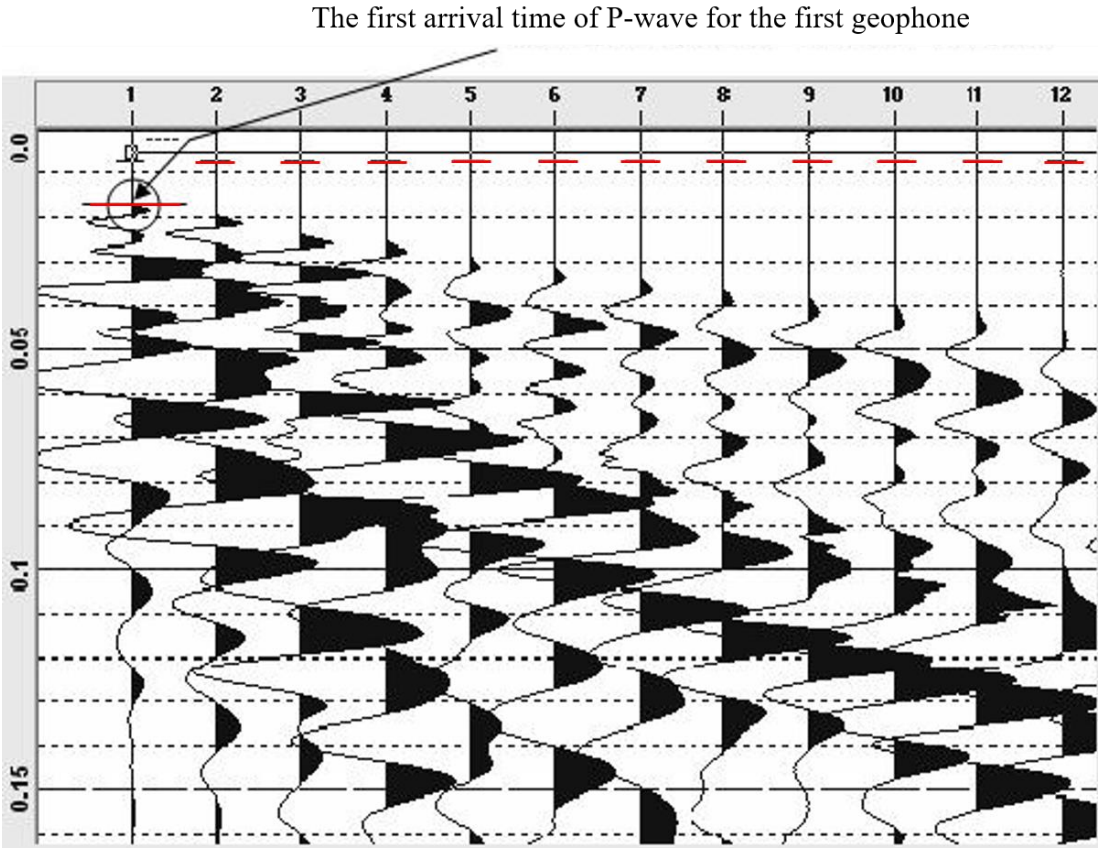

Figure 2.17. Example of picking first arrival times for one seismic spread

- A traveltime curve is generated through the layer assignment technique in interpretation model like Plotrefa (Figure 2.18).

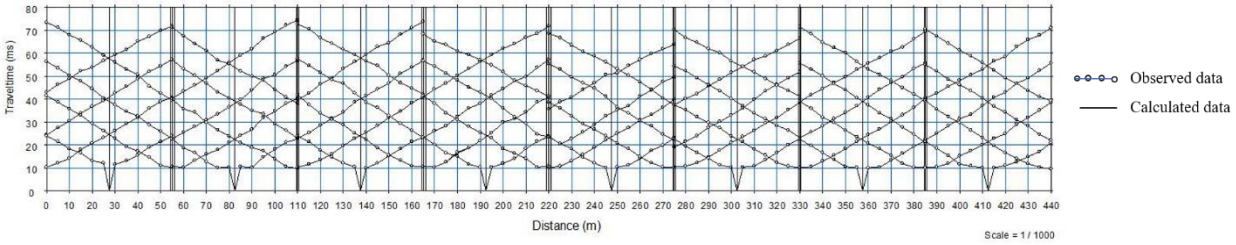

Figure 2.18. Example of the traveltime curves for seismic profile

- The model is divided into a large number of smaller constant velocity grid cells. The model is then inverted by performing ray tracing with the grid cells adjusted in an attempt to match the calculated traveltimes to produce a 2D initial velocity model.

- This is repeated until the number of pre-defined iterations within the software has been completed as the resulting final subsurface model or earth velocity model. The velocity model is inverted by performing ray tracing, via an initial velocity model and comparing the modelled traveltimes to field data, and adjusting the model grid-by grid in order to match the calculated traveltimes to the field data. This then generates the resulting subsurface velocity model also known as tomogram/inverted velocity model after the number of program predefined iterations has been completed (Figure 2.19).

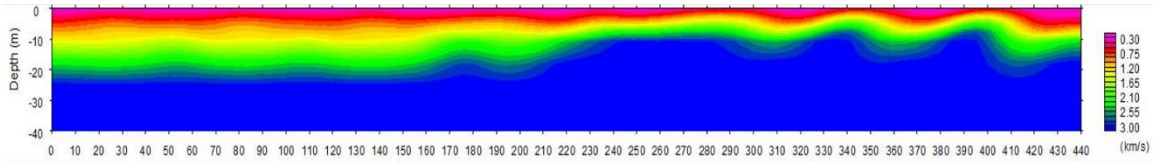

Figure 2.19. Example of velocity model for seismic profile

The advantages of the seismic refraction method are refraction observations generally employ fewer source and receiver locations and are thus relatively cheap to acquire. Meanwhile, because such a small portion of the recorded ground motion is used, developing models and interpretations is no more difficult than other geophysical surveys. While limitations of the seismic refraction method are refraction seismic only works if the speed at which motions propagate through the Earth

increases with depth. Refraction seismic observations are generally interpreted in terms of layers with the same velocities.

CONCLUSION OF CHAPTER 2

This chapter addressed methodology used in research work which consists of basis geophysical methods theory, geophysical data acquisition and geophysical data processing and interpretation as follows:

✓ The basic theories and principles of electrical and seismic refraction methods were explained in subsections that related to many purposes of different objectives of research work particularly groundwater investigation to obtain a reliable information based on all integrated geophysical methods to apply for groundwater investigation. These geophysical methods could provide concerning the relevant geological information such as the first concerns the aquifer geometry and the second concerns the parameters describing the groundwater quantity, including identifying fresh and saline groundwater by physical properties of earth subsurface such electrical resistivity or electrical conductivity and density of the earth subsurface.

✓ The designing of electrical and seismic refraction surveying like electrode arrays and geophone spacing were chosen during data acquisition are important in obtaining precise results based on the main objective of the research work. In this thesis, the Wenner electrode array was selected for 2D ERT data acquisition with manual electrode system whereas Dipole-Dipole electrode array was used for 2D IMEE data acquisition with multi-electrode system and 7 shot points were used for seismic refraction data acquisition.

✓ Geophysical data processing and interpretation used EarthImager 2D [6] for electrical resistivity and induced polarization data and used SeisImager software for seismic refraction data in order to analyze and process data to get the results of the geoelectric sections and seismic velocity models. The success in geophysical data processing and interpretation based on the understanding of the geological conditions, structural conditions and hydrogeological conditions in the three selected research areas.

✓ The simultaneous use of the multi-electrode electrical exploration and seismic refraction methods, especially for the first time using the improved multi-electrode electrical exploration method (both resistivity and induced polarization) to survey groundwater in Laos have complemented each other and increased the accuracy of research results.

CHAPTER 3
GROUNDWATER SURVEY RESULTS IN CENTRAL LAOS

3.1. GEOLOGICAL CHARACTERISTICS OF THE RESEARCH AREAS

Laos is located in mainland South East Asia, which is a landlocked country bordered by Thailand, Cambodia, Vietnam, Myanmar, and China. Laos has a population of approximately 7 million and land area of 236,800 km^2, the country extends intimately of 1,050 km from northwest to southeast. Flowing of the Mekong River from China and exiting through Cambodia into Vietnam, which is one of the largest rivers of the world. Mountains extend over the vast majority of the north of the country, and south wards along the border with Vietnam. The lowlands cover the central and southern part of the country from the Vientiane Plain, and along the Mekong River, towards Cambodia. The country is a topical monsoon climate, rainy season runs from May to October, a dry and cool season run from November to February and a hot dry season prevailing in March and April. The temperature varies from 5°C to 40°C depends on local regions. The country's average humidity varies between 87% in rainy season and 69% in hot dry season. Rainfall varied from 1300 mm to 3700 mm [78]. The geological information of Laos is a little known of the Asian regions whereas characteristic of geological subsurface is similar to the neighboring countries. Metamorphic rocks are considered to be Proterozoic outcrop, which found in some parts of the country can be summarized as follows:

During the Paleozoic 250 to 500 million years, deep waters that extended in a NW–SE axis along the Vietnamese border resulted in extensive sandstone and mudstone deposits. The mid-Carboniferous period (320 M.y.) was important striking and faulting along both the NW to SE and SW to NE directions that induced the current topography of the country. The Paleozoic sequences of sandstone, siltstone, limestone, and shale were deposited mainly in the Annamite range area and northern Laos. The Mesozoic era (65 to 250 M.y.) is characterized by important marine deposits, particularly in the south of Laos were shallow lagoon conditions created evaporite layers in some places [60-61, 86, 89]. These Mesozoic sandstones, of a

thickness of several hundred meters, constitute the Khorat Plateau found in Thailand that extends into Laos within lowland parts of Vientiane Plain, Vientiane, Savannakhet, and Champassak Basins. Basaltic lava flows, particularly in south of Laos in Champasack province let to the formation of the Volcanic Bolaven Plateau. On the other hand, the origin tectonics and erosion process created intra montane basins that were filled by freshwater alluvial sediments such as gravel, sands, silts, clays, and freshwater sandstones. These Tertiary and Quaternary deposits are found remarkably in the Vientiane Plain and in the south around Bolaven Plateau and occasionally along rivers in upland areas.

The three study areas were selected in the central part of Laos named Vientiane, Khammouane and Savannakhet Basins. The first study area is located in Vientiane Province whereas the second and third study areas are located in Savannakhet and Khammouane Provincees respectively. The three Basins were considered as a northwest extension of the Sakon Nakhon basin of the Khorat Plateau, Thailand. The Khorat Plateau covers an area of about 170 000 km^2 between latitudes 101° and 106° and longitudes 14° and 19° in the region of north-eastern Thailand and central Laos (Figure 3. 1). The plateau is mostly gently undulating, without extreme topography, and has an average elevation of about 200m.

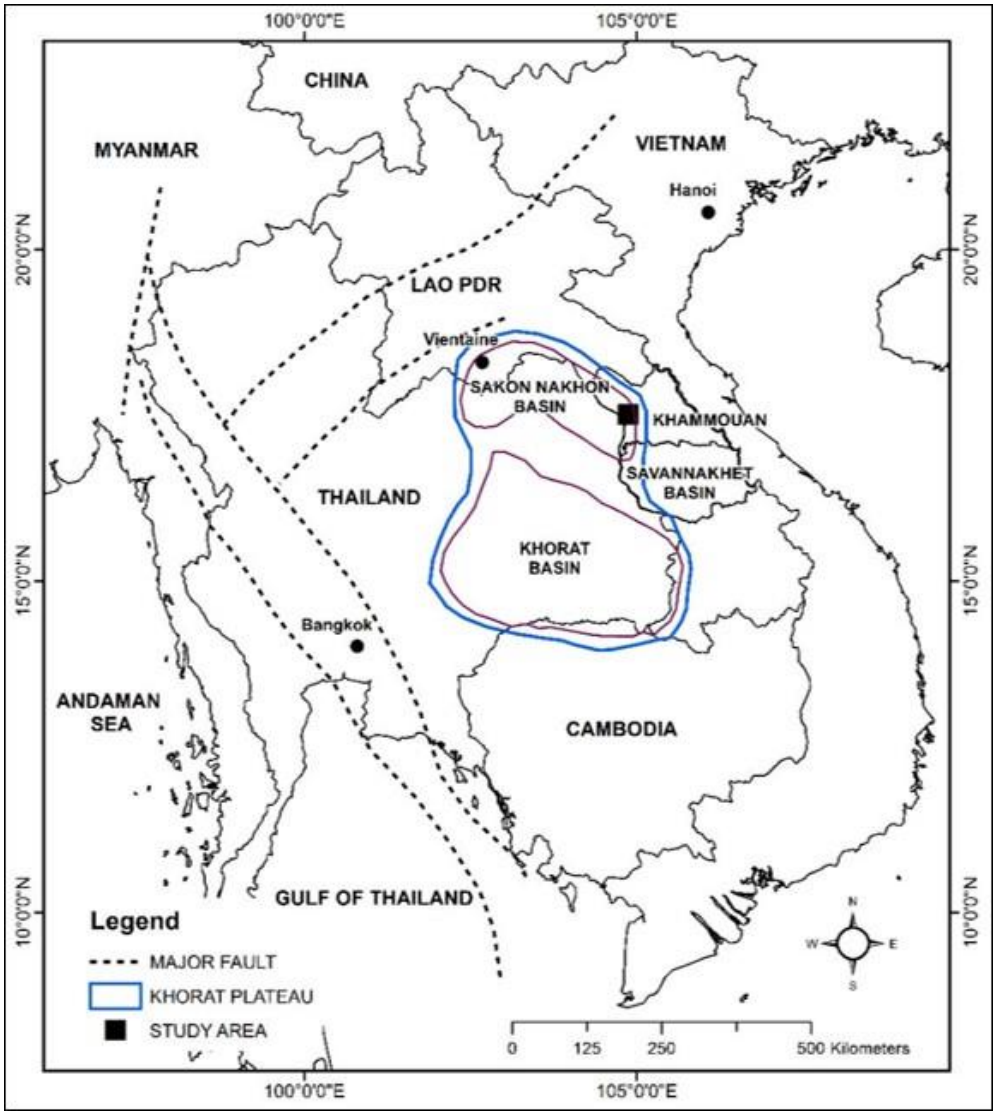

Figure 3. 1. Map of the Khorat and the SakonNakon basins on the Khorat Plateau, Thailand [25]

The PhuPhan range separates Khorat Plateau into two basins, namely the Khorat basin in the south covering an area of about 36,000 square kilometers and SakonNakhon basin in the north covering area of about 21,000 square kilometers [25, 35, 42, 89]. Laos has two main seasons, the rainy season, which runs between May to October, and the dry season, which runs from November to April [60]. Thus, it is necessary to conduct geophysical surveys to identify the saturated groundwater layers and groundwater information such the water table depth, the aquifers thickness, and the quality of groundwater in the research areas.

3.1.1. Vientiane Province

Vientiane province is located in the central Laos, it's far from Vientiane capital about 80 km. The landscape in Vientiane province varies from the flat, fertile alluvial plains of the Mekong River Valley to rugged limestone mountains in the northern and western part of the province. Vientiane province is well-known for the highest mountain peak of Phou Bia, 2,819 meters in Laos. The first selected study area is located in Phonhong and Thoulakhom districts, are located in the Vientiane Basin of Vientiane province, a large area of about 15,927 km^2 located in the central part of Laos with a population of ~ 419,090 people. Annual rainfall is around 2500 mm but is largely concentrated within the five-month-long rainy season. The flat lowlands, with elevations varying from 170 to190 meters above sea level, are flanked to the east and west by mountains covered by forests with elevations ranging up to 1600 m, and by the Mekong River to the south (Figure 3.2) [60].

The sedimentary rocks represented in the Vientiane Basin vary from Mesozoic to Cenozoic in age. The sedimentary rocks of the Mesozoic period consist of 5 main formations, from bottom to top, PhuLekPhai (T1-2pp), Nam Sait (T3ns), PhuPha Nang (J-Kpn), Champa (K2cp) and ThaNgon (K2tn) (Fig. 3.2). These formations were described as following: The first formation (T1-2pp) consists of sandstone, claystone, and lenticular conglomerates of the Middle Triassic age, with its thickness of around 650 m, while the second formation (T3ns) of same age as the first formation consists of sandstone with claystone, shale and sandstone with gypsum and coal, the thickness of this formation is between 700 and 850 m. The third formation consists of sandstone with micas with laminate sandstone of Jurassic to Cretaceous age, with the thickness of around 350 m. whereas both Champa (K2cp) and ThaNgon (K2tn) formations of Middle Cretaceous ages, which quartzite sandstone, siltstone with sandstone exist in (K2cp) formation, with the thickness of estimate 400 m. ThaNgon formation consists of sandstone, siltstone, conglomerate and halite of potassium and magnesium salts, the thickness of this formation is greater than 550 m. Quaternary sediments overlie these Mesozoic sediments that in the Vientiane Basin are located

along the valleys of the major rivers, which mainly consist of sand, gravel, clay and laterite [62].

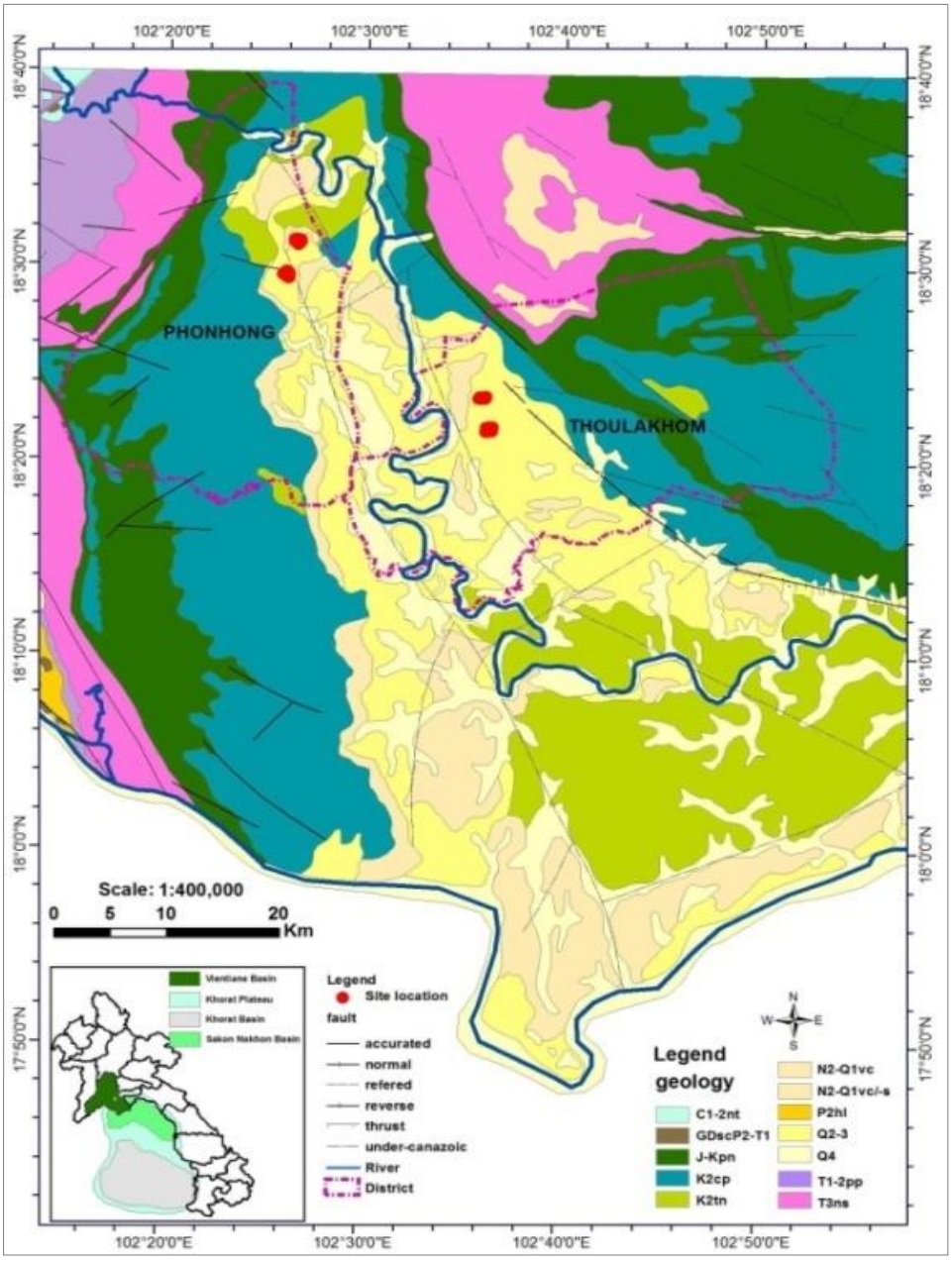

Figure 3.2. Geology of the Vientiane Basin [62], key map shows the extent of Khorat Plateau and the site locations [25]

The comparison between the stratigraphy of the Khorat Plateau and Vientiane Basin is explained in Table 1. The shallower geological units of the Vientiane Basin comprise alluvium such as sand, gravels and clays (Fig. 3.2). Porous

sandstone formations promote groundwater flow from the high-land to the low-land areas, and communities regularly encounter problems of insufficient yields from shallow wells in the high land areas. Problematic salt content of groundwater is encountered, especially in central Laos and northeast Thailand [85].

Table 3.1. Stratigraphy of Khorat Plateau [64] and Vientiane Basin [62].

Vientiane Basin, Laos				Khorat Plateau, Thailand		
Peroid	Thickness(m)	Lithology	Formation	Thickness(m)	Formation	Peroid
Quaternary	0.5		Quaternary Sediments (Q4:Q2-3)	4-40	Sediments(Qa)	Quaternary
	20-25					
	70		Vientiane (N2-Q1)			
Cretaceous	>550		Tha Ngon (K2tn)	50-785	Phu Thok(KTpt)	Cretaceous-Tertiary
				156-1294	Maha Sarakham (KTms)	
	400		Champa (K2cp)	100-350	Khok Kruat(Kkk)	Cretaceous
Jurassic-Cretaceous	350		Phu Pha Nang (J-Kpn)	120-150	Phu Phan(Kpp)	Cretaceous
				280-420	Sao Khua(Ksk)	
				50-136	Pra Wiharn(JKpw)	Jurassic-Cretaceous
Midle Triassic	700-850		Nam Sait (T3ns)	800-1100	Phu Kradung(Jpk)	Cretaceous
Early Midle Triassic	650		Phu Lek Phai (T12pp)	600-750	Nam Phong(Trnp)	Triassic

The main potash deposits can be found in two areas namely Vientiane and Khammouane sub-basins that are considered as extension parts of potash deposits, Thailand. [36]. The sandstone layers in the mountainous areas cannot recharge large quantities of groundwater and could not provide water supply in community from shallow wells in these areas. There is lack of acknowledgement of groundwater system to access the deeper aquifer systems. In additionally, there is found rock salt, rich potash, and gypsum deposits at shallow depth of about 25 to 50 m and are associated with a confining layer [13, 89].

3.1.2. Savannakhet Province

Savannakhet province is located in the Southern of Lao PDR. Savannakhet has a total area of 21,774 km^2, with a population of 125,760 in 2018. The second study area is located in Outhomphone district of Savannakhet province, Laos. The study area is situated in the northwestern part of the province with elevation between 175 to 200 m and most areas are covered by rice farm and forests. The annual rainfall is estimate 1780 mm, but it depends on regional parts [87]. The geology of eastern Savannakhet Province, extending further north to Thakhek and central Laos is considered similar to that of Northeast Thailand, as these areas all locate within the Khorat Plateau, a large saucer-shaped basin tilted to the east. The Plateau consists of Mesozoic and Tertiary aged sedimentary rocks known as the Khorat Group [86]. They reported that saline soils have recently been identified in parts of Laos, including in the Xe Champhone catchment, near Thakkek and in Vientiane Province, noting that the by evaporite beds and clastic sedimentary rocks of the Khorat Group are a source of salt found in groundwater and surface soils. Geology information of Savannakhet basins is similar geological information to the MahaSarakham Formation, which consist of claystone, shale, siltstone, sandstone, anhydrite, gypsum, potash, and rock salt [21, 38].

3.1.3. Khammouane Province

Khammouane province is a province in the center of Laos, covers an area of 16,315 km^2, with a population of ~ 392,052 people. The province is mostly of forested mountainous terrain. The vast forests of the Nakai-Nam Theun National Parkare an important watershed that feed many Mekong tributaries as well as form the catchment area for Nam Theun 2, the largest hydropowerproject in Laos. The third study was selected in Thakhek district of Khammouane province, far from 350 kilometers south of Vientiane capital with a population of ~85,000 people, located across the Mekong River from the Nakhon Phanom province, Thailand. Thakhek district cover area of about 980 km^2, with the Mekong River to the west and mountains to the east. The study area is one of the main tobacco producing areas of Laos. There are two major

operating mining companies in the Thakhek district namely Mining Development Economy Corporation mining gypsum and V.S.K. Co. Ltd mining limestone. The average annual rainfall during 2007 to 2011 was 2,350 mm and the average temperature was 26.7 °C [40]

The geology of Khammouane basin comprised of carbonate rocks of limestone, dolomitic limestone or dolomite lithology, which are hard, compact and pure. The Khammouane Formation is underlain by the sandstones of the early Carboniferous Boualapha Formation [63, 79]. During the Mesozoic Era the Khammouane Formation was covered unconformably by continental red beds of the early to middle Jurassic Ban Lao Formation, which in turn was covered by the red beds of the late Jurassic Nam Phouan and early Cretaceous Nam Xot Formations (Figure 3.3). The stratigraphic gap of the unconformity between the Paleozoic carbonates and Mesozoic red beds reaches up to 60 million years in central Laos. This gap in the sedimentary record indicates a long erosion period favorable to karst formation, before burial by the Mesozoic continental red beds created a paleokarst [63]. The geology in Thakhek district of Khammouane Basin, is mainly Carboniferous overlain by Permian limestone, a predominantly carbonific series composed of thick limestone beds with some intercalations of chert and shale beds. The limestone forms the cliffs and steep mountains. The Carboniferous causes high-hardness in groundwater [40].

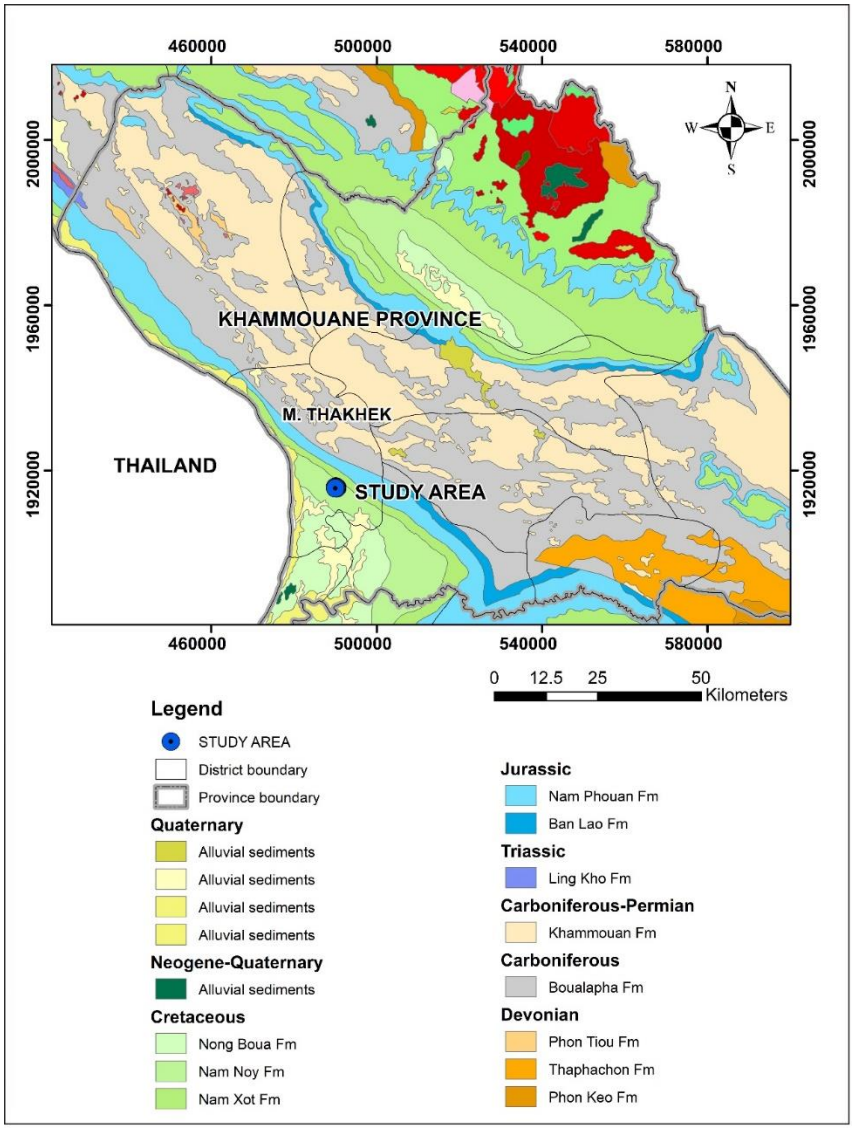

Figure 3.3. Detailed geology of the study region in Khammouan Province overlaid with the boundaries of the province and districts [79]

3.2. NETWORK OF SURVEY PROFILES AND USED GEOPHYSICAL METHODS

The various subsurface geophysical methods will be selected depends on the geological conditions and purposes of target surveying. In this research work, the 2D ERT, seismic refraction and improved multi-electrode electrical exploration, induced polarization methods were selected for groundwater investigation in three research areas of Laos. These geophysical methods, the measured parameters and the exist

contrast in physical properties of subsurface earth in the selected study areas are seen in the (Table 3.2).

Table 3.2. The surface geophysical methods and relevant physical properties [41]

Method	Measured parameter	Operative physical property	Study areas
Induced polarization	Polarization voltages	Electrical capacitance	Vientiane
Seismic refraction	Travel times of refracted seismic waves	Density and elastic moduli	Vientiane, Savannakhet Khammouane
Electrical resistivity	Earth resistance	Electrical conductivity	Vientiane, Savannakhet Khammouane

3.2.1. Vientiane Province

Ten electrical resistivity (numbered from 1 to 10) and three induced polarization (numbered 3, 4, 7) profiles were conducted at the four sites using the IMEE methods with the MC array presented above with 10 m electrode spacing and profile lengths of 550 m (Figure 3.4). Additionally, two boreholes were drilled on electrical resistivity profile 1 and 8 for verification comparison with geophysical results at Phonhong and Thoulakhom sites. Some of the important information that have been used include:

- Regarding field work: The number of electrodes used for each profile: 56; The total number of resistivity or induced polarization readings for each profile: 557; The measured error value is set on the unit to be 3% so the number of bad readings rejected for each profile is 1.

- Regarding the processing of data: The number of iterations used by the inversion software to obtain each resistivity or polarization profile is 3 to 8; The highest RMS error of the model reached at the last iteration was 12.57%; The inverse type used is the finite element method.

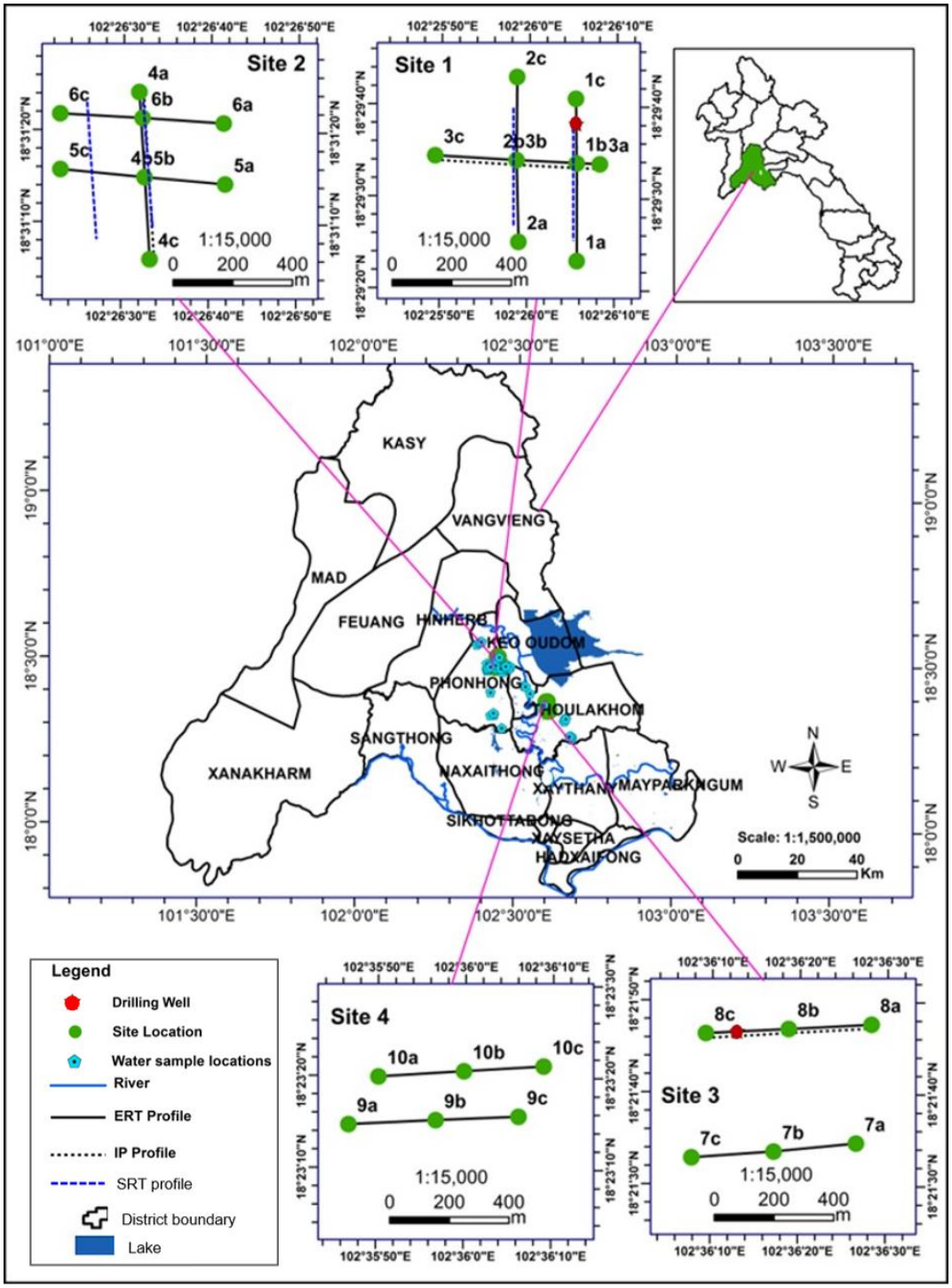

Figure 3.4. Map of geophysical survey profiles in Vientiane Province

The data were recorded by multi-electrodes system and automatically by using a SuperSting R8/IP system with 56 electrodes (Figure 3.5).

Figure 3.5. SuperSting R8/IP system with 56 electrodes and Switch box connection for IMEE data acquisition

The SmartSeis ST with 12 channels seismograph (Figure 3.6) was selected to use for seismic refraction data acquisition at the two study sites for 4 seismic profiles (Figure. 3.4), which seismic survey profile length of 440 m, with geophone interval of 5 m, and consists of 8 spreads for each seismic profile. The technique consisted of laying out 12 geophones in a straight line and recording arrival times from shot points produced by striking a 5kg sledge hammer into a steel plate at 7 shots per spread: one inter-spread shot, three forward and three reverse shots (Figure. 3.7).

Figure 3.6. Smartseis ST with 12 channels for seismic data acquisition

The seismographs setting for data acquisition for each profile at two sites are the same. The first geophones of spread 1 located at 0 m and the 12th geophone at 55 m; while the first geophone of spread 2 located at 55 m and the 12th geophone at 110 m then move to next spread until reach to the first geophone of spread 8 located at 385 m and the 12th geophone at 440 m. The geophone and seismic shot locations for the first seismic spread were shown details in Table 3.3.

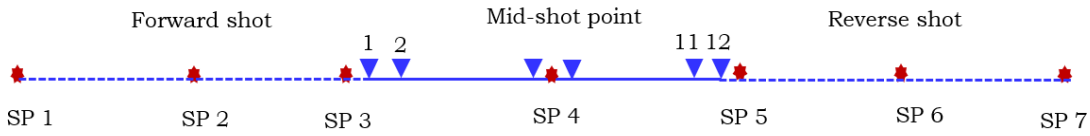

Figure. 3.7. A typical seismic refraction data acquisition layout and location of shot points for seismic refraction survey profile.

Table 3.3: The geophone and seismic shot for the first seismic spread

Geophone No.	**Location (m)**	**Shot No.**	**Shot location**
1	0	1	-44
2	4	2	-22
3	8	3	-1
4	12	4	22
5	16	5	45
6	20	6	66
7	24	7	88
8	28		
9	32		
10	36		
11	40		
12	44		

3.2.2. Savannakhet Province

The five ERT profiles were conducted in Outhomphone district of Savannakhet province, in which there are 4 profiles were oriented in the NE - SW directions, whereas another profile left was oriented in the NW - SE directions, maximum length of profile of 480m. The data were recorded by manually and automatically in the Terrameter ABEM SAS 1000 (Figure. 3.8). The Wenner electrode array was selected to conduct with electrode spacing of a=10 up to 160 m.

The two seismic refraction profiles were conducted at selected ERT profiles, used the SmartSeis ST with 12 channels seismograph. The two seismic refraction profiles were conducted on overlies on two selected ERT profiles (2 and 4) in the study area was presented (Figure 3.9), seismic profile length of 330 m, with geophone interval of 5m, and consists of 6 spreads for each seismic profile. In this measurement, consisted of laying out 12 geophones in a straight line and recording arrival times from shot points produced by striking a 6.5 kg sledge hammer into a steel plate at 7 shots per spread: one inter-spread shot, three forward and three reverse shots (Figure 3.7).

Figure 3.8. ABEM Terrameter SAS 1000 for 2D ERT data acquisition

The first geophones of the first spread placed at 0 m and the 12th geophone at 55 m; while the first geophone of the second spread located at 55 m and the 12th

geophone at 110 m then move to next spread until reach to the first geophone of the 6th spread placed at 275 m and the 12th geophone at 330 m. Additionally, two boreholes were drilled on ERT and seismic profiles 2 and 4 at the study area to match, demonstrate and complement the results of integrated ERT and seismic refraction methods.

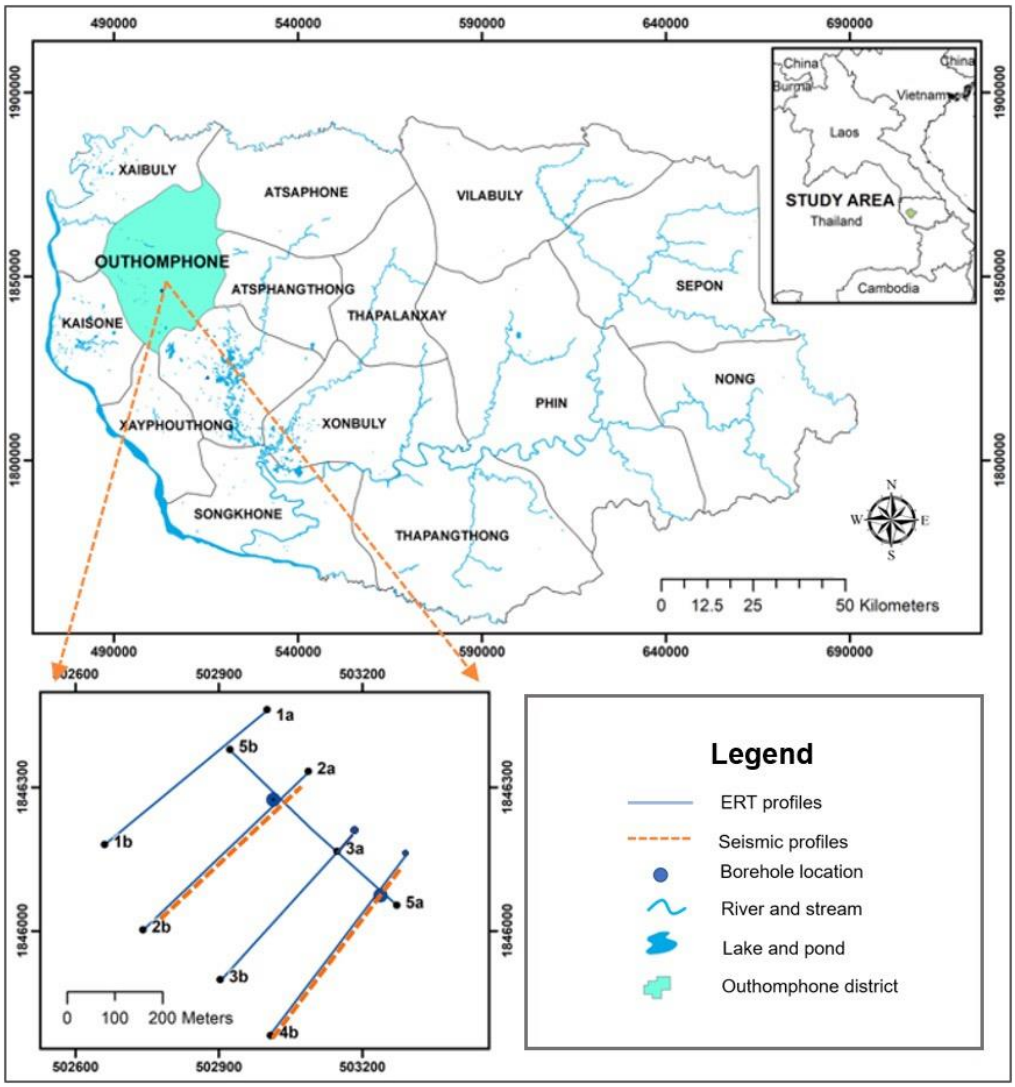

Figure. 3.9. Map of the ERT and SRT profiles in Savannakhet Province

3.2.3. Khammouane Province

The four ERT profiles were conducted in Thakhek district, in which there are three profiles were oriented in the W - E directions, another profile was oriented in the N - S direction, maximum length of profile of 480m (Figure 3.10). The Wenner

electrode array was selected to conduct with electrode spacing of a=10 up to 160 m. The data were recorded by manually and automatically in the Terrameter ABEM SAS 1000.

The three seismic refraction profiles were conducted at selected ERT profiles, used the SmartSeis ST with 12 channels seismograph. The three seismic refraction profiles were conducted on overlies on three selected ERT profiles (1, 2 and 4) in the study area was presented (Figure 3.10), seismic profile length of 352 m, with geophone interval of 4m, and consists of 8 spreads for each seismic profile.

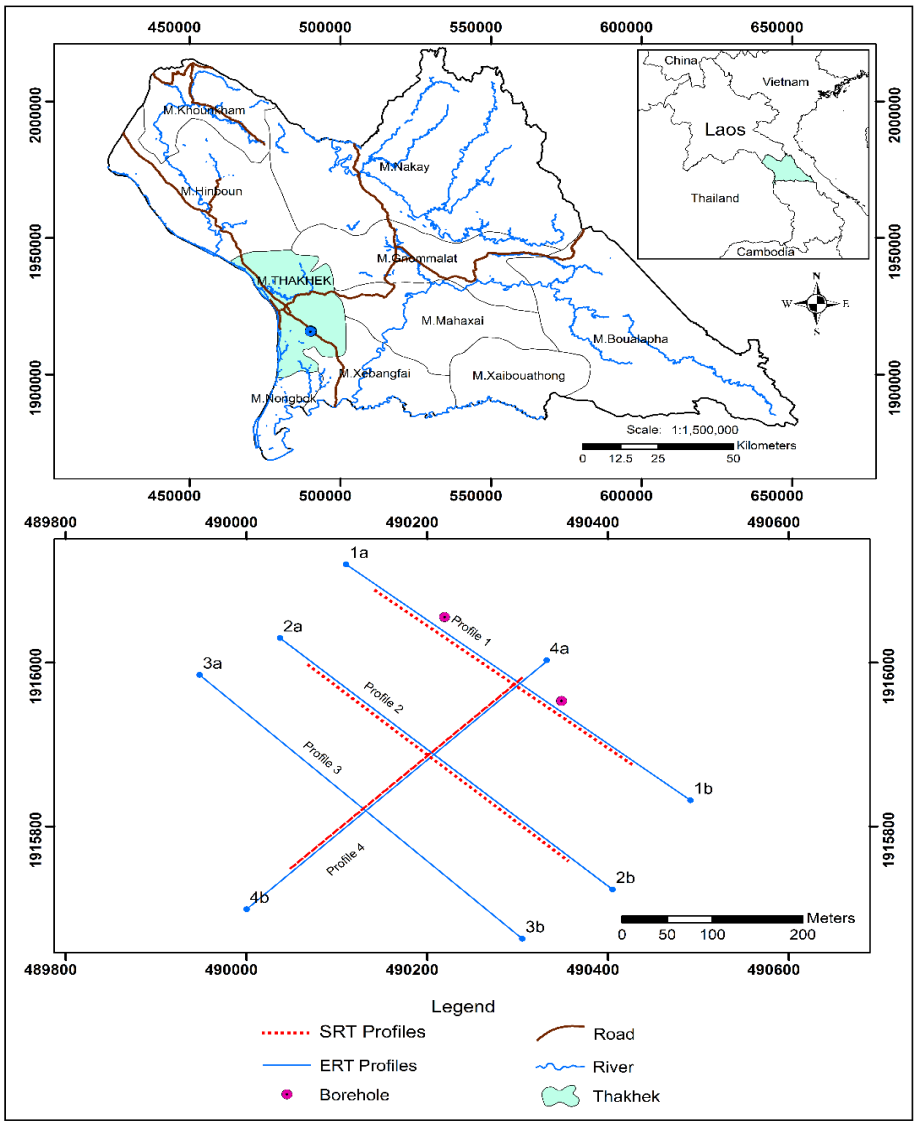

Figure 3.10. Map of the ERI and SRT profiles in Khammouane Province

In this measurement, consisted of laying out 12 geophones in a straight profile and recording arrival times from shot points produced by striking a 6.5 kg sledge hammer into a steel plate at 7 shots per spread: one inter-spread shot, three forward and three reverse shots (Figure 3.7). The first geophones of the first spread placed at 0 m and the 12^{th} geophone at 44 m; while the first geophone of the second spread located at 44 m and the 12^{th} geophone at 88 m then move to next spread until reach to the first geophone of spread 8 placed at 308 m and the 12^{th} geophone at 352 m. Additionally, two boreholes were drilled on ERT and SRT profile 1 at the study area to match, demonstrate and complement the results of integrated ERT and seismic refraction methods.

3.3. RESULTS AND DISCUSSIONS

3.3.1. Vientiane Province

✓ *For IMEE methods*

The results obtained on ten resistivity and three induced polarization profiles from IMEE methods showed that two parallel south-north transverse profiles showed similar results with regions of high resistivity greater than 150 Ohm.m at depths of up to 12 m. These are interpreted as sand and a clay top soil layer. The relatively low to moderate resistivities range from 5 to 18 Ohm.m at depths of 12 to 22 m are considered to be a thick saturated clay layer. However, moderately resistive regions from 18 to 80 Ohm.m are observed at depths of 22 to 70 m and extended downward in a deeper depth at profile 1 and some zones at profile 2, indicating possibly suitable areas for groundwater extraction (Figure 3.11) that correlated well with the previous studies on groundwater zones range from 22 m to 70 m in the Vientiane region [60]. While, found low resistivity values less than 18 Ohm.m at depths of 70m to bottom layers are interpreted as thick clay layers of the profile 2.

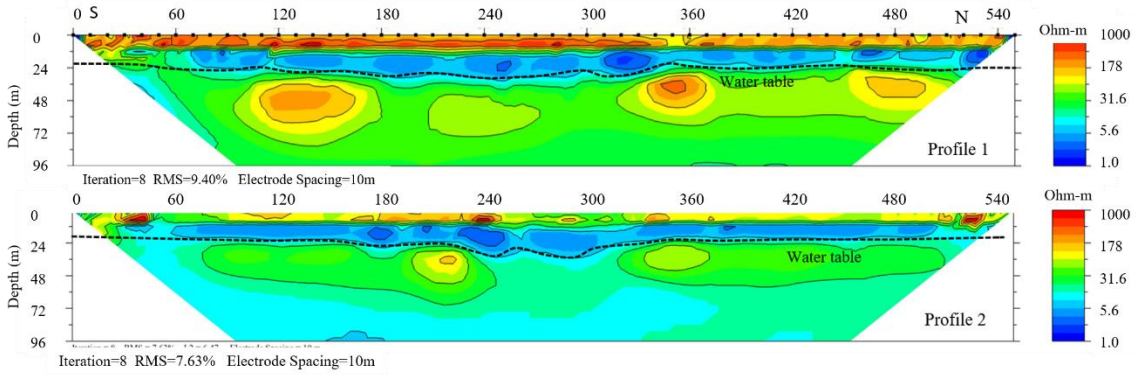

Figure 3.11. 2D Resistivity cross sections under profiles 1 and 2 at site1

Regarding to the obtained geoelectrical cross-sections of geoelectrical profiles 1 and 2 at site 1 in the Phonhong district, the moderate resistivity values from 18 to 80 Ohm.m have been found at a depth of 22 to 24 m, so it is determined at this depth to be groundwater surface or water table because it is suitable for the resistivities range of fresh groundwater varies from 20-160 Ohm.m in Table 2.1 [66].

In order to compare with electrical resistivity results, one borehole VBH-1 was drilled at the profile 1 for matching the positions of water table or aquifers layers (Figure 3.12 a, b). The obtained results from the borehole VBH-1 indicated the water table at around 22 m depth at profile 1. The soil samples collected from the borehole was classified as gravel and siltstone at water table level (Figure 3.12 b), which respond well with resistivity regions of 18 to 80 Ohm.m at depth of 22m (Figure 3.12 a).

The obtained results of this resistivity cross section indicated that RMS error between the measured field data and the theoretical model of 9.40% for the first resistivity profile. The results of this resistivity cross section agree well with data from borehole VBH-1 drilled in the Phonhong district, which indicated the location of the water table at 22 m depth where samples extracted from the drill cores have been identified as gravel and siltstone.

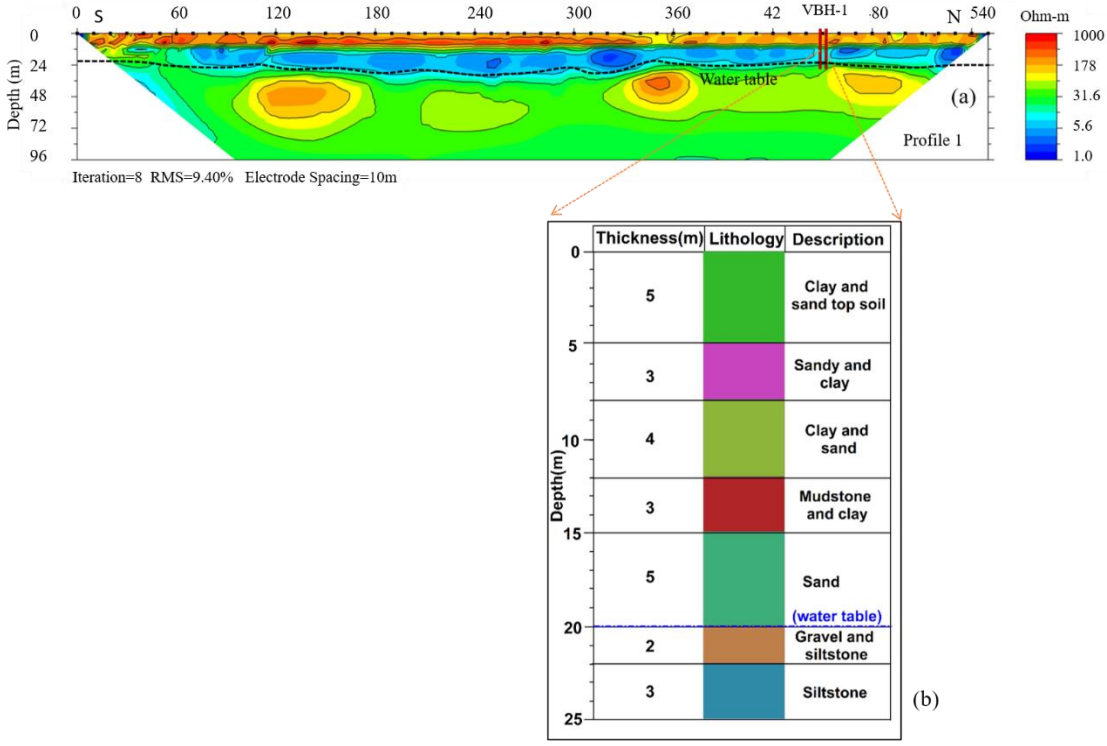

Figure 3.12. (a). 2D Resistivity cross sections under profiles 1 at site1; (b). Vertical geological section under borehole VBH-1 at 450m on profile 1

The different geological formations observed from the borehole VBH-1 stratigraphy data matched well with the resistivity results (Table 3.4).

Table 3.4: Comparison between drilling results at borehole VBH-1 and results of IMEE model

Drilling results at borehole VBH-1		**IMEE results at profile 1**		
Depth (m)	**Stratigraphy**	**Depth (m)**	**Resistivity (Ohm.m)**	**Stratigraphy**
0-5	Clay and sand top soil	0-12	>150	Clay and sand top soil
5-8	Sand and clay			
8-12	Clay and sand			
12-15	Mudstone and clay	12-22	5-18	Sandy clay
15-20	Sand			
20-22	Gravel and siltstone			

	(watertable)			
22-25	Siltstone	22-70	18-80	Gravel and siltstone (Water tale, aquifers)

In order to verify the existence and position of earth layers at site 1, a third profile (profile 3) was oriented crossing the two parallel profiles (1 and 2) in a west to east direction, with points at 78 m and 280 m along profile 3. High resistivity and chargeability regions, greater than 150 Ohm.m and less than 40 ms, at depths up to 12 m are interpreted as a sandy clay top soil layer. The relatively low resistivity and high chargeability regions, 5 to 18 Ohm.m and 40 to 160 ms, at depths of 12 to 24 m are considered to be a thick saturated clayey layer. Moderate resistivity and low chargeability vary from 18 to 80 Ohm.m and 0 to 21 ms respectively were found at depths of 24 to 70 m, indicating suitable areas for groundwater. However, found low resistivity values less than 18 Ohm.m and high chargeability values greater than 100 ms at depths of 70m to bottom layers are considered as thick clay layers of this profile (Figure 3.13).

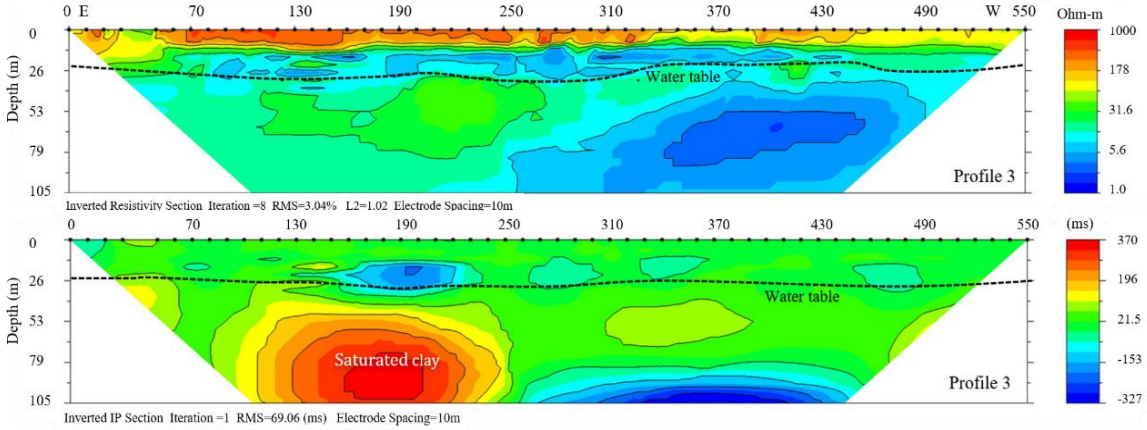

Figure 3.13. 2D Resistivity and IP cross sections under profile 3 at site1

Similarly, as at site 1, profile 4 at site 2 was oriented north to south, cutting though two parallel profiles (profiles 5 and 6) with crossing points 87 m and 285 m along profile 4. High resistivity and chargeability regions greater than 150 Ohm.m and less than 10 ms, at depths of up to 12 m are interpreted as a sandy clay top soil

layer. The relatively low resistivity and chargeability regions from 5 to 18 Ohm.m and 29 to 100 ms respectively, at depths of 12 to 24 m are interpreted as a thick saturated clay layer. As at site 1, the moderate resistivity and low to high chargeability regions from 18 to 80 Ohm.m and 0 to 29 ms at depths of 24 to 70 m, indicate possible suitable areas for groundwater. However, found low resistivity values less than 18 Ohm.m and high chargeability values greater than 100 ms at at depths of 70m to bottom layers are considered as thick clay layers of this profile (Figure 3.14).

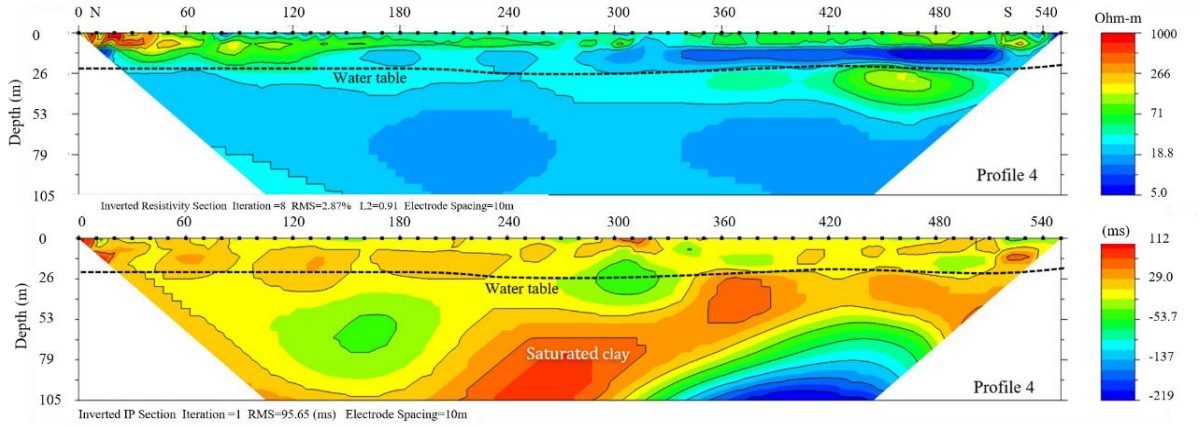

Figure 3.14. 2D Resistivity and IP cross sections under profile 4 at site2

Two parallel east-west profiles (5 and 6) at site 2, show similar results (Figure 3.15) with high resistivity regions of greater than 150 Ohm.m at depths up to 12 m, interpreted as a sand and clay top soil layer. The relatively low vary from 5 to 18 Ohm.m resistivity regions at depths of 12 to 24 m are interpreted as a thick saturated clayey layer. Along these two profiles moderate resistivities vary from 18 to 60 Ohm.m at depths from 24 to 70 m, indicate possibly suitable areas for groundwater. However, found low resistivity values less than 18 Ohm.m at at depths of 70m to bottom layers are considered as thick clay layers of the both profiles (Figure 3.15).

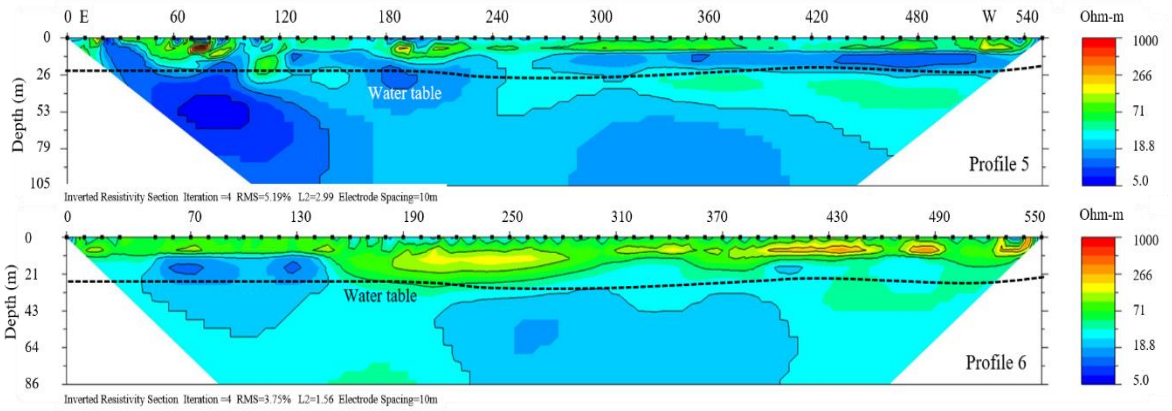

Figure 3.15. 2D Resistivity cross sections under profiles 5 and 6 at site 2

Profile 7 at site 3 was situated parallel with profile 8 in east to west direction (Figure 3.16). The inverse resistivity and IP models show high resistivity greater than 50 Ohm.m and chargeability regions of 50-100 ms at depths up to 12 m, interpreted as a sandy clay top soil layer. The relatively low resistivity less than 5 Ohm.m and chargeability greater than 100 ms at 12 to 95 m depth are considered to be a thick saturated clay layer.

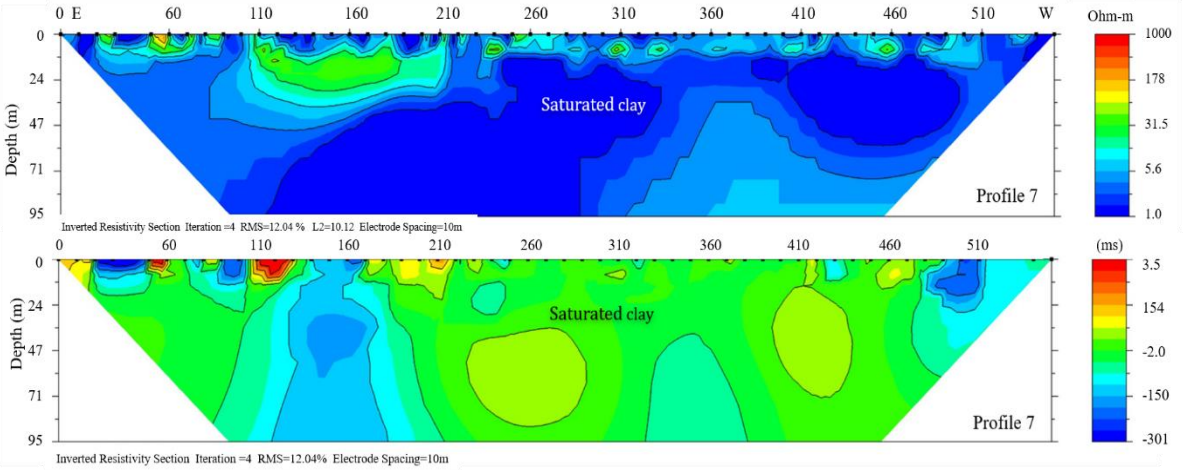

Figure 3.16. 2D Resistivity and IP cross sections under profile 7 at site 3

Similarly, results from profile 8 (Figure 3.17 a) show high resistivity regions of greater than 50 Ohm.m at depths up to 12 m, interpreted as a sand and clay top soil layer, underlain by a thick saturated clay layer with relatively low resistivities of less

than 5 Ohm.m at depth of 12 to 95m. The results at this site do not indicate the presence of a zone suitable for groundwater extraction.

The drilling results verified that did not found water table at this borehole, which correlated well with resistivity results. The geological information on the soil profile (Figure 3.17b). The different geological formations were identified by comparing the resistivity regions to the borehole lithology (Table 3.5).

Table 3.5: Comparison between drilling results at borehole VBH-2 and results of IMEE model

Drilling results at borehole VBH-2		**IMEE results**		
Depth (m)	**Stratigraphic**	**Depth (m)**	**Resistivity (Ohm.m)**	**Stratigraphic**
0-5	Clay and sand top soil	0-12	>50	Clay and sand top soil
5-13	Siltstone			
13-18	Sand	12-95	<5	Clay and mudstone
18-21	Clay and siltstone			
21-25	Clay and mudstone			

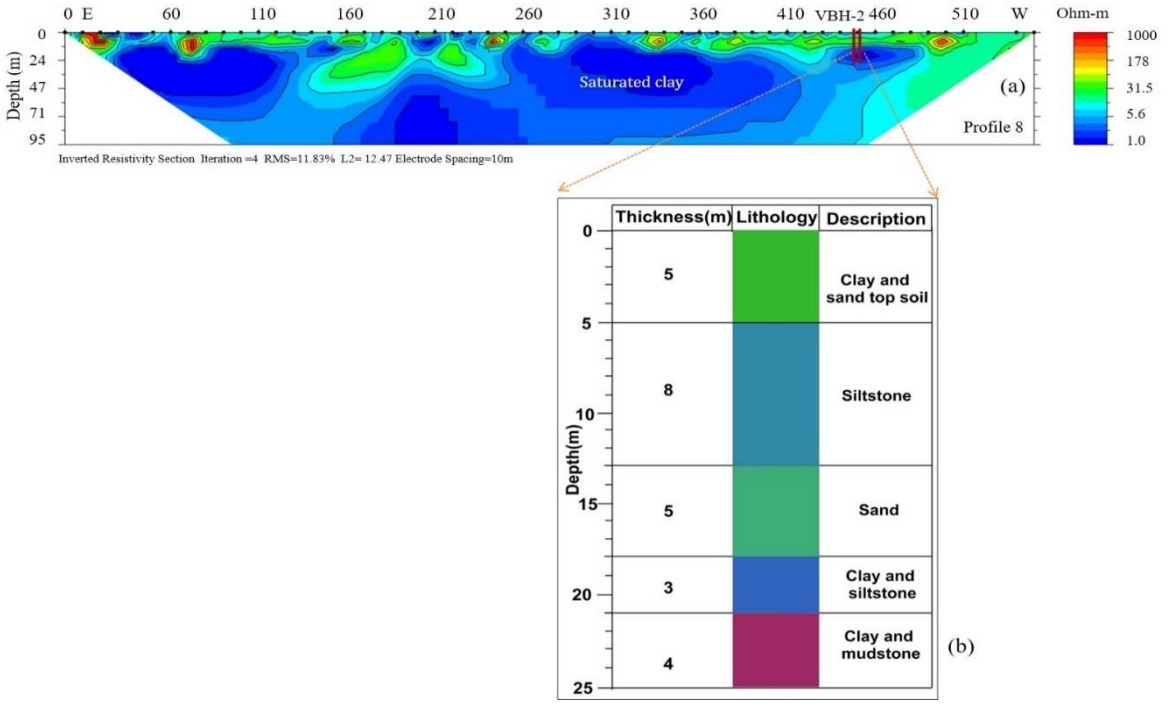

Figure 3.17. (a). 2D Resistivity cross sections under profile 8 at site3
(b). Vertical geological section under borehole VBH-2 at 450m on profile 8

Similarly, inversion of resistivity data from two parallel profiles, 9 and 10 (Figure 3.18) at site 4, shows high resistivity regions of greater than 50 Ohm.m at depths up to 12 m, interpreted as a sand and clay top soil layer, with relatively low resistivity of less than 5 Ohm.m at depth of 12 to 95m considered to indicate a thick saturated clayey layer, indicating it's not a suitable area for groundwater extraction.

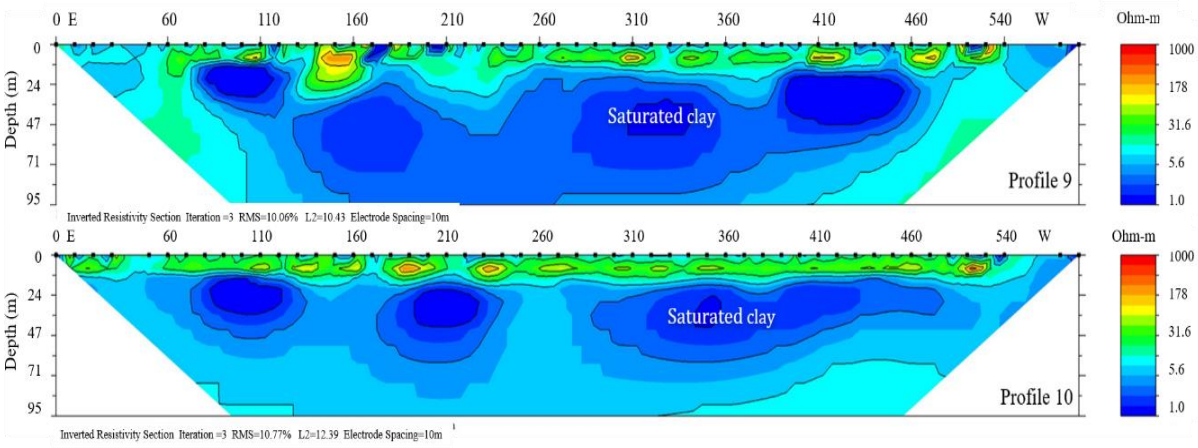

Figure 3.18. 2D Resistivity cross sections under profiles 9 and 10 at site 4

The thirteen water samples were collected from different existing deep wells and the new drilled test boreholes in the first study area in order to measure physical properties such as Total dissolved solids (TDS), Electrical conductivity (EC) and potential of hydrogen (pH). Each water sample was measured for three physical properties such as TDS, EC and pH. The results of measurement from these water samples compared with standard values based on World Health Organization (WHO) and United State Environmental Protection Agency (USEPA) advice a maximum level of 500mg/l for TDS. A TDS level greater than 1000mg/l, EC level greater than 2500 $\mu S/cm$, and pH level greater than 9.0 are generally considered to indicate water unfit for human consumption [74, 84].

The observed TDS values range from 30 to 860 mg/l with the mean value 287.69 mg/l, i.e., lower than the contamination threshold (Figure 3.19). In additional, the Electrical conductivity (EC) of water is strongly related to salt concentration, the

European Union directive on water quality sets an upper limit of 2500 $\mu S/cm$ for the electrical conductivity of drinking water.

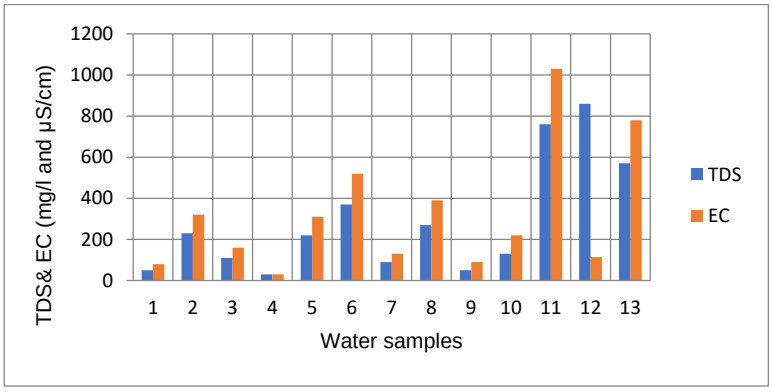

Figure 3.19. Distribution of physical properties (TDS and EC) from 13 water samples in existing shallow wells

The observed EC values range from 30 to 1030 $\mu S/cm$ with the mean value is 321.08 $\mu S/cm$. The observed pH values range from 6.5 to 8.3 with the mean value of pH is 7.4. Therefore, TSD, EC and pH values from different existing wells and the drilled test boreholes in the study area indicate levels below the contamination thresholds (Figure 3.19 and 3.20).

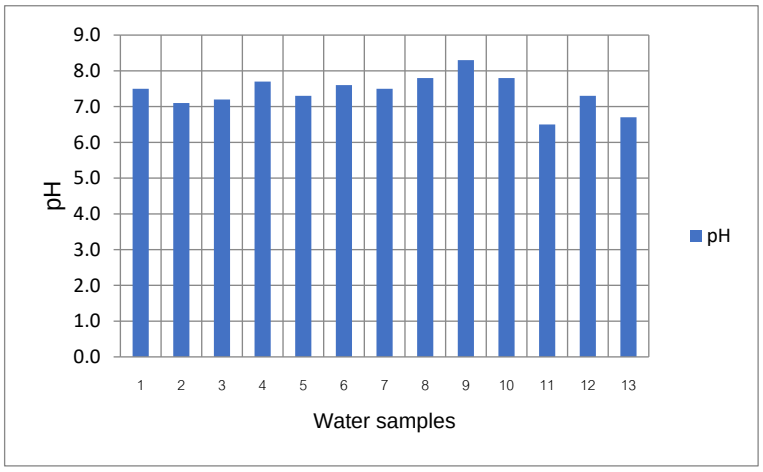

Figure 3.20. Distribution of physical properties (pH) from 13 water samples in existing shallow wells

✓ *For seismic refraction method*

The results obtained from the seismic refraction data analysis in the two sites revealed these regions can be categorized as a three earth layers with the velocity of

each layer increasing with depth in the composition of the earth subsurface. Two parallel south to north transverse seismic profiles namely profile 1 and 2 at sites 1 showed similar result. The traveltime curves and velocity models are shown in the (Figures 3.21 and 3.22).

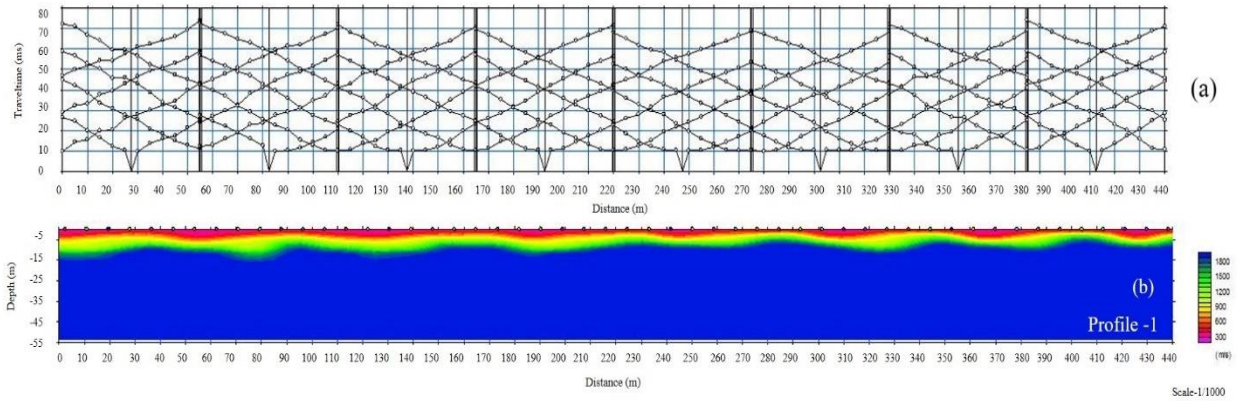

Figure 3.21. (a) The traveltime curves; (b) velocity model for seismic profile 1at site 1

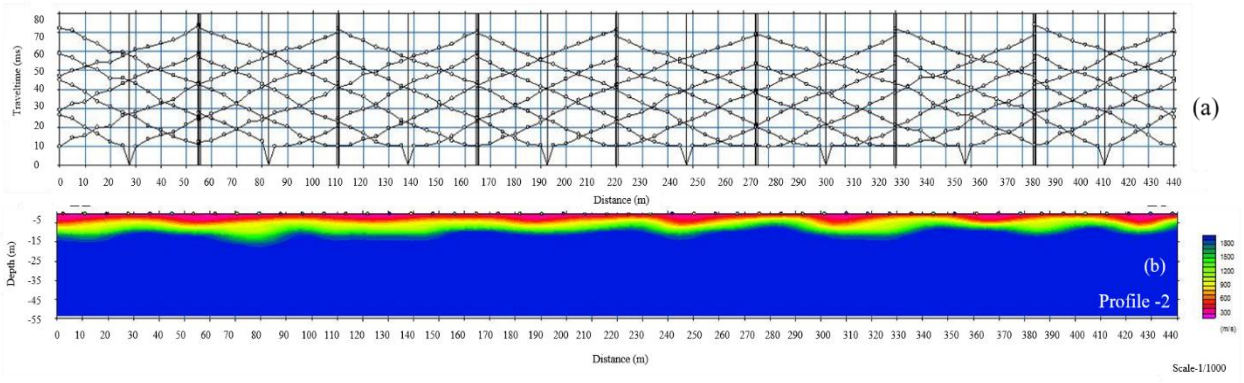

Figure 3.22. (a) The traveltime curves; (b) velocity model for seismic profile2 at site 1

The P-wave velocity of topmost layers, where lowest seismic velocities ranging from 300 to 700 m/s with an average velocity of 500 m/s were detected, corresponds to an area within the sand and clay top soil which is mainly as dry alluvial sediments, whereas the thickness of the first layers range from 0 to 5 m. The second layers found the yellowish green colours and seismic velocity vary from 700 to 1500 m/s with an average of 1100 m/s, corresponds to an area which is mainly thick saturated clayey layer and the thickness of the second layers range between 5 m to 15

m. The third layers found blue colours and seismic velocity range from 1500 to 2000 m/s with an average of 1750m/s, corresponds to an area which is mainly gravel and siltstone with the depth from ground surface to the third layer is greater than 15 m indicating suitable areas for groundwater zones. It is clear when we compare the velocity with that of water or saturated sand materials (Table 3.6)

Meanwhile, two parallel north to south transverse seismic profiles namely profile 3 and 4 at site 2 showed similar results. The traveltime curves and velocity models are shown in (Figure 3.23 and 3.24). The P-wave velocity of topmost layers, where lowest seismic velocities ranging from 300 to 750 m/s with an average velocity of 525m/s were detected, corresponds to an area within the sand and clay top soil which is mainly as dry alluvial sediments, whereas the thickness of the first layers range from 5 to 10 m. The second layers made up of the yellowish green colours and seismic velocity ranges from 750 to 1650 m/s with an average of 1200 m/s were detected, corresponds to an area which is mainly thick saturated clayey layer and the thickness of the second layer ranges between 10 to 20 m. The third layers made up blue colours and seismic velocity range from 1650 to 2100 m/s with an average of 1875 m/s were detected, corresponds to an area which is mainly gravel and siltstone with the depth from ground surface to the third layer is greater than 20 m indicating suitable areas for groundwater zones.

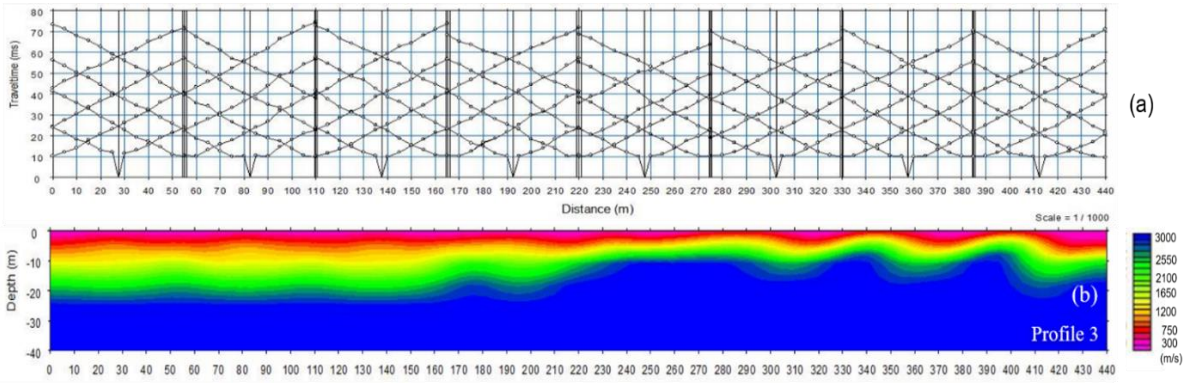

Figure 3.23. (a) The traveltime curves; (b) velocity model
for seismic profile 3 at site 2

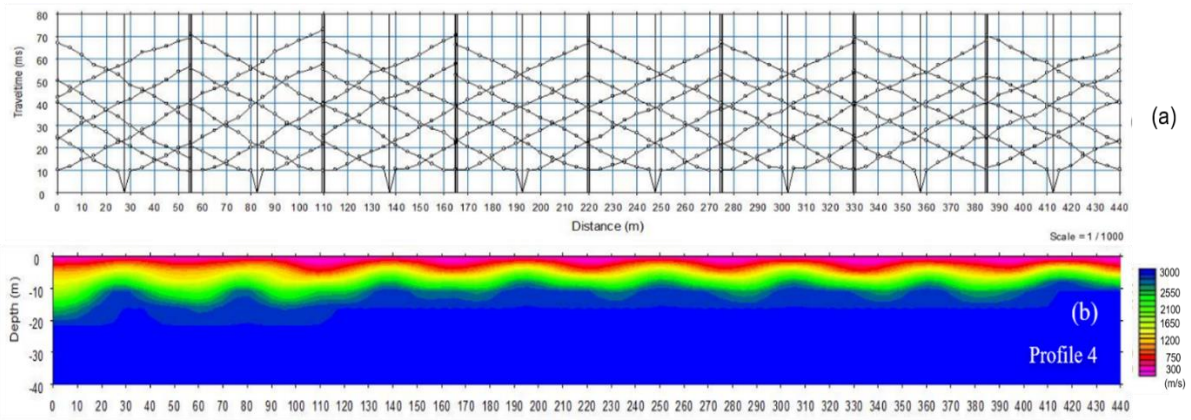

Figure 3.24. (a) The traveltime curves; (b) velocity model
for seismic profile 4 at site 2

The results of seismic refraction technique found the depth of the main aquifer ranges from 20 to 25 m that respond well with Magnetic Resonance Sounding and Vertical Electrical Sounding at three areas namely Xaythani (Thangon), Thoulakhom and Phonhong districts of Vientiane Basin [60]. The results from the MRS measurements show that the aquifer thickness ranges from 10 to 40 m and the depth of the main aquifer ranges from 5 to 15 m. The free water content is up to 30% and the decay times vary between 100 and 400 ms, suggesting a mean pore size equivalent to fine sand to gravel while the resistivity of the aquifers is highly variable but is usually higher than 10 Ohm.m suggesting that the water is fresh.

Meanwhile, determining water quality parameters of aquifers in the Vientiane basin, Laos used geophysical and water chemistry data [56]. The results found water layers are identified with the main water layer situated between 13 and 30 m in depth with no water below. From the VES models it becomes clear that the low resistive layer of 3 Ohm.m starts between 34 to 37 m, which is an indication that this layer is most likely clay (Figure 3.25). In additionally, drilling found the water table at a depth of 20-22 m in Phonhong district. Soil samples collected from this depth have been identified as gravel and siltstone, matching the velocity model result. The detailed soil profile is included in Figure 3.25 b. The different geological formations observed from the borehole VBH-1 stratigraphy data matched well with the seismic results (Table 3.6).

Table 3.6: Comparison between drilling results at borehole VBH-1 and seismic results of seismic velocity model

Drilling results at borehole VBH-1		**Velocity model results at profile 1**		
Depth (m)	**Stratigraphy**	**Depth (m)**	**Velocity (m/s)**	**Stratigraphy**
0-5	Clay and sand top soil	0-10	300-750	Clay and sand top soil
5-8	Sandy and clay			
8-12	Clay and sand			
12-15	Mudstone and clay	10-20	750-1650	Sandy clay
15-20	Sand			
20-22	Gravel and siltstone (Water table)			
22-25	Siltstone	>20	1650-2100	Gravel and siltstone (Water table, aquifers)

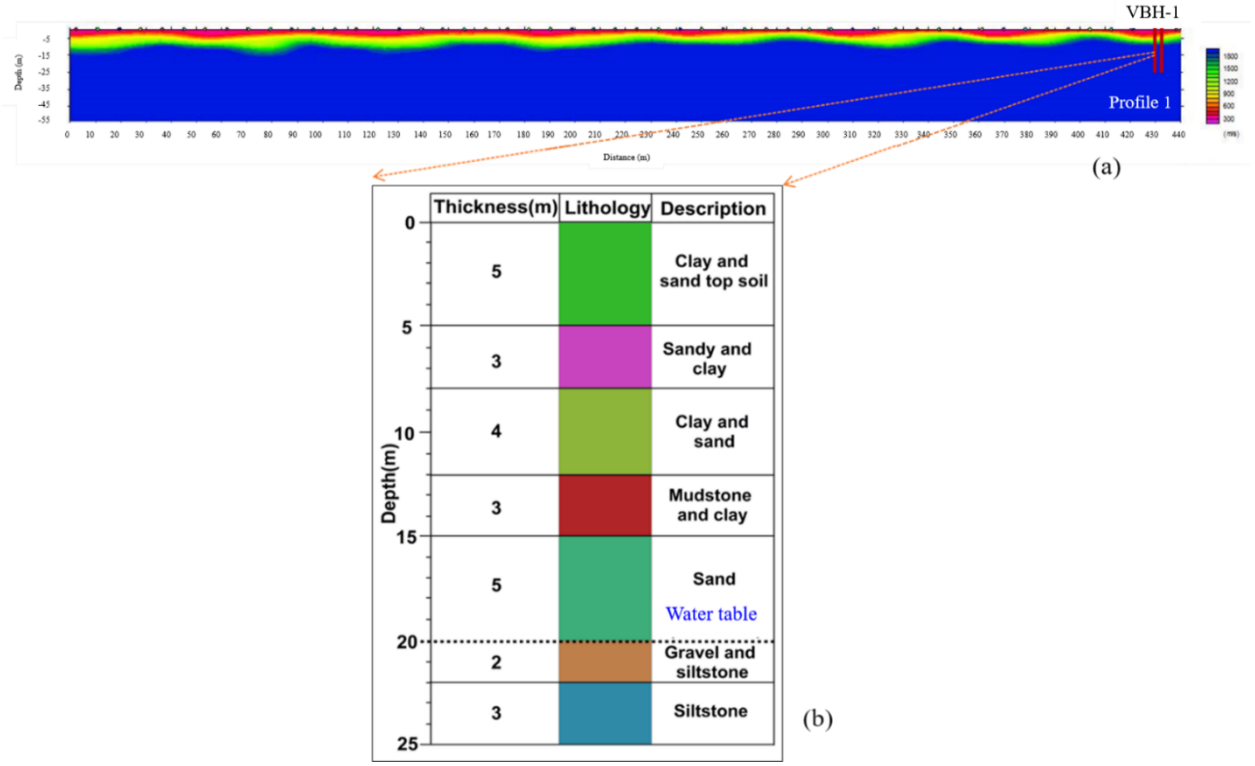

Figure 3.25. (a) Seismic velocity model under profile 1 at site1 and (b) Vertical geological section of borehole VBH-1 at 440 m along profile 1

Integrated seismic and drilling results at seismic profile 1 where is Naxou village, which correlated well with vertical electrical sounding at site S19 [60], indicated that found water table range from 15 to 30m with average seismic velocity around 1875m/s is considered as gravel and siltstone aquifers in research sites. According to the seismic exploration results, the thickness of all three layers of site 2 at Phonhor village is larger than that of site 1 at Naxou village. It means that the aquifer layer (N2Q1) at site 2 is thicker than that at site 1(Figure 3.26).

In short, according to the obtained geoelectrical cross-sections in Vientiane province, the thickness of the aquifer or groundwater zones is from 22 to 70m, which agreed well with the previous studies on the groundwater zones in the Vientiane region [60]. While, found low resistivity less than 18 Om-m and high chargeability greater than 100 ms at depths of 70m to bottom layers in some places on several profiles (see details above) are considered as thick clay layers of obtained specific cross-section.

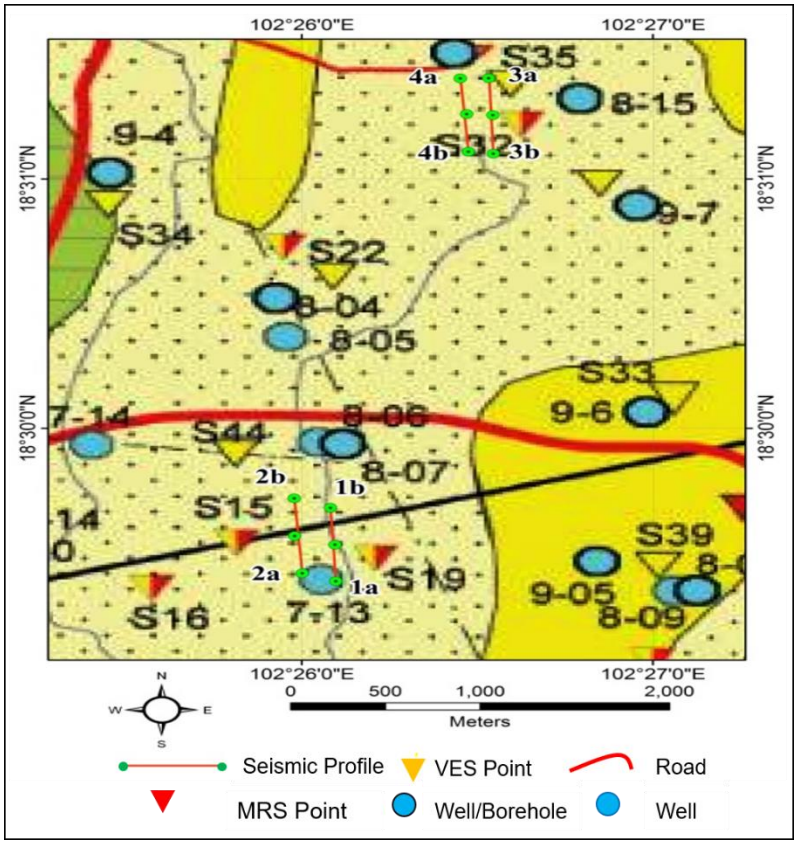

Figure 3.26. Location of the orientation of seismic refraction survey profiles compared with geophysical sites [60]

3.3.2. Savannakhet Province

Four parallel NE - SW oriented profiles (1, 2, 3 and 4) at the study area showed similar results (Figure 3.27). High resistivity regions greater than 100 Ohm.m found at 15-80 m depth along these profiles with unclear thickness are considered as sandstone or bedrocks layers of these profiles. The relative low resistivity regions less than 10 Ohm.m appear at some zones for each profile with unclear thickness are considered to be a thick clay zone. However, moderate resistivity values of 15 to 60 Ohm.m are observed at 16 to 80 m depth along these profiles are interpreted to be appropriate groundwater zones.

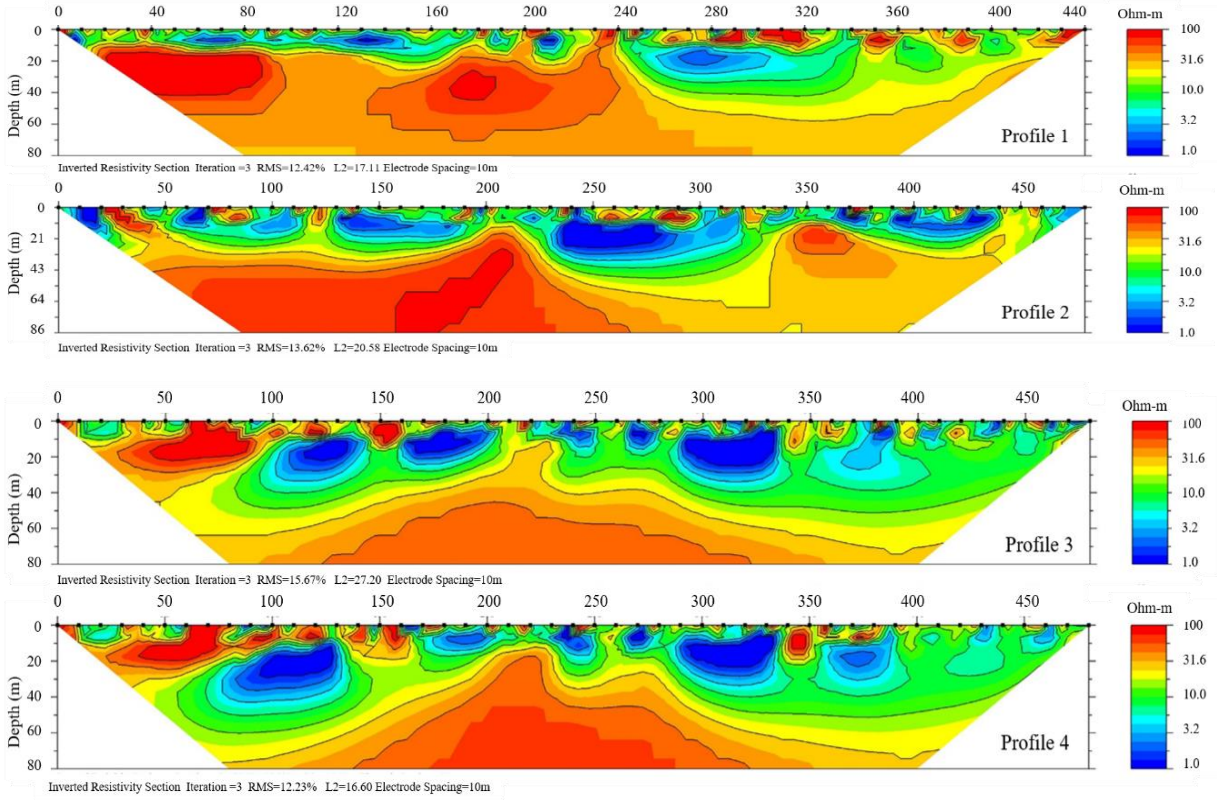

Figure 3.27. 2D resistivity cross sections at profiles 1, 2, 3 and 4.

In order to correlate the positions of the earth subsurface layers in research site, a fifth profile (profile 5) was arranged crossing the two parallel profiles (2 and 4) in an ES - WN direction, with crossing points of profiles 2 and 4 at 60 m and 330 m respectively (Figure 3.28). High resistivity values greater than 100 Ohm.m found at 10 to 80 m depth, distances between 0 and 160 m at the depths of unclear, is considered as sandstone or bedrocks layers of the profile. The relative low resistivity regions less than 10 Ohm.m appear at some zones for this profile with unclear thickness are considered to be a thick clay zone. However, moderate resistivity regions of 15 to 60 Ohm.m are observed at 18 to 80 m depth along these profiles are interpreted to be suitable groundwater zones.

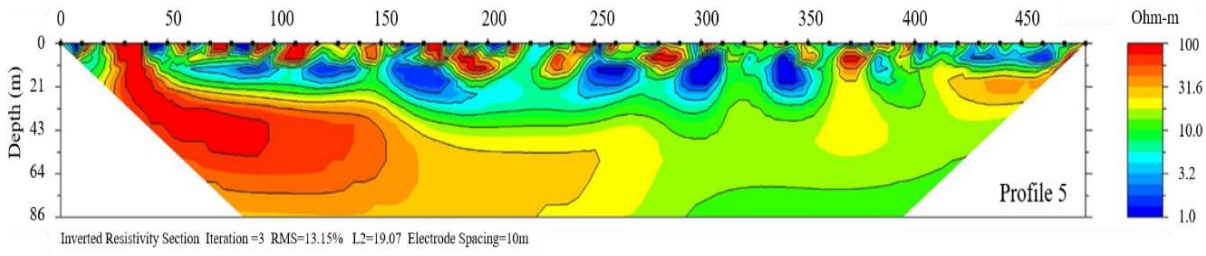

Figure 3.28. 2D resistivity cross section at profile 5.

In additionally, two seismic refraction profiles (1 and 2) were conducted at over lied on selected ERT profiles (2 and 4), the starting point of seismic profile located at 55 m of ERT profiles while the end of seismic profile located at 385 m of ERT profile (Figure 3.29). The results of both two seismic profiles (1 and 2) were well correlated with 2D geoelectric cross section of ERT profiles 2 and 4. The ERT and seismic results show moderate resistivity values of 15 to 60 Ohm.m and seismic velocity range from 1200 to 1800 m/s are considered to be the water table at depth of about 16 to 20m. The low resistivity regions less than 10 Ohm.m and seismic velocity range from 800 to 1200 m/s are interpreted to be a thick clay zone with unclear thickness, whereas high resistivity regions greater than 100 Ohm.m and seismic velocity greater than 1800 m/s are interpreted as sandstone or bedrocks subsurface earth layers.

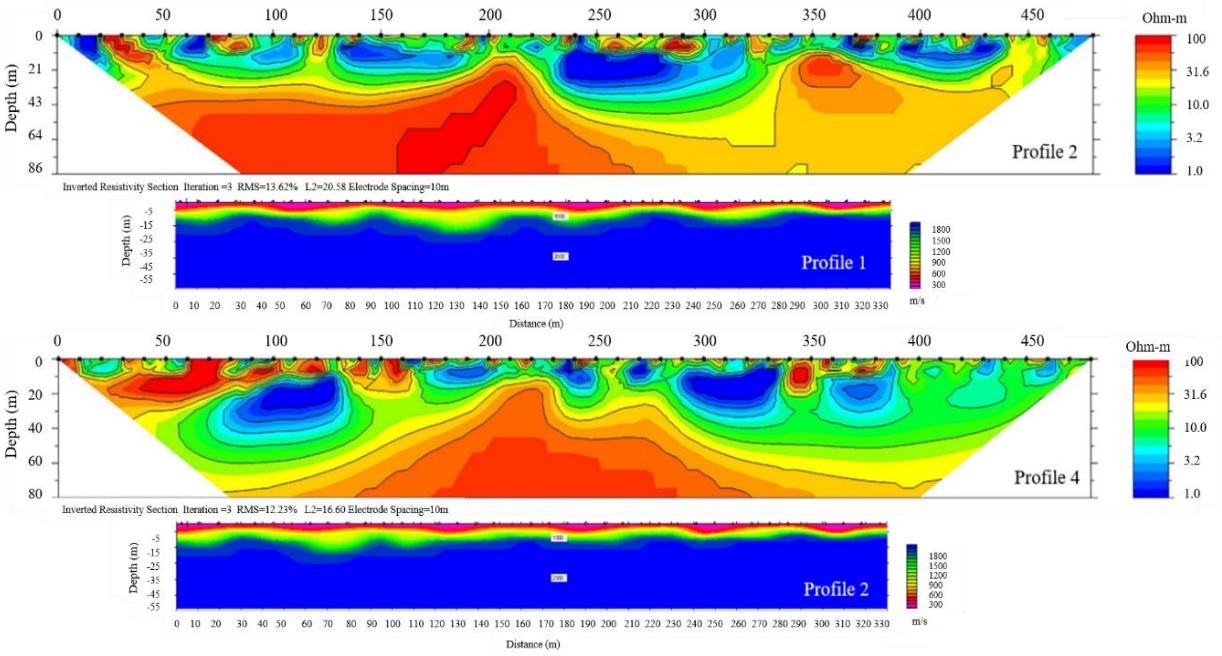

Figure 3.29. 2D geoelectric cross sections at profiles 2 and 4 versus seismic velocity models at profiles 1 and 2.

In order to match electrical resistivity and seismic results, two boreholes were drilled at these profiles for verifying the positions of water table or aquifers layers (Figure 3.30a, b, c and Figure 3.31a, b, c). The obtained results from the borehole SBH-1 and borehole SBH-2 showed the water table at about 16 m depth for borehole SBH-1 and 20 m depth for borehole SBH-2. The soil samples collected from both two boreholes have been classified as sandstone and siltstone at water table level (Figure 3.30c and 3.31c), which respond well for electrical resistivity regions of 15 to 60 Ohm.m (Figure 3.29a and 3.30a) and seismic velocity range from 1200 to 1800 m/s were identified for groundwater zones (Figure 3.30b and 3.31b).

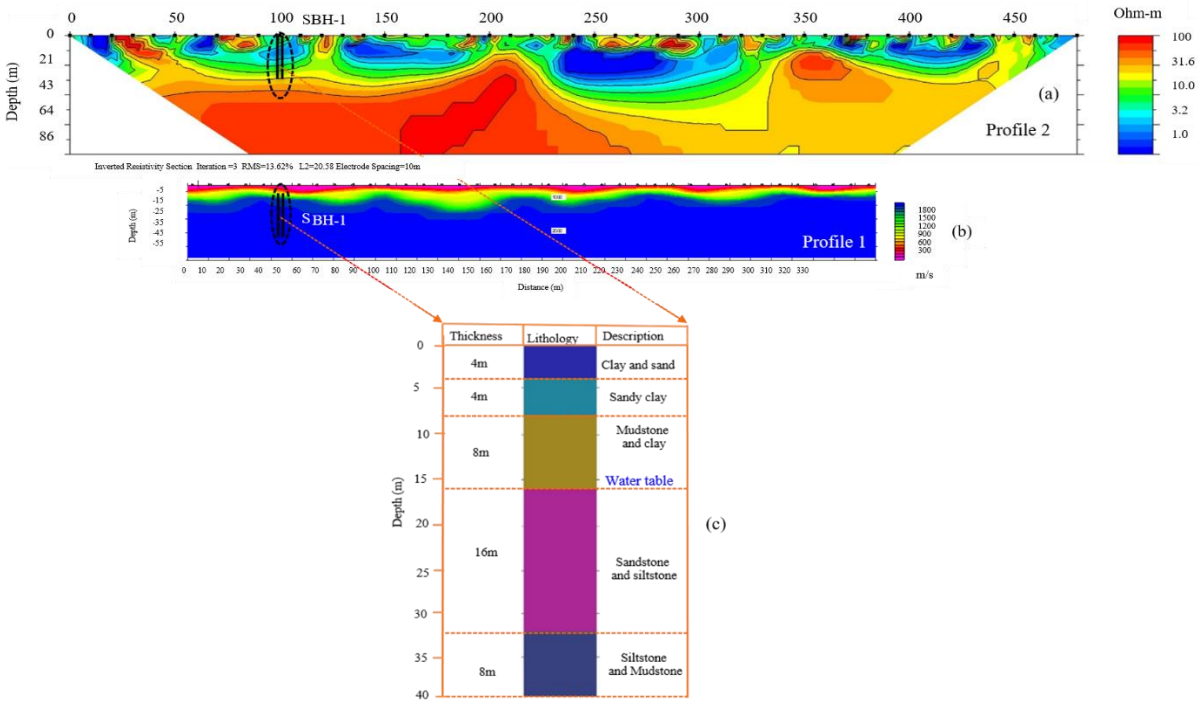

Figure 3.30. (a) 2D geoelectric cross section at profile 2; (b) The seismic velocity model at profile 1; (c) Vertical geological section of borehole SBH-1 at 100 m along ERT profile 2 and 45 m along seismic profile 1.

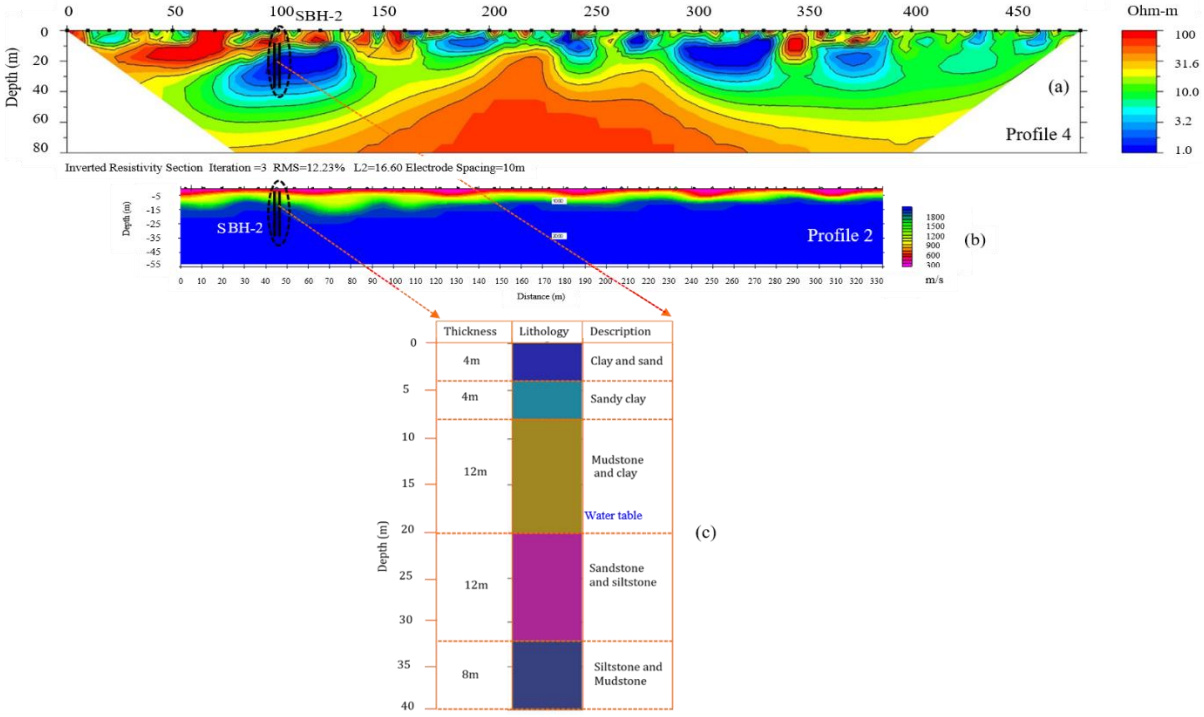

Figure 3.31. (a) 2D geoelectric cross section at profile 4; (b) The seismic velocity model at profile 2; (c) Vertical geological section of borehole SBH-2 at 100 m along ERT profile 4 and 45 m along seismic profile 2.

3.3.3. Khammouane Province

Three parallel NW - SE oriented profiles (1, 2 and 3) at the study site showed similar results (Figure 3. 32). A high resistivity region is higher than 100 Ohm.m was observed at shallow depths of approximately 10 m and some zones at depths between 40 and 80 m with fuzzy thicknesses are considered as sandy clay topsoil layers for shallow depths and sandstone bedrocks layers for deeper depths. A relatively low resistivity region is lower than 10 Ohm.m, which appear some zones of unclear thickness are interpreted to be a thick clay layers for each profile. However, a moderate resistivity ranges from 18.8 to 71 Ohm.m are observed at 12 to 30 m depth along these profiles are considered as appropriate water table.

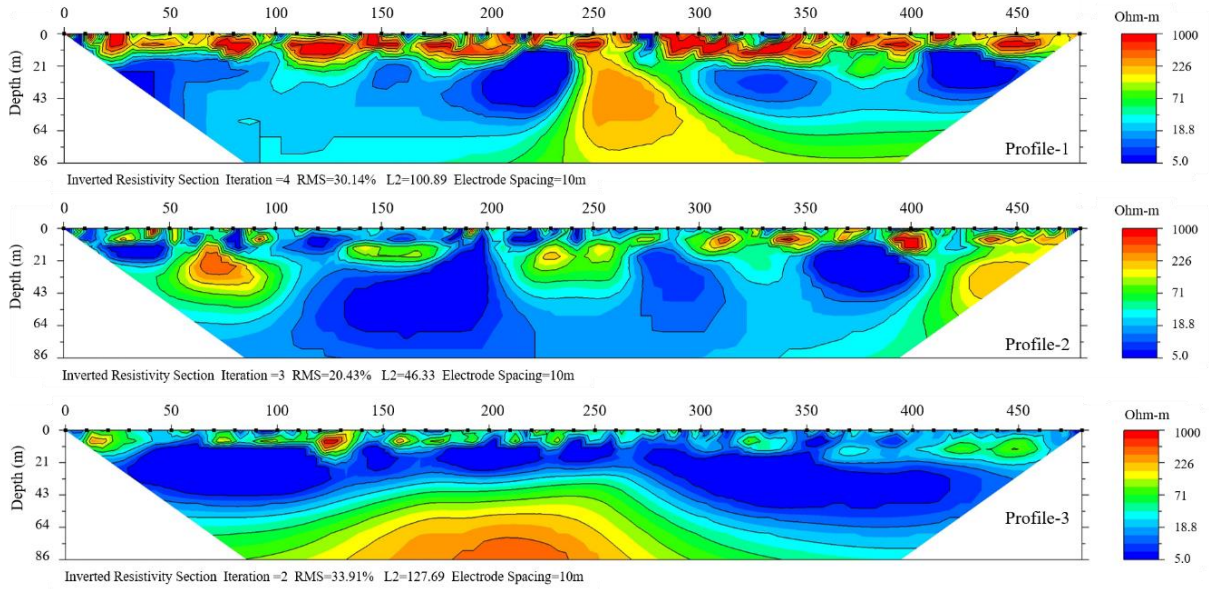

Figure 3.32. 2DERT cross sections at profiles 1, 2 and 3

In order to link the location of the earth subsurface layers in the survey area, a fourth profile is arranged crossing the three parallel profiles (1, 2 and 3) in the NE - SW direction with the intersection of profiles 1, 2 and 3 at 50 m, 200 and 300 m, respectively (Figure 3.33). The relatively low resistivity regions below 10 Ohm.m appears in some zones for this profile with an unclear thickness to be interpreted as a

thick clay region, approximately 12 to 30 m deep, which is interpreted as an appropriate groundwater zone or aquifer in the profile.

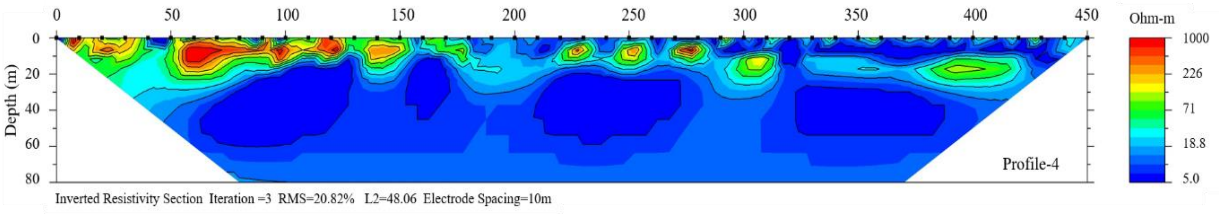

Figure 3.33. 2D ERT cross section at profile 4.

Additionally, two parallel SRT profiles (1 and 2) were superimposed on selected ERT profiles (1 and 2). The beginning of the seismic profile was 44 m of the ERT profile while the end of the profile was located at 352 m of the ERT profile (Figure 3.34). The results of the two SRT profiles (1 and 2) correlated well with the 2D ERT cross-sections of profiles 1 and 2. These two geophysical results show a moderate resistivity of 18.8 to 71 Ohm.m and a seismic velocity range from 1220 to 2140 m/s is considered to be water level at a depth of about 12 to 30 m. The regions with low resistivity below 10 Ohm.m and seismic velocity ranges from 760 to 1220 m/s are considered as thick clay layers of unclear thickness, whereas high resistivity is greater than 100 Ohm.m and seismic velocity varies from 300 to 760 m/s found at shallow depths of about 10 m, it is considered a sandy clay topsoil.

On the other hand, a third seismic profile was carried out at the fourth ERT profile (Figure 3.35.). High resistivity values greater than 100 Ohm.m and seismic velocity vary from 300 to 760 m/s found at shallow depth of about 10m, with unclear thickness are considered to be sandy clay topsoil layers. The relative low resistivity regions less than 10 Ohm.m and seismic velocity vary from 760 to 1220 m/s appear at some zones for this profile with unclear thickness are interpreted to be a thick clay zone. However, medium as resistivity regions of 18.8 to 71 Ohm.m and seismic velocity vary from 1220 to 2140 m/s are observed at 12 to 30 m depth along this profile is interpreted to be suitable groundwater layers.

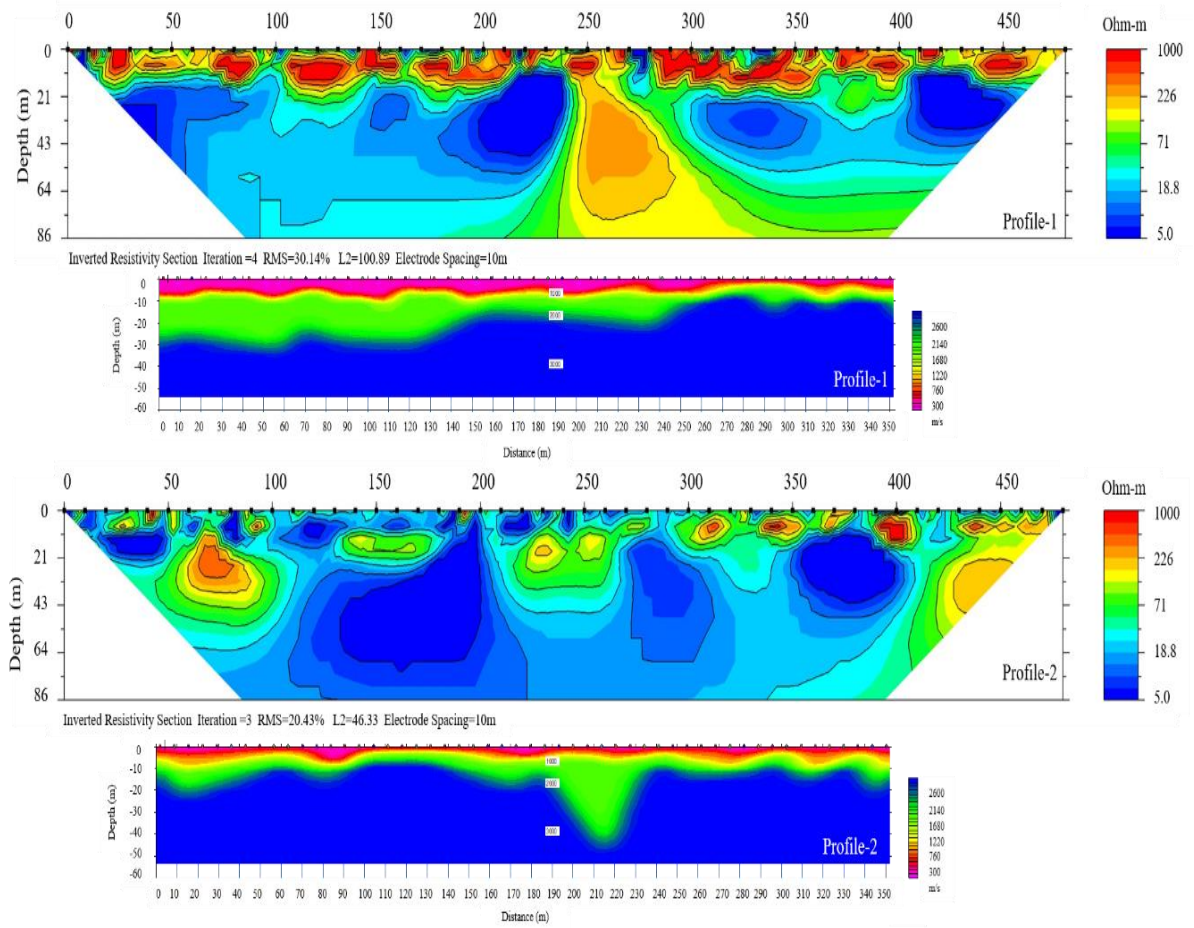

Figure 3.34. 2D ERT and SRT cross sections at profiles 1 and 2.

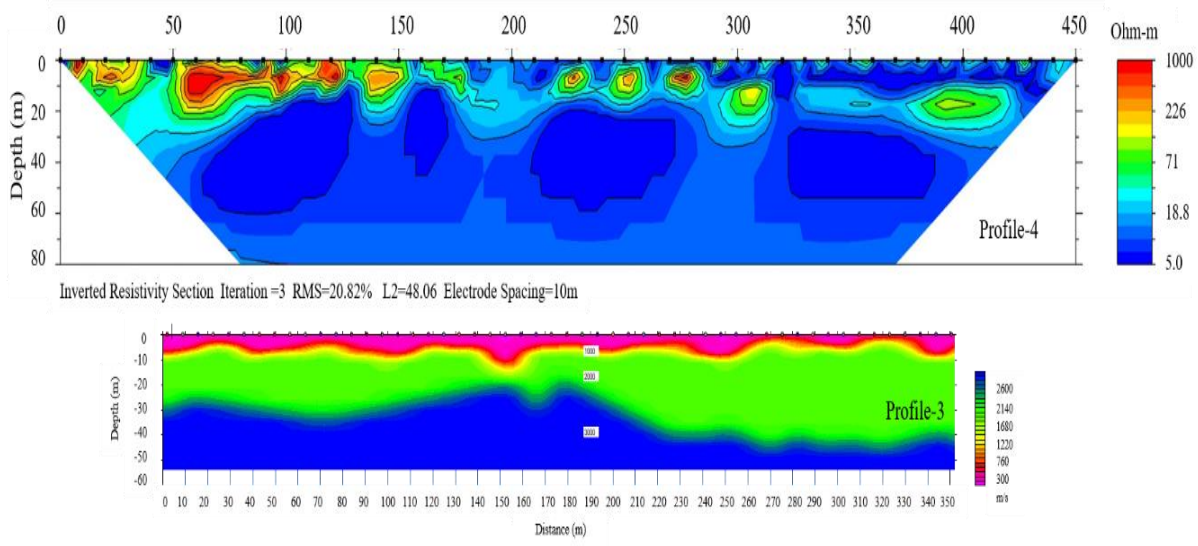

Figure 3.35. 2D ERT and SRT cross sections at ERT profile 4 and SRT profile 3.

In order to compare between 2D ERT and SRT results, two boreholes were drilled at the profile 1 for matching the positions of water table or aquifers layers (Figure 3.36a, b, c, d). The obtained results from the both borehole KBH-1 and borehole KBH-2 indicated the water table at around 12 m depth for borehole KBH-1 and 15 m depth for borehole KBH-2 in the first ERT and SRT (profile 1). The soil samples collected from both two boreholes were classified as sand and gravel at water table level (Figure 3.36c, d), which respond well with resistivity regions of 18.8 to 71 Ohm.m (Figure 3.36a) and seismic velocity regions between 1220 to 2140 m/s are identified for groundwater layers (Figure 3.36b).

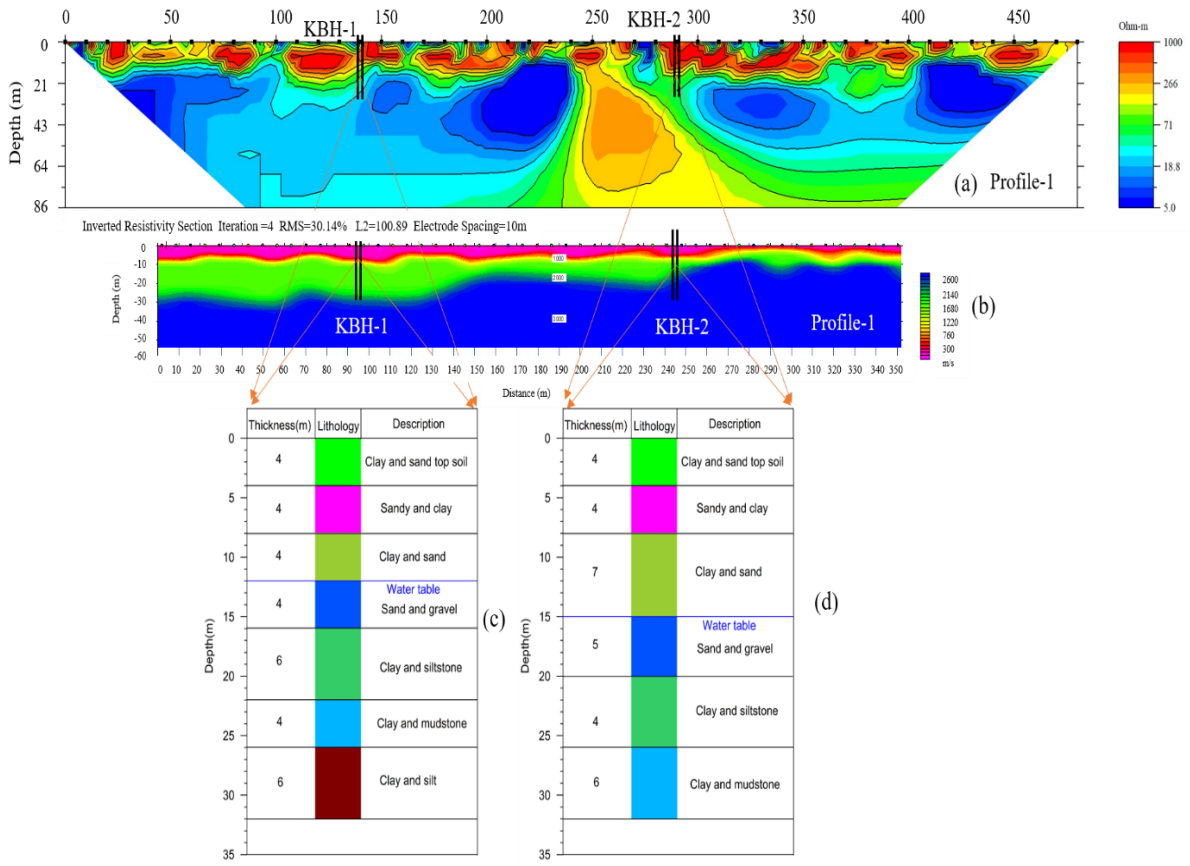

Figure 3.36. (a) 2D ERT cross section at profile 1; (b) The SRT cross section at profile 1; (c) Vertical geological cross section of borehole KBH-1 at 140 m at ERT profile 1 and 96 m at SRT profile 1; (d) Vertical geological cross section of borehole KBH-2 at 290 m at ERT profile 1 and 246 m at SRT profile 1.

CONCLUSION OF CHAPTER 3

This chapter addressed methodology used in research work which consists of characteristics of the research areas, network of survey profiles and used geophysical methods, and results and discuss of each research area as follows:

- The three selected study areas in different provinces of central Laos were chosen in this thesis work. The country is a topical monsoon climate, rainy season runs from May to October, a dry and cool season run from November to February and a hot dry season prevailing in March and April. The temperature varies from 5°C to 40°C depends on local regions whereas rainfall varied from 1300 to 3700 mm. The geological information of Laos is similar to the neighboring countries. Metamorphic rocks are considered to be Proterozoic outcrop, which found in some parts of the country. These Mesozoic sandstones, of a thickness of several hundred meters, constitute the Khorat Plateau found in Thailand that extends into Laos within lowland parts of Vientiane Plain, Vientiane, Savannakhet, and Champassak Basins.

- The three selected geophysical methods were carried out at different study areas.

+ In Vientiane province: ten electrical resistivity and three induced polarization profiles were conducted at four sites using the IMEE methods with the MC array presented above with 10 m electrode spacing and profile lengths of 550 m. On the other hand, four seismic profiles were conducted at two sites in Phonhong district, which seismic survey profile length of 440 m. In addition, two boreholes were drilled to compare with the geophysical results at the Phonhong and Thoulakhom districts.

+ The five 2D ERT profiles were conducted in Outhomphone district of Savannakhet province with maximum length of profile of 480 m. The Wenner electrode array was selected to conduct with electrode spacing of a=10 up to 160 m. The two SRT profiles were also conducted at selected ERT profiles with seismic profile length of 330 m, including two boreholes were drilled to compare with the geophysical results at the selected study areas.

+ The four ERT profiles were conducted in Thakhek district, Khammouane province with maximum length of profile of 480 m. The Wenner electrode array was selected to conduct with electrode spacing of a=10 up to 160 m. The three seismic refraction profiles were conducted at elected ERT profiles, with seismic profile length of 352 m, including two boreholes were drilled to compare with the geophysical results at the selected study areas.

- The geophysical methods like ERT, seismic refraction, and especially the IMEE methods have proven useful in subsurface mapping of water table or aquifers in selected research areas. The drilling results of the boreholes in around research sites, including the results of TDS, EC and pH from water samples in different existing and new wells in the first survey areas confirmed that the water is suitable for drinking without causing health risk. The results of this research work indicate that the application of the ERT, seismic refraction, and IMEE methods to finding groundwater in Laos is feasible and effective. Induced polarization analysis can reduce the ambiguities in the resistivity data, being able to distinguish between clay and groundwater zones whereas seismic refraction results to confirm water tables or good groundwater zones in the three studied areas. As following details below:

+ The study area 1 in Vientiane province: the results obtained from IMEE methods indicated that a moderate resistivity region of 18 to 80 Ohm·m and low chargeability region of 0 to 21 ms found at depth from 22 to 70 m and extended downward in a deeper depth at profile 1 and some zones at profile 2 is considered as possible groundwater or good quality of aquifers. The results of IMEE methods were well correlated with water level at a depth of 22 m of the borehole in Phonhong district and correlated well with the previous studies on groundwater ranges from 22 m to 70 m in the Vientiane region [60]. While results from seismic refraction method found that water table at depth from 20 to 25 m that the aquifer is a sand and gravel aquifer with a thickness of unclear. The results of TDS, EC and pH values indicated that the water is suitable for eating without causing health risks.

+ The study area 2 in Savannakhet province: the results obtained from ERT and SRT methods showed that the moderate resistivity regions vary from 15 to 60 Ohm.m and seismic velocities ranging from 1200 to 1800 m/s found at the depth of 16 to 80m, is considered as possible groundwater aquifers. These results also agree well with information obtained from two boreholes in the Outhoumphone district, where samples at depth of 16 to 20 m have been identified as sandstone and siltstone.

+ The study area 3 in Khammouane province: the obtained results showed the moderate resistivity regions of 18.8 to 71 Ohm.m and seismic velocity vary from 1220 to 2140 m/s found at 12 to 30 m depth are considered as possible groundwater aquifers. These results correlate well with those obtained from boreholes which show the groundwater level at a depth of about 12 m for borehole KBH-1 and a depth of 15 m for borehole KBH-2.

CONCLUSION

1. A combination of Electrical Resistivity Tomography / Improved Multi-electrode Electrical Exploration and Seismic Refraction Tomography methods have been chosen to search for groundwater zones in the three research areas of central Laos. The results obtained of the geophysical methods was compared to the results of boreholes were drilled at along geophysical profiles. In addition, the TDS, EC, and pH values are also analyzed from water samples in different existing and new wells in the first survey area.

- The obtained results from IMEE methods in Vientiane province indicated that a moderate resistivity region of 18 to 80 Ohm.m and low chargeability region of 0 to 21 ms found at depths from 22 to 70m and extended downward in a deeper depth at profile 1 and some zones at profile 2 is considered as possible groundwater or good quality of aquifers that correlated well with the previous studies on the groundwater zones range from 22 m to 70 m in the Vientiane region [60]. The results of IMEE methods were well correlated with the water level at a depth of 22 m of the borehole in the Phonhong district. While results from seismic refraction method found that water table at depth from 20 to 25 m. In addition, the TDS, EC, and pH analysis from water samples in different wells in the survey area confirm that water is suitable for drinking without causing health risks.

- The results of ERT and SRT methods in Savannakhet province showed that the moderate resistivity region of 15 to 60 Ohm.m and the seismic velocity of 1200 to 1800 m/s at a depth of 16 to 80 m was considered as possible groundwater aquifers, which correlates well with the water table obtained from the boreholes at depths of 16 m and 20 m respectively.

- The results of ERT and SRT methods in Khammouane Province found that moderate resistivity values of 18.8 to 71 Ohm.m and the seismic velocity of 1220 to 2140 m/s at a depth of 12 to 30 m are considered as possible groundwater aquifers, which correlates well with the water table obtained from the boreholes at depths of 12 m and 15 m respectively.

Regarding to the recent obtained electricity results indicated, it can be delineated fresh water zones and other zones based on their electrical properties contrast. On the basic of resistivity values range from 20-160 Ohm.m and very low chargeability 0 ms is considered as fresh groundwater or good aquifers. These results are consistent with the TDS, EC and pH results from water samples in existing wells and new borehole.

The obtained results of the three studied areas indicated that water tables or depth to aquifers are slightly different from each other, which found water tables at 20 to 22 m in Vientiane province, whereas found water tables at 15 to 20 m and 12 to 15 m in Savannakhet and Khammouane provinces respectively.

2. The research results indicated that the combination of the geophysical exploration methods such as the Improved Multi-electrode Electrical Exploration (both electrical resistivity and induced polarization)/2D Electrical Resistivity Tomography and Seismic Refraction methods to search for groundwater is feasible and efficient in the three research sites of central Laos. There are a few geophysical profiles were conducted in the three study areas due to limitation on budget and time. Therefore, the obtained geophysical results, including results from water samples analysis of TSD, EC and pH parameter for groundwater studies in this thesis work to assess the quality and availability of groundwater at specific locations of the 3 selected study areas. The results of induced polarization and seismic refraction methods can reduce ambiguity in resistivity data analysis, which can distinguish between clay content or saturated water earth subsurface. The combination of resistivity and induced polarization methods can identify fresh and saline groundwater and high groundwater zones in these areas. While seismic refraction method to identify water tables or aquifers. The obtained results indicated that these geophysical methods can provide new and higher resolution results in the three research areas of central Laos. The results demonstrated the benefits of using these geophysical methods to find groundwater zones in the research areas and they can be used for other areas with similar geology formations in further research work.

3. The results of this thesis will be reported to the Department of Water Resources, Ministry of Natural Resources and Environment, Lao PDR. The results will be useful for researchers who are interested in groundwater exploration as references. At the same time, these results will attract directly for managers in planning exploitation and the use of groundwater resources as well as use these results will be useful for a public awareness strategy to promote safe and sustainable use of groundwater in the future in Laos.

LIST OF SCIENTIFIC WORKS OF THE AUTHOR RELATED TO THE THESIS

1. **Viengthong Xayavong**, Vu Duc Minh, Do Anh Chung, Sonexay Xayheuangsy, Thiengsamone Sounsuandao, (2019), "Study the possibility of applying the advanced 2D multi-electrode electrical exploration method to find groundwater in Vientiane province, Laos", *Proceedings of the 6th International Conference on Applied and Engineering Physics (ICAEP – 6)*, pp. 105-111, Thai Nguyen.

2. **Viengthong Xayavong**, Vu Duc Minh, Nguyen Anh Duong, Vu Minh Tuan, (2020), "Seismic Refraction Exploration for Groundwater Potential Evaluations: A Case Study of Vientiane Province, Laos", *VNU Journal of Science: Earth and Environmental Sciences*, 36(4), pp. 90-101, DOI: https://doi.org/10.25073/2588-1094/vnuees.4651.

3. **Viengthong Xayavong**, Minh Duc Vu, Duong Anh Nguyen, Tuan Minh Vu, Chung Anh Do, (2021), "Application of the electrical resistivity tomography and seismic refraction methods for groundwater investigation in Savannakhet province, Laos", *Proceedings of the 7th Academic Conference on Natural Science of ASEAN Countries (CASEAN –7)*, Ha Noi.

4. Minh Duc Vu, **Viengthong Xayavong**, Chung Anh Do, Luan Thanh Pham, David Gómez-Ortiz, Ahmed M. Eldosouky, (2021), "Application of the improved multi-electrode electrical exploration methods for groundwater investigation in Vientiane Province, Laos", *Journal of Asian Earth Sciences: X*, 5, 100056,DOI: https://doi.org/10.1016/j.jaesx.2021.100056.

5. **Viengthong Xayavong**, Minh Duc Vu, Duong Anh Nguyen, Tuan Minh Vu, Chung Anh Do, Luan Thanh Pham, Ahmed M. Eldosouky, (2022), "Application of the Electrical Resistivity Tomography and Seismic Refraction Methods for

Groundwater Investigation in Savannakhet Province, Laos", *Frontiers in Scientific Research and Technology*, 3, pp. 62 -69, DOI: 10.21608/fsrt.2021.105000.1052.

6. **Viengthong Xayavong**, Vu Duc Minh, Sounthone Singsoupho, Nguyen Anh Duong, K.N.D. Prasad, Vu Minh Tuan, Do Anh Chung, (2023), "Combination of 2D-Electrical Resistivity Imaging and Seismic Refraction Tomography methods for groundwater potential assessments: A case study of Khammouane province, Laos", *Vietnam Journal of Earth Sciences*, 45(2), p. 1-13, https://doi.org/10.15625/2615-9783/18348**.**

REFERENCES

1. Vietnamese

[1] Đỗ Anh Chung, Vũ Đức Minh, (2019), "Áp dụng phương pháp Thăm dò điện đa cực 2D cải tiến để khảo sát hiện trạng, góp phần đánh giá độ ổn định của đê", *Tạp chí khoa học Đại học Quốc gia Hà Nội, Khoa học Tự nhiên và Công nghệ*, số 35(1), tr. 104-118. DOI: https://doi.org/10.25073/2588-1140/vnunst.4855.

Do Anh Chung, Vu Duc Minh, (2019), "Application of the Advanced 2D Multi-electrode Electrical Exploration Method in Surveying Dyke's Current Condition and Its Contribution to Assessing the Stability of Dyke", *VNU. Journal of Science, Natural Sciences and Technology,* 35(1), pp.104-118 (in Vietnamese).

[2] Lê Viết Dư Khương, Vũ Đức Minh, (2001), "Các phương pháp mới trong đo sâu điện trở dùng tổ hợp hệ cực đo hợp lý", *Tạp chí Các Khoa học về trái đất,* số 23(3), tr. 217-224.

Le Viet Du Khuong, Vu Duc Minh, (2001), "A new method by using the reasonable combination of electrode array for Resistivity Sounding", *Vietnam Journal of Earth Sciences,* 23(3), pp. 217-224 (in Vietnamese).

[3] Vũ Đức Minh, (2010), "Phương pháp Thăm dò điện đa cực cải tiến", *Tạp chí khoa học Đại học Quốc gia Hà Nội, Khoa họcTự nhiên và Công nghệ*, số 26(4), tr. 233-241. DOI: https://js.vnu.edu.vn/NST/article/view/1983

Vu Duc Minh, (2010), "The Improved Multi-electrode Electrical Sounding Method", *VNU. Journal of Science: Natural Sciences and Technology*, 26(4):233-241 (in Vietnamese).

[4] Đỗ Anh Chung, Vũ Đức Minh, (2013), "Nghiên cứu cải thiện khả năng tiếp đất của các điện cực trong phương pháp điện đa cực cho các môi trường khó tiếp đất", *Tạp chí khoa học Đại học Quốc gia Hà Nội, Khoa họcTự nhiên và Côngnghệ*, số 29(2), 2013, tr. 57-69. DOI: https://js.vnu.edu.vn/NST/article/view/1253

Do Anh Chung, Vu Duc Minh, (2013), "Research on improvement of the electrodes' soil connection when using the multi-electrode method in media which are typical for

soil connection difficulty", *VNU. Journal of Science, Natural Sciences and Technology,* No. 29(2), pp. 57-69 (in Vietnamese).

2. English

[5] Adewoyin O.O., Joshua E.O., Akinyemi1 M.L. (2016), "Application of Shallow Seismic Refraction Method and Geotechnical Parameters in Site Characterization of a Reclaimed Land", *Indian Journal of Science and Technology,* 9 (45), pp.1-7.

[6] Advanced Geosciences. (2002-2009), *EarthImager 2D resistivity and IP Invasion*, Advanced Geosciences inc, Austin, Texas 78726, USA.

[7] Aizebeokhai A.P. (2010), "2D and 3D geoelectrical resistivity imaging: Theory and field design", *Academic Journals*, 5(23), pp. 3592-3605.

[8] Akingboye A.S., ChrisOgunyele A. (2019), "Insight into seismic refraction and electrical resistivity tomography techniques in subsurface investigations", *The Mining-Geology-Petroleum Engineering Bulletin,*34 (1), pp. 93-111.
DOI: 10.17794/rgn.2019.1.9

[9] Anomohanran O. (2012), "Geophysical interpretation of seismic reflection data obtained from Umureute and Amiynaibo area of Delta state, Nigeria", *Nigerian. J. Sci. Environ,* 11, pp.148- 153.

[10] Arjwech R., Everett M.E. (2015), "Application of 2D electrical resistivity tomography to engineering projects: three case studies", *Songklanakarin Journal of Science and Technology,* 37 (6), pp. 675-681.

[11] Azwan M., Zawawi M., Toridi N.M., Wayayok A. (2015), "Detection of fractured aquifer using combination of resistivity and induced polarization analysis", *Technology Journal,*76:15, pp. 119-124. DOI: 10.11113/jt. v76.5962

[12] Banks E.W., Post V.E.A., *Meredith* K., Ellis J., Cahill K., Noorduijn S., Batelaan O. (2021), "Fresh groundwater lens dynamics of a small bedrock island in the tropics, Northern Australia", *Journal of Hydrology,* 595, 125942.
Doi: 10.1016/j.jhydrol.2020.125942.

[13] Banks E.W., Hatch M., Douangsavanh S., Pavelic P., Singsouph, S., Xayavong V., Xayviliya O., Vongphachanh S., Viossanges M., Batelaan O. (2022), "Cooperation

in hydrogeophysics: Enhancing practitioners and institutions' groundwater assessment capacity, Vientiane Plain, Lao PDR", *Geophysics,*87(1): WA49-WA63. https://doi.org/10.1190/geo2021-0100.1**.**

[14] Banks, E.W., Hatch M., Smith S., Underschultz J., Lamontagne S., Suckow A., Mallants D. (2019), "Multi-tracer and hydrogeophysical investigation of the hydraulic connectivity between coal seam gas formations, shallow groundwater, and stream network in a faulted sedimentary basin", *Journal of Hydrology*, 578, 124132. Doi: 10.1016/j.jhydrol.2019.124132.

[15] Bery A.A. (2013), "High Resolution in Seismic Refraction Tomography for Environmental Study", *International Journal of Geosciences*, 4 (4), pp.792-796.

[16] Binley A., Kemna A. (2005), "DC resistivity and Induced Polarization Methods", *Hydrogeophysics Springer*, 50, pp. 129-156.DOI:10.1007/1-4020-3102-5_5

[17] Burger H. R. (1992), *Exploration Geophysics of the Shallow Subsurface. Englewood Cliffs*, Prentice- Hall, Inc.

[18] Butler D.K. (2005), "Near-Surface Geophysics. Society of Exploration Geophysicists", 13, pp. 478.

[19] Castagna J.P., Batzle M.L., Eastwood R.L. (1985), "Relationship between compressional-wave and shear-wave velocities in clastic silicate rocks", *Geophysics,* 50 (4), pp. 571-581. https://doi.org/ 10.1190/1.1894108.

[20] Colangelo G., Lapenna V., Loperte A., Perrone A., Telesca L. (2008), "2D electrical resistivity tomography for investigating recent activation landslides in Basilicata Region (Southern Italy)", *Annals of Geophysics,* 51, pp.275-285.

[21] Contanont T., Srisuk K. (2005), "Determination of Groundwater Recharge at Nong Bo Area, MahaSarakham Province, Thailand", *International Conference on Geology, Geotechnology and Mineral Resources of Indochina*, pp. 143-148.

[22] Daily W., Ramirez A., Binley A., LaBrecque D. (2005), "Electrical resistance tomography - Theory and practice: in D. K. Butler (ED).", *Near-surface geophysics, SEG*, 13, pp. 525-550.

[23] Dahlin T., Leroux V., Nissen J. (2002), “Measuring techniques in induced polarization imaging”, *Journal of Applied Geophysics*, 50, pp. 279-298.

[24] Do C.A., Vu M.D., Pham L.T., Eldosouky A.M. (2022), “Surveying the seepage area in the Dong Do dam by the improved multi-electrode electrical exploration method”, *Frontiers in Scientific Research and Technology*, 3, pp. 70-77.

[25] El Tabakh M., Utha-Aroon C., Schreiber B.C. (1999), “Sedimentology of the Cretaceous MahaSarakham evaporites in the Khorat Plateau of northeastern Thailand”, *Sedimentary Geology*, 123 (1), pp.31-62. DOI:10.1016/S0037-0738(98)00083-9

[26] Fan P. (2000), “Accreted terranes and mineral deposits of Indochina”, *Journal of Asian Earth Sciences*, 18, pp. 343-350.

[27] Foti S., Lai C.G., Lancellotta R. (2002), “Porosity of fluid saturated porous media from measured seismic wave velocities”, *Geotechnique*, 52 (5), pp. 359-373. http://dx.doi.org/10.1680/geot.52.5.359.38702.

[28] Gabr A., Murad A., Baker H., Bloushi K., Arman H., Mahmoud A. (2012), “The use of seismic refraction and electrical techniques to investigate groundwater aquifer, wadi al-ain, United Arab Emirates (UAE)”, *Conference: Water resources and wetlands, Tulcea (ROMANIA)*, pp. 1-7.

[29] Grelle G., Guadagn F.M. (2009), “Seismic refraction methodology for groundwater level determination”: “Water seismic index”, *Journal of Applied Geophysics*, 68, pp. 301-320. https://doi.org/10. 1016/j.jappgeo.2009.02.001.

[30] Griffiths D.H., Barker R.D. (1993), “Two-dimensional resistivity imaging and modelling in areas of complex geology”, *Journal of Applied Geophysics*, 29, pp. 211-226.

[31] Griffiths D.H., Barker, R.D. (1994), “Electrical imaging in archaeology”, *Journal of Archaeology Science*, 21 (2), pp.153-158.

[32] Ha K., Nguyen N.T., Lee E., Jayakumar R. (2015), “Current Status and Issues of Groundwater in the Mekong River Basin”, *Korea Institute of Geoscience and Mineral*

Resources (KIGAM), CCOP Technical Secretariat, UNESCO Bangkok Office, pp. 1-121.

[33] Haeni F.P. (1986), "Application of seismic refraction methods in groundwater modelling studies in New England", *Geophysics,* 51 (2), pp. 236-249. http:// dx.doi.org/10.1190/1.1442083.

[34] Hasselstroem B. (1969), "Water prospecting and rock investigation by the seismic refraction method", *Geoexploration,* 7 (2), pp.113-132. https://doi.org/ 10.1016/0016-7142(69)90026-x.

[35] Hite R.J., Japakasert W. (1979), "Potash deposits of the Khorat Plateau, Thailand and Laos", *Economic Geology*, 74, pp. 448-458.

[36] Inthavong T. (2005), "Lao Mineral Resources Development, Management and Research Cooperation in Indochina", *International Conference on Geology, Geotechnology and Mineral Resources of Indochina, (GEOINDO 2005), KhonKaen, Thailand,* pp.1-12.

[37] Jagadeshan G., Gosaye B, Zinabe S., Abeje A. (2018), "Assessment of Groundwater Potential Using Seismic Refraction Method in Secha, Arba Minch, Ethiopia", *Journal of Applied Geology and Geophysics,* 6 (1), pp. 18-24.

[38] Jenkunawat P. (2005), "Results of Drilling to Study Occurrence of Salt Cavities and Surface Subsidence Ban Non Sabaeng and Ban Nong Kwang Amphoe Ban Muang, Sakon Nakhon", *International Conference on Geology, Geotechnology and Mineral Resources of Indochina (GEOINDO 2005), KhonKaen, Thailand,* pp. 259-267.

[39] JICA. (2000), "The study on rural water supply and sanitation improvement in the northwest region in the Lao People´s Democratic Republic, Ministry of health, National center for environmental health and water supply", *Progress report 2,* pp.14.

[40] JICA. (2013), "Preparatory survey on Thakhek water supply development project in Khammouane province in the Lao People´s Democratic Republic", *Final report 2,* pp.1-24

[41] Kearey P., Brooks M., Hill I. (2002), "An Introduction to Geophysical Exploration". *Blackwell Science,* 3rd edition, pp. 99-205

[42] Keith S., Crosby P. (2005), "Overview of the Geology and Resources of the APPC Udon Potash (Sylvinite) Deposits, Udon Thani Province, Thailand", *International Conference on Geology, Geotechnology and Mineral Resources of Indochina (GEOINDO 2005), KhonKaen, Thailand*, pp.283-299.

[43] Kim J.H., Yi M.J., Park S.G., Kim J.G. (2009), "4 D inversion of DC resistivity monitoring data acquired over a dynamically changing earth model", *Journal of Applied Geophysics*, 68 (4), pp.522-532.

[44] Knodel K., Lange G., Voigt H.J. (2007), *Environmental Geology: Handbook of Field Methods and Case Studies*, Springer- Verlag Berlin Heidelberg.
DOI: https://doi.org/10.1007/978-3-540-74671-3.

[45] Knudsen J.B.S., Ruden F., Smith, B.T. (2004), "The Online Support and Training Project for the Groundwater Sector of Lao PDR",*30th WEDC International Conference, Vientiane, Lao PDR*, pp.434- 437.

[46] Lee N., Lopez A., Katz J., Oliveira R., Hayter S. (2018), "Report Assessment of Data Availability to Inform Energy Planning Analyses", *Energy Alternatives Study for the Lao People's Democratic Republic, Smart Infrastructure for the Mekong Program*, pp. 1-71.

[47] Lees J.M., Wu H. (2000), "Poisson's ratio and porosity at Coso geothermal area, California", *Journal of volcanology and geothermal research*, 95, pp.157-173. https://doi.org/10.1016/S0377-0273(99) 00126-2.

[48] Loke M.H. (2000), "Electrical imaging surveys for environmental and engineering studies", *A practical guide to 2D and 3D surveys*, pp.1-61.

[49] Loke M.H., Chambers J.E., Rucker D.F., Kuras O., Wilkinson P.B. (2013), "Recent developments in the direct current geoelectrical imaging method", *Journal of Applied Geophysics*, 95, pp.135-156.

[50] Loke M. H. (2015), *Tutorial: 2-D and 3-D electrical imaging surveys*, Copyright (1996-2015), pp. 1-176

[51] Marutani M. (2006), “Final Report for Economic Geology: Sector Plan for Sustainable Development of the Mining Sector in the Lao PDR”, *The World Bank WASHINGTON D*C, pp.1-36.

[52] Medlicott K. (2001), *Water sanitation and environmental health in rural Lao PDR*, KAP Study. UNICEF WES; National Centre for Environmental Health and Water Supply (Nam Saat), Lao PDR.

[53] Mohamed A., Mohamed Z., Noorellimia M.T., Aimrun W. (2015), “Detection of fractured aquifer using combination of resistivity and induced polarization analysis”, *Technology Journal*, 76 (15), pp. 119-124.

[54] Nicholson C., Simposon D.W. (1985), “Changes in V_P /V_S with depth: implication for appropriate velocity models, improved earthquake locations, and material properties of the upper crust”. *Bulletin of the Seismological Society of America*, 75, pp. 1105-1124.

[55] Ngangnouvon I. (2019), “Mining in Laos, Economic growth, and price fluctuation”. *United Nations Conference on Trade and Development, Geneva,* pp. 1-19.

[56] Olowokudejo A. J. (2007), *Master’s thesis: Targeting of High-quality Groundwater in the province of Vientiane, Lao PDR*.

[57] Orojah O.J., Agayina K.E. (2014), “Hydro-geophysical investigation using seismic refraction tomography to study the groundwater potential of Ahmadu Bello University Main Campus, within the basement complex of Northern Nigeria”, *Journal of Environment and Earth Science,* 4 (2), pp. 15-22.

[58] Owen R., Gwavava O., Gwaze P. (2006), “Multi-electrode resistivity survey for groundwater exploration in the Harare greenstone belt, Zimbabwe”, *Hydrogeology journal*, 14 (1), pp. 244-252.

[59] Pellerin L. (2002), “Application of electrical and electromagnetic methods for environmental and geotechnical investigations”, *Surveys in Geophysics*, 23, pp.101-132.

[60] Perttu N., Wattanasen K., Phommasone K., Elming S.Å. (2011a), "Characterization of aquifers in the Vientiane Basin, Laos, using magnetic resonance sounding and vertical electrical sounding", *Journal of Applied Geophysics*, 73, pp. 207-220. doi: 10.1016/j.jappgeo.2011.01.003.

[61] Perttu N., Wattanasen K., Phommasone K., Elming S.Å. (2011b), "Determining water quality parameters of aquifers in the Vientiane Basin, Laos, using geophysical and water chemistry data", *Near Surface Geophysics*, 9, pp. 381-395, doi: 10.3997/1873-0604.2011014.

[62] Phommakaysone K. (2001), "Urban geology of Vientiane municipality, capital of the Lao people's Democratic Republic", *Atlas of Urban Geology*,14, pp.341-346.

[63] Phommavong K. (2015), *Groundwater Flow Systems and Aquifer Storage for Agriculture and Domestic Water Use in Kiet Ngong Village, Pathoumphone District, Champasak Province, Lao PDR*, 4th Batch Masters Programme in Environmental Engineering and Management. Master's Thesis, NUOL Faculty of Engineering, National University of Laos, Vientiane, Lao PDR.

[64] Raksaskulwong M., Monjai D. (2007), "Relationship between the MahaSarakham Formation and high terrace gravels along the Khon Kean-Kalasin provinces", *(Geothai'07), Department of Mineral Resources, Bangkok, Thailand*, pp. 288-296.

[65] RES2DINV ver. 3.59. (2010), Rapid 2-D Resistivity & IP inversion using the least-squares method. *Geotomo Software, Minden Heights, 11700 Gelugor, Penang, MALAYSIA*, pp. 1-151.

[66] Reynold J.M. (1997), *An Introduction to Applied and Environmental Geophysics*, John Wiley and Sons Ltd, pp. 209-415.

[67] Ronczka M., Hellman K., Günther T., Wisén R., Dahlin T. (2017), "Electric resistivity and seismic refraction tomography: a challenging joint underwater survey at Äspö Hard Rock Laboratory", *Solid Earth*, 8, pp. 671-682.

[68] Rosli S., Muhammad S., Nordiana M.M., Nur A. I. (2013), "Water table Delineation for Leachate Identification using 2-D Electrical Resistivity Imaging (2-DERI) and Seismic Refraction at GampongJawa, Banda Aceh", *EJGE*, 18, pp.1529-1535.

[69] Rucker D.F, Loke M.H., Levitt M.T., Noonan G.E. (2010), "Electrical resistivity characterization of an industrial site using long electrodes", *Geophysics*, 75 (4), pp. 95-104.

[70] Saad R., Syukri M., Nordiana M.M., Ismail N.A. (2013), "Water table Delineation for Leachate Identification using 2-D Electrical Resistivity Imaging (2D-ERI) and Seismic Refraction at GampongJawa, Banda Aceh", *Electronic Journal of Geotechnical Engineering*, 18, pp.1529-1535.

[71] Saad R., Muztaza, M.N., Zakaria, M.T., Saidin, M.M. (2017), "Application of 2D Resistivity Imaging and Seismic Refraction Tomography to Identify Sungai Batu Sediment Depositional Origin", *Journal of Geology & Geophysics*, 6, pp.1-5.

[72] Sander J.E. (1978), "The blind zone in seismic groundwater exploration", *Ground Water*, 165, pp. 394- 395. https://doi.org/10.1111/j.1745-6584.1978.tb0 3252.x.

[73] Schicht T., Wieser B., Allendorf-Schicht A. (2013), "Case study of a geophysical investigation with seismic refraction tomography and the Ohm Mapper to estimate the brine content of a Salar/Salmuera", *Near Surface Geoscience*, 31, pp. 85-90.

[74] SEPA. (200), "Environmental Quality Criteria-Groundwater". *REPORT 5051, Swedish Environmental Protection Agency (SEPA), Kalmar*, pp.142.

[75] Stümpel H., Kähler S., Meissner R., Milkereit B. (1984), "The use of seismic shear waves and compressional waves for lithological problems of shallow sediments", *Geophysical Prospecting*, 32, pp. 662-675. https://doi.org/10.1111/j.1365-2478. 1984.tb01712.x.

[76] Sundararajan N., Srinivas Y., Chary M.N., Nandakumar G., Chary A.H. (2004), "Delineation of structures favorable to groundwater occurrence employing seismic refraction method: A case study from Tiruvuru, Krishna district, Andhra Pradesh", *Journal of Earth System Science*, 113 (3), pp. 259-267.

[77] Takayanagi K. (1993), *Basic Design Study Report on the Project for Groundwater Development in Vientiane Province in Laos PDR*, Japan International Cooperation Agency (JICA).

[78] Viossanges M., Pavelic P., Rebelo L.M., Guillaume L., Sotoukee T. (2017), "Regional Mapping of Groundwater Resources in Data-Scarce Regions, The Case of Laos", *Hydrology journal*, 5(2), pp.1-24. DOI:10.3390/hydrology5010002.

[79] Vote C., Newby J., Phouyyavong K., Inthavong T., Eberbach P.L. (2015), "Trends and perceptions of rural household groundwater use and the implications for smallholder agriculture in rain-fed Southern Laos", *Int. J. Water Resource*, 31 (4), pp. 1-17. DOI:10.1080/07900627.2015.1015071

[80] Vu M.D. (2001), "Induced-Polarization Sounding methods in a new manner", *Journal of Geology*, Series B 17-18:94.

[81] Vu M.D., Do C.A. (2015a), "Introduction to the Advanced Multi-electrode Electrical Sounding method", *VNU Journal of Mathematics-Physics*, 31(3), pp.1-14.

[82] Vu M.D., Do C.A. (2018), "Perfecting the Advanced Multi-electrode Electrical Sounding method", *VNU Journal of Mathematics-Physics*, 34(3), pp. 90-103.

[83] Vu M.D. (2016), "Application of Interpolation Algorithm in Data Processing of the Advanced Multi-electrode Electrical Sounding Method to Determine Saturation Line in the Earth Dam", *VNU Journal of Science: Mathematics-Physics*, 32(3), pp.86-95.

[84] WHO. (1996), "Guidelines for drinking-water quality, third edition, incorporating, first and second addenda", *Recommendations, Geneva*, pp.210-220.

[85] Williamson D.R., Peck A J., Turner J.V., Arunin S. (1989), "Groundwater hydrology and salinity in a valley in Northeast Thailand", *Groundwater contamination IAHS-AISH Publication,*185, pp.147-154.

[86] Wiszniewski I., Lertsirivorakul R., Merrick N.P., Milne-Home W.A., Last R. (2005), "Groundwater flow section modelling of salinization processes in the Champhone catchment, Savannakhet province, Lao PDR", *Conference Proceeding*, pp. 1-9.

[87] Xayavong V., Vu M.D., Duong A.N., Vu M.T., Do C.A., Pham L.T., Eldosouky A.M. (2022), "Application of the Electrical Resistivity Tomography and Seismic Refraction Methods for Groundwater Investigation in Savannakhet Province, Laos", *Journal of Frontiers in Scientific Research and Technology*, 3, pp. 62 -69, DOI: 10.21608/fsrt.2021.105000.1052.

[88] Yusuf T.U. (2016), “Overview of Effective Geophysical Methods Used in the Study of Environmental Pollutions by Waste Dumpsites”, *An International Multi-Disciplinary Journal*, 10(2), pp.123-143.DOI: 10.4314/ afrrev. v10i2.8.

[89] Zhang X., Ma H., Yungi M., Tang Q., Yuan X. (2013), “Origin of the late Cretaceous potash-bearing evaporites in the Vientiane Basin of Laos”, *Journal of Asian Earth Sciences,* 62, pp. 812-818. DOI:10.1016/j.jseaes.2012.11.036